

UNCLASSIFIED

AD NUMBER

AD803949

LIMITATION CHANGES

TO:

Approved for public release; distribution is unlimited.

FROM:

Distribution authorized to U.S. Gov't. agencies and their contractors;
Administrative/Operational Use; 28 NOV 1966.
Other requests shall be referred to Office of Naval Research, Arlington, VA 22203.

AUTHORITY

ONR ltr 27 Jul 1971

THIS PAGE IS UNCLASSIFIED

803949

PUMPED TRANSFORMER LASERS

FINAL REPORT

Contract Nonr-4718(00), ARPA No. 306
GPL Division, Aerospace Group, General Precision, Inc.

C.B. Ellis (Sections 1-5)
J.H. Simpson and E.C. Eberlin (Sections 6-12)
I.A. Greenwood, Project Manager

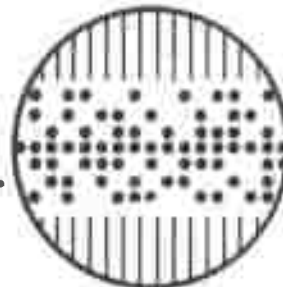
This research is part of Project DEFENDER under the joint sponsorship of the Advanced Research Projects Agency, the Office of Naval Research, and the Department of Defense. Reproduction of this report in whole or in part is permitted for any purpose of the United States Government.

28 November 1966

GPL DIVISION

 **GENERAL
PRECISION INC.**

**AEROSPACE GROUP
PLEASANTVILLE, NEW YORK**



**BEST
AVAILABLE COPY**

GPL-A-31-4

PUMPED TRANSFORMER LASERS

FINAL REPORT

Contract Nonr-4718(00)

ARPA No. 306

C.B. Ellis (Sections 1-5)

J.H. Simpson and E.C. Eberlin (Sections 6 -12)

I.A. Greenwood, Project Manager

This research is part of Project DEFENDER under the joint sponsorship of the Advanced Research Projects Agency, the Office of Naval Research and the Department of Defense. Reproduction of this report in whole or in part is permitted for any purpose of the United States Government.

28 November 1966

ABSTRACT

A number of laser-pumped-laser systems have been studied which offer promise of development into sources for very high intensity beams of excellent parallelism.

The arrangement proposed is to pump a vapor volume from many directions simultaneously with the output light from a large number of primary lasers -- which do not have to be of good optical quality.

Absorption of the pump light by molecules of the vapor produces inversion in some of the molecular transitions, in such a manner that the vapor volume can lase out most of the total absorbed energy as a single output beam.

Analysis based on molecular properties recorded in the existing literature pointed to at least five combinations of materials, with outputs between 7000Å and 5μ, which look potentially useful for such a system, *provided* no new unfavorable properties of the gas molecules under intense irradiation are established.

All of these combinations appeared deserving of serious experimental investigation.

Laboratory work under the contract has dealt entirely with one of these possible combinations: saturated cesium vapor near 400°C in a helium atmosphere, pumped at 1.06μ with Nd glass lasers.

The experiments so far indicate a strong probability of serious trouble from some dissipative reaction occurring in the cesium vapor at high pumping fluxes. However, the origin of the trouble has not yet been definitely settled.

TABLE OF CONTENTS

	<u>Page No.</u>
1. INTRODUCTION	1
1.1 Summary of Previous Contract Reports	2
1.2 New Work Covered in this Report	4
2. THE CO-ER GLASS TRANSFORMER LASER CONCEPT	7
2.1 General Description of Proposed Arrangement	7
2.2 Pumping CO with Er Glass Lasers	10
2.3 Choice of the Lasing Wavelength	16
2.4 Collisional Energy Transfers	18
2.5 Resistance of CO to Waste Heat Production	23
2.6 The Molecular Heat Balance	26
3. POLYATOMIC MOLECULES IN IR TRANSFORMERS	29
3.1 The HCN-Er Glass Possibility	29
3.2 The Polyatomic Situation in General	31
4. NOTES ON THE Na ₂ -RUBY TRANSFORMER COMBINATION	34
4.1 Location of the (A-X) System and of its Neighbors	34
4.2 Calculated Band Origins for (A-X)	38
4.3 General Remarks on Na ₂ -Ruby	42
5. SOME PROPERTIES OF CESIUM MOLECULES	45
5.1 Expected Intensity of the Cs ₂ -(A-X) Band System	46
5.2 Molecular Concentrations in Superheated Vapor	51
6. INTRODUCTION TO EXPERIMENTAL WORK	61
7. TRANSFORMER LASER EXPERIMENT	62
7.1 Experimental Arrangement	62
7.2 Discussion of Results	66
8. INVESTIGATION OF NEODYMIUM AND RUBY LASER CHARACTERISTICS	68
8.1 Experimental Methods	69
8.2 Summary of Results	71
9. PHOTOELECTRIC ABSORPTION SPECTRA	75
9.1 Experimental Arrangement	75
9.2 Presentation of Cesium Results	77
9.3 Discussion of Cesium Results	77
9.4 Rubidium Absorption Spectrum	81

	<u>Page No.</u>
10. LASER-EXCITED FLUORESCENCE	82
10.1 Experimental Procedures	82
10.2 Presentation of Results	89
10.3 Discussion of Results	89
10.4 Effect of Varying Laser Power	95
10.5 Fluorescence With Ruby Excitation	95
11. TIME-DEPENDENT ABSORPTION STUDIES OF CESIUM VAPOR	98
11.1 Experimental Arrangement and Procedures	98
11.2 Presentation of Results	101
11.3 Discussion of Results	105
12. DISCUSSION OF EXPERIMENTAL RESULTS	109
13. CONCLUSION	117
14. BIBLIOGRAPHY	119

LIST OF FIGURES AND TABLES

<u>Figure</u>		<u>Page No.</u>
1.	A Simple Transformer Laser Arrangement	8
2.	The Er-CO Pumping and Lasing Spectral Region	14
3.	Collision Relaxation Rate vs. Temperature for CO	25
4.	Energy Level Chart for Na ₂	37
5.	Franck-Condon Diagram for the Na ₂ ⁺ (A-X) System	41
6.	Concentrations of Higher Polymers in Alkali Metal Vapors	53
7.	Molecular Concentrations in Superheated Vapor	55
8.	Schematic Drawing of Transformer Laser Experiment	63
9.	Portion of Apparatus for Transformer Laser Experiment Showing Optical Cavity and Oven	65
10.	Experimental Arrangement for Investigation of Neodymium and Ruby Laser Outputs	70
11.	Neodymium and Ruby Laser Spectra	73
12.	Apparatus for Photoelectric Absorption Spectra Measurements	76
13-a.	Absorption Spectrum of Cesium Vapor With Helium Between 7000 and 9000Å	78
13-b.	Absorption Spectrum of Cesium Vapor With Helium Between 9000 and 11000Å	79
13-c.	Absorption Spectrum of Cesium Vapor With Helium Between 11000 and 13000Å	80
14-a.	Absorption Spectrum of Rubidium Vapor Between 6000 and 7000Å	83
14-b.	Absorption Spectrum of Rubidium Vapor Between 7000 and 9000Å	84
14-c.	Absorption Spectrum of Rubidium Vapor Between 9000 and 11000Å	85

<u>Figure</u>		<u>Page No.</u>
14-d.	Absorption Spectrum of Rubidium Vapor Between 11000 and 13000Å	86
15.	Apparatus for Photoelectric Fluorescence Measurements	88
16-a.	Fluorescence Spectrum Between 5600 and 8000Å of Neodymium Laser-Excited Cesium Vapor (Without Helium)	90
16-b.	Fluorescence Spectrum Between 7900 and 10300Å of Neodymium Laser-Excited Cesium Vapor (Without Helium)	91
16-c.	Fluorescence Spectrum Between 7900 and 10300Å of Neodymium Laser-Excited Cesium Vapor (With Helium)	92
16-d.	Fluorescence Spectrum Between 1.00 and 1.24μ of Neodymium Laser-Excited Cesium Vapor (With and Without Helium)	93
17.	Cesium Fluorescence as a Function of Neodymium Laser Energy	96
18.	Experimental Arrangement for Observing Time Dependent Absorption Spectra	99
19.	Time Dependent Absorption Curves for Saturated Cesium Vapor ($\lambda = 9800\text{\AA}$)	102
20.	Time Dependent Absorption Curves for Saturated Cesium Vapor With Helium ($\lambda = 7530\text{\AA}$)	103
21.	Time Dependent Absorption Curves for Saturated Cesium Vapor With Helium ($\lambda = 9800\text{\AA}$)	104
22.	Energy Level Diagram for Atomic Cesium	113

<u>Table</u>	<u>Page No.</u>
1. The Lower Vibrational Levels of CO·X	11
2. Rotation Lines and Levels of the CO·X (3-0) Band	12
3. Spontaneous Lifetimes of CO Harmonic Bands	17
4. Rotational Population Distribution in (v=0) at 100°K	19
5. Wavenumbers of Origins of Observed Na ₂ ⁺ (A-X) Bands	39
6. Molecular Radiative Cross Sections	48
7. Energy Required for Suppressing the Molecules	58
8. Summary of Neodymium and Ruby Laser Characteristics	72
9. Summary of Time-Dependent Absorption Measurements on Cesium-Helium Cell	106

1. INTRODUCTION

The transformer laser concept is an arrangement proposed for combining the outputs of numerous auxiliary lasers, which do not need to be in phase, *and which do not need to be of the best optical quality*, into a single coherent diffraction-limited beam containing a power close to the sum of the auxiliary laser output powers. This is to be done by absorption of the pumping laser beams by the molecules of a transformer gas medium, in such a manner that inversion occurs and the gas re-emits most of the absorbed energy as a single new laser beam.

The present contract was established with two major aims:

- (a) to analyze theoretically a great many possible combinations of pumping laser types, and gas transformer media types, so as to identify those combinations which would probably be most suitable for various practical applications of the concept, and
- (b) to choose as quickly as possible the most likely of these combinations and to begin its experimental testing in the laboratory.

In pursuit of these aims, a great many possible combinations have now been considered analytically under the contract. From a preliminary comparison of the expected merits of these, one combination was chosen fairly early in the contract period for laboratory investigation, and no reason was found later for altering this choice of a first combination for laboratory study.

This combination was a transformer medium of hot saturated cesium vapor mixed with helium, to be pumped by neodymium glass

lasers at 1.06 μ . All of the experimental work of the contract has been carried out on this single combination of materials.

1.1 Summary Of Previous Contract Reports

Three Technical Summary Reports have already been issued at six month intervals under the present contract. They are identified as follows:

<u>GPL Div. No.</u>	<u>Issue Date</u>	<u>Defense Dept. No.</u>	<u>NASA No.</u>
GPL-A-31-1	17 May 1965	AD-618896	
GPL-A-31-2	22 November 1965	AD-624481	
GPL-A-31-3	25 May 1966	AD-633839	N66-33813

These reports are available to the general public through the Clearinghouse for Federal Scientific and Technical Information, Springfield, Virginia.

The first report was entirely analytical and, after outlining numerous possibilities for different transformer media to be pumped by various primary lasers, dealt chiefly with a design for pumping cyanogen gas monomer molecules, CN, with a battery of Nd glass lasers. This analysis was continued in the second report, with the conclusion that transformer maximum output energy densities of the general order of 1 joule/cm³ in a lms pulse might be attainable with this combination insofar as could be judged from information already existing in the scientific literature.

The principal analytical topic of the second report was a proposed design for pumping metastable nitrogen gas molecules with a battery of Nd glass lasers. The conclusion reached, again limited to analysis based on information already existing in the

literature, was that this combination should indeed act as a transformer laser, but that one could not yet be optimistic about reaching a 1 ms pulse energy output density of 1 joule/cm³, while maintaining good optical quality of the output beam.

During the period covered by the second report, experimental work was begun on the transformer laser concept. The system chosen for first study in the GPL Division laboratory was a Cs₂ plus He molecular vapor medium, pumped by Nd glass laser light. This choice was made because this combination appeared potentially capable of operating satisfactorily at much greater output pulse energy densities than any other, *provided multiple quantum excitation effects did not lead to excessive generation of waste heat in the vapor.* This latter crucial point could only be settled by experimental tests at high irradiation densities.

Techniques for handling cesium in a manner to exclude impurities were tested, and the near infrared molecular absorption spectrum of the vapor at about 280°C was mapped at low dispersion, using a Pyrex glass vapor container. Besides extending the known Cs₂ (A-X) band, centered at 1μ, farther into the infrared than it had ever been observed previously, two entirely new absorption bands were found near 1.13μ and 1.21μ.

In the third report, the existing scientific literature on all the alkali metals was analyzed, in order to be able to estimate and extrapolate those molecular constants of the Cs₂ molecule needed for initial understanding of the behavior to be expected from cesium vapor under strong Nd laser light irradiation.

Experimentally, the Cs_2^+ (A-X) absorption band system was measured under higher dispersion than before, at vapor temperatures up to about 400°C , using containers made of specially corrosion resistant Corning 1720 glass. In this period the hot cesium vapor was also irradiated with 1 ms pulses of 1.06μ Nd glass laser light at a maximum pulse energy of about 0.02 joules. The highest average pulsed beam intensity used was about 80 watts/cm^2 . The amount of Nd light absorbed by the vapor was found to depend strongly on the laser beam intensity, in a manner which made it seem that bleaching of the absorbing transition was occurring.

Fluorescence of the cesium molecules as a result of the absorbed 1.06μ energy was also studied, at various vapor temperatures. Fluorescence throughout the Cs_2^+ (A-X) band was observed, indicating the expected (and desired) collisional transfer of the excited molecular population from those levels excited initially to many other nearby vibrational and rotational levels of the Cs_2^+ A state. In addition, particularly at the higher temperatures, irradiation of the vapor with 1.06μ light caused strong fluorescence in the newly discovered spectral features at 1.13μ and 1.21μ . Apparently, collisions were also transferring excitation energy in a considerable fraction of the molecules from the Cs_2^+ A state to the upper states of these other transitions.

1.2 New Work Covered In This Report

The experimental contract work during the most recent period has been a continuation of studies on the behavior of hot cesium vapor irradiated by 1.06μ Nd glass laser light. Both

atomic and molecular cesium fluorescent emission has been observed at numerous wavelengths, arising from about 5 cm^3 of vapor irradiated with 1 ms pulses containing as much as 8 joules of 1.06μ energy. These investigations have dealt with pure Cs vapor near 350°C , and also with a mixture of Cs saturated at this temperature in about 1 atm of helium gas. The extent to which the vapor absorbed Nd light has also been studied at this new higher irradiation beam intensity.

Attempts were made to detect initial transformer laser action in this system by surrounding the irradiated vapor with a cavity, constructed from a pair of almost confocal concave mirrors. No lasing has been observed from the cesium vapor so far. Lasing at the very start of the pulse may have been blocked by losses within the vapor, or possibly by losses arising from the poor optical quality of the only available 1720 glass containers, or by any of several other possible effects. A vapor container having windows of good quality made of either sapphire or MgO , which are believed to be unattacked by alkali metal vapors up to about 800°C , should give additional information on the problem. Lasing at later times in the pulse should probably not be expected in view of the finding that a probable major decrease in the molecular concentration during the pulse is occurring in all the work so far.

All of this new experimental work will be detailed in Sections 6 - 12 of this report.

Much of the theoretical work of the recent period has consisted of special auxiliary studies on alkali metal vapor

properties needed for the explanation of particular questions which arose in the laboratory work. Some of these are recounted in Section 5 below. Section 4 describes a small amount of the design work on a proposed transformer system of sodium vapor pumped by a battery of ruby lasers which had received extensive analysis under GPL Division funding before the start of the present contract.

A considerable analytical effort was also placed on the search for a suitable gas or vapor transformer medium which could be pumped by a battery of Er glass lasers. As described in Section 3, the most likely *polyatomic* gas, HCN, does not seem completely satisfactory. However, it is believed that a *diatomic* gas, CO at high pressure, could be pumped by Er glass lasers to yield a very high intensity output beam near 1.66μ of excellent optical quality. The CO-Er design concept will be discussed in Section 2 of this report. The description will include repetition of enough details of the transformer laser cyclic process that this concept may be understood by readers who do not have available the previous reports of this series.

2. THE CO-ER GLASS TRANSFORMER LASER CONCEPT

2.1 General Description of Proposed Arrangement

Figure 1 is a schematic diagram of the type of arrangement proposed for a transformer laser assembly. An array of erbium glass pumping lasers, whose output beams do not need to be extremely parallel, feed energy from all directions at about 1.57μ into the transformer medium, which is CO gas at 100 atm pressure and about 100°K . By absorption of this light, a major fraction of the CO molecules is excited to various rotational levels of the ($v = 3$) vibrational level belonging to the ground electronic state. Molecular collisions quickly cause vibrational energy exchanges which will tend to produce a pseudo-Boltzmann distribution of all the molecules among all the vibrational levels of the CO-X electronic state. The collisions will also maintain pseudo-Boltzmann distributions of molecules over the rotational levels belonging to each of the vibrational levels, separately.

In the early stages of a 1 ms pumping pulse, if the pumping is sufficiently intense, the combined effects of energy absorption and collisional redistribution over the molecular energy levels will produce inversions between

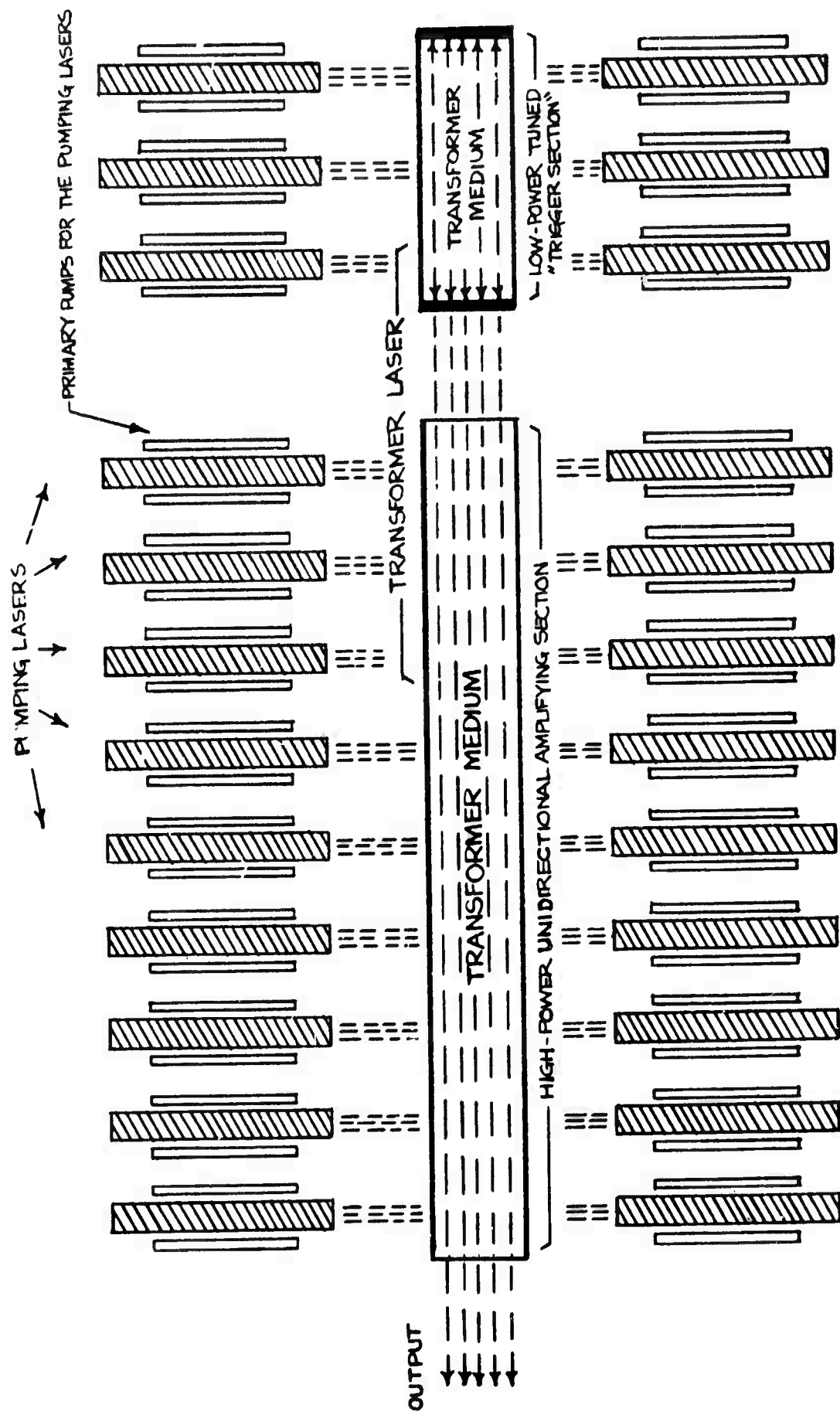


Figure 1
Schematic Diagram for One of Many Simple Transformer Laser Arrangements

many pairs of these levels -- in the manner first proposed by GPL Division in 1963, and which has now become well known from the operation of various gas lasers. Thus, Hocker, Kovacs, Rhodes, Flynn, and Javan (1966) have reported detailed experiments on the development of such collisionally-fed inversions in the CO_2 laser powered by an electric discharge.

The "trigger section" shown at the right side of Figure 1 has a selectively tuned cavity, which causes lasing to begin and to build up preferentially on those of the transitions with inverted populations which will yield output wavelengths most desirable for the system as a whole. These wavelengths are amplified by the main body of the transformer as a once-through travelling wave. The plane wave-front initiated by the trigger section will be amplified in the main section and sent on to the output as a high-energy plane wave, provided there is no waste heat in the gas to create thermal inequalities which would reduce the optical quality of the path. It is precisely because of this latter point that CO is such an extremely desirable transformer medium. Low temperature carbon monoxide gas and nitrogen gas probably have the greatest resistances of any known substances toward wasteful transfer of vibrational

excitation energy into sensible heat by collision. (The possibilities for the use of nitrogen gas in a transformer were surveyed in report GPL A-31-2.)

In the next section the important pumping process will be considered more carefully.

2.2 Pumping CO with Er Glass Lasers

Snitzer and Woodcock (1965) obtained lasing of the Er^{+++} ions in an Er-K-Ba-Na silicate glass at 6480.8 cm^{-1} , or 1.5426μ , with a pulse of about $1/3 \text{ ms}$. Gandy, Ginther, and Weller (1965) used an Er-Li-Mg-Al silicate glass and measured its lasing frequency with a low resolution spectrometer as lying in the range $6580 - 6330 \text{ cm}^{-1}$, with some theoretical reasons for suspecting it to be near 6410 cm^{-1} . They obtained pulses of several μsec duration. As Figure 2 shows, these locations are quite close to the (3-0) vibration-rotation band of $\text{CO}\cdot\text{X}$, whose origin is at 6350.4 cm^{-1} .

The set of molecular constants for $\text{CO}\cdot\text{X}$ recently derived by Patel (1965) agrees very closely with the latest experimental measurements, not only for the low levels but also for levels with as high vibrational quantum number as ($v = 18$). Table 1 gives the location of the first twenty five vibrational levels as calculated from these constants, and Table 2 lists the rotational levels and lines involved

TABLE 1. The Lower Vibrational Levels Of CO·X

<u>v</u>	<u>Vibrational Level Energy</u>
0	0 cm ⁻¹
1	2,143
2	4,260
3	6,351
4	8,415
5	10,452
6	12,464
7	14,449
8	16,409
9	18,342
10	20,250
11	22,132
12	23,987
13	25,818
14	27,622
15	29,402
16	31,155
17	32,884
18	34,587
19	36,264
20	37,916
21	39,544
22	41,147
23	42,724
24	44,276
25	45,804

TABLE 2. Locations of Rotation Levels and Lines
For the CO-X (3-0) Bands

J	Rotation Levels		Band Lines	
	v=0	v=3	P-branch	R-branch
0	0 cm ⁻¹	0 cm ⁻¹		6354 cm ⁻¹
1	4	4	6347 cm ⁻¹	6358
2	12	11	6343	6361
3	23	22	6339	6365
4	39	37	6334	6368
5	58	56	6330	6371
6	81	79	6326	6374
7	108	105	6321	6377
8	138	135	6317	6380
9	173	168	6312	6383
10	211	206	6307	6386
11	254	247	6302	6388
12	300	292	6297	6391
13	350	340	6292	6393
14	404	393	6287	6394
15	461	448	6282	6398
16	523	508	6275	6400
17	588	572	6271	6402
18	657	639	6265	6403
19	730	710	6260	6405
20	806	784	6254	6407
21	887	863	6248	6408
22	971	945	6242	6410
23	1059	1030	6236	6411
24	1151	1120	6230	6412
25	1247	1213	6223	6413
26	1347	1310	6217	6414
27	1450	1410	6210	6415
28	1557	1515	6204	6416
29	1668	1622	6197	6416
30	1783	1734	6190	6417
31	1901	1849	6183	6417
32	2023	1968	6176	6418
33	2149	2091	6169	6418
34	2279	2217	6162	6418
35	2413	2347	6154	6418
36	2550	2480	6147	6418
37	2691	2617	6140	6417
38	2836	2758	6132	6417
39	2984	2902	6124	6416
40	3137	3050	6116	6416
41	3292	3202	6108	6415
42	3452	3357	6100	6414
43	3616	3516	6092	6413
44	3783	3679	6084	6412
45	3953	3845	6076	6411
46	4128	4014	6067	6410
47	4306	4188	6059	6409
48	4488	4364	6050	6407
49	4673	4545	6041	6406
50	4863	4729	6033	

in the (3-0) band, all to the nearest cm^{-1} . The high precision available from Patel's constants is not actually needed in the present application, since at 100 atm and 100°K each line will be about 12 cm^{-1} broad.

It is uncertain what alteration, if any, needs to be made to either of the existing Er glass lasers to render its output light adequately absorbable by CO gas. Figure 2 shows that the absorption band of the type of glass used by Snitzer and Woodcock completely overlaps the R branch of the CO absorption, and *presumably* lasing could be promoted to some degree anywhere within that band of the glass. Regardless of whether or not Gandy, Ginther, and Weller's glass lased 70 cm^{-1} closer to the CO band than did the other glass, it seems probable that some glass could be found which would shift the emission frequency this much and more. Thus, Maurer (1963) found as much as 110 cm^{-1} difference between the centers of the 1.06μ Nd absorption bands in various kinds of Nd-bearing glasses, and there is 100 cm^{-1} difference between the Nd lasing frequency in silicate glass measured by Snitzer (1965) and the Nd lasing frequency in BeF_2 glass measured by Petrovsky, et al (1966). The maps by Dieke et al (1961) show that crystal field splitting in the lower level of the Er lasing transition is fully as broad as that for the Nd 1.06μ lasing transition

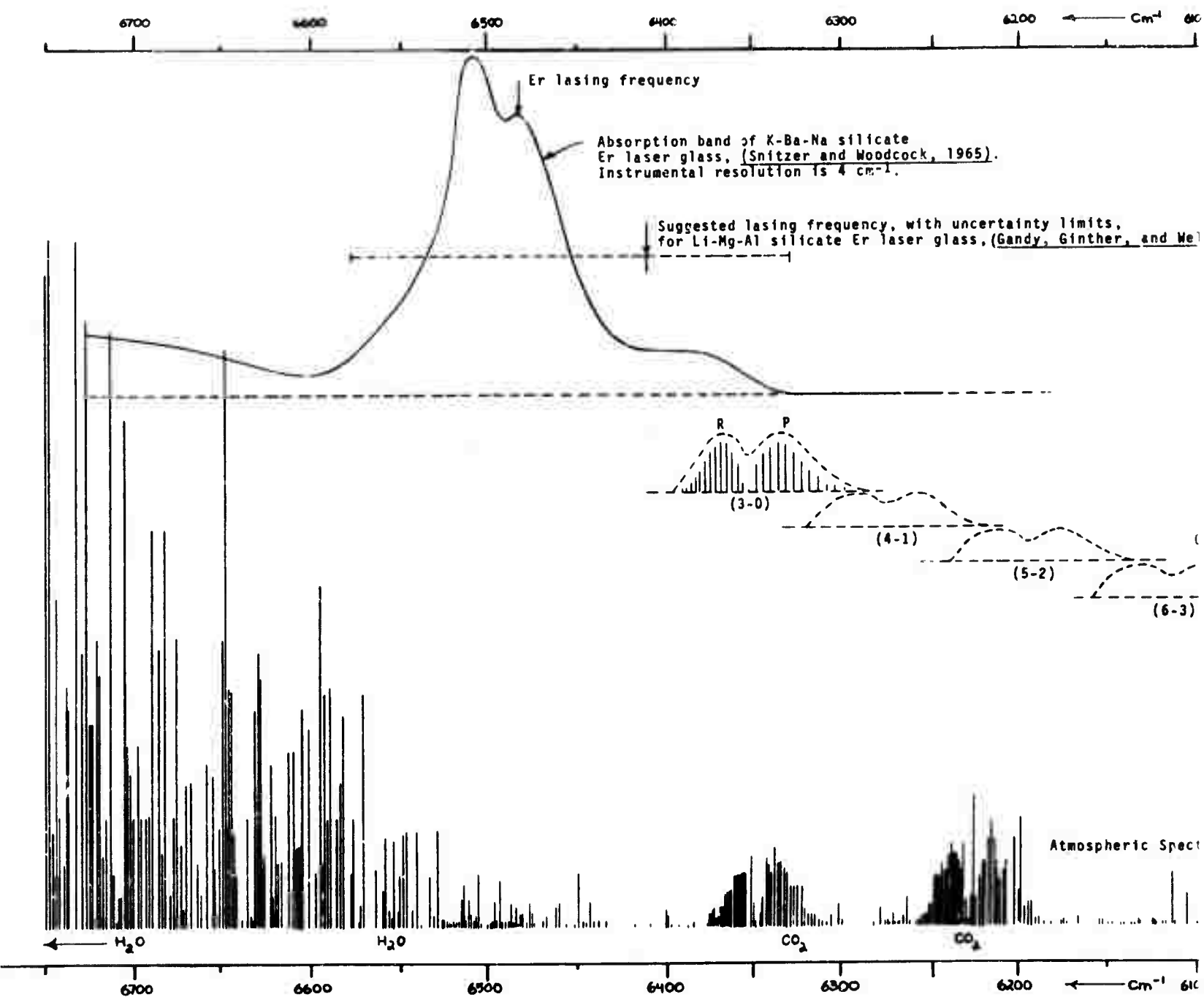
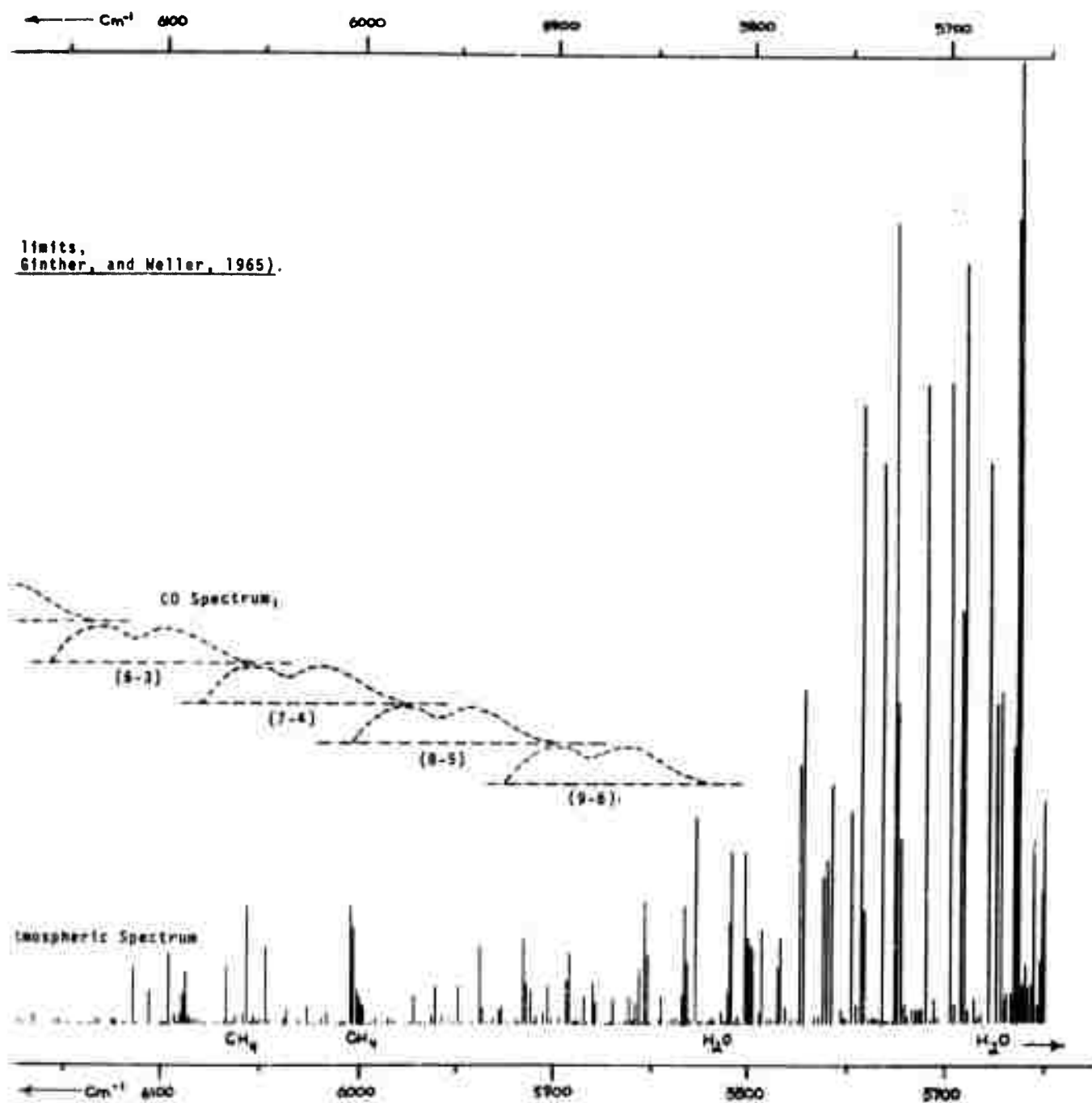


Figure 2. Location of Er glass 1



limits.
Ginther, and Meller, 1965).

Location of the $\Delta v = 3$ bands of CO with respect to the
Er glass laser spectra and the atmospheric absorption lines.

B

in the same crystal. This is one indication that these two states are equally susceptible to the influence of neighboring atoms in a solid.

Let us assume that the output spectra from a battery of suitable Er glass lasers can be made to cover a region a few wavenumbers wide, centered near the maximum R-branch intensity of the (3-0) band at 100°K, near 6370 cm⁻¹ or 1.5694μ. For the beginning of the pumping flash, the absorption coefficient of the gas for this light can be determined from the work of Young (1966), who found $k_0 \approx 1.5 \times 10^{-4}$ cm⁻¹/amagat for this region in CO at 300°K. (This unit is equivalent to the unit labelled "cm⁻² atm⁻¹ at STP" by some writers. One amagat = 2.69 x 10¹⁹ particles/cm³.) His results for higher temperatures imply that extrapolation back down to 100°K would lead to $k_0 \approx 1.0 \times 10^{-4}$ cm⁻¹/amagat near 6370 cm⁻¹. The number density of gas at 100 atm and 100°K is (100 x 273/100) = 273 amagat. The absorption coefficient of the gas at the beginning of pumping would then be $k_0 \approx 2.7 \times 10^{-2}$ cm⁻¹. In a single pass across a transformer tube width of 10 cm, for example, approximately the fraction

$$\left(1 - \frac{I}{I_0}\right) \approx \left(1 - e^{-2.7 \times 10^{-2} \times 10}\right) \approx 24\%$$

of the pump light would be absorbed.

It would seem, therefore, that even in the later stages of a power pulse, when the transitions would be partially bleached, the number of passes required for rapid absorption of the pumping energy would not be excessive. That is, if the CO volume was placed within the resonant cavity of each Er glass laser, through the use of TIR prism reflectors, the fraction of the pumping energy which must be absorbed by the various pieces of glass should remain acceptable throughout the pulse.

2.3 Choice of the Lasing Wavelength*

In order to reach high output pulse energy levels with a CO-Er transformer laser it would probably be desirable to lase in transitions requiring less radiation field strength for reaching a very short stimulated emission lifetime than do the transitions of the (3-0) band. For space applications of this device, it would probably be easiest to lase in various P-branch lines of the (3-2) band near 4.7μ . The spontaneous emission lifetime of the upper levels for this band is relatively short, and so it is correspondingly easier to produce a high probability for stimulated emission. For ground-based applications it would be desirable to use wavelengths outside of the strong atmospheric absorption bands.

* Much of the information about the CO molecule used in sections 2.3 - 2.6 was developed during a detailed analysis of a CO-CaF₂:Dy²⁺ transformer laser concept carried out by GPL Division with Company funds before the start of the present contract.

Figure 2 diagrams the atmospheric absorptions in the neighborhood of the (3-0) band, and of some of the other members of the ($\Delta v = -3$) series, from the data of Mohler (1955). The higher members of this series have shorter and shorter spontaneous emission lifetimes. As shown in various texts, such as Penner (1959), the squared matrix element for transitions between the rotation levels of ($v=n+s$) and the rotation levels of ($v=n$), in a diatomic molecule electronic state having vibrational anharmonicity constant $\omega_e x_e$, is approximately proportional to

$$x_e^{s-1} \cdot \frac{(n+s)!}{s^2 n!}.$$

Since the spontaneous emission lifetime is proportional to the reciprocal of this expression, one may start with the well known value of $\tau_{\text{spont}} = 33 \text{ ms}$ for the (1-0) band (Young and Eachus (1966)), and obtain the results in Table 3 by proportion.

TABLE 3

Spontaneous Emission Lifetimes of
Third Harmonic IR Bands of CO

<u>Band</u>	<u>τ_{spont}</u>	
(3-0)	300	sec.
(4-1)	75	"
(5-2)	30	"
(6-3)	15	"
(7-4)	8.6	"
(8-5)	5.3	"
(9-6)	3.6	"

It would probably be most desirable to lase in the lower P-branch lines of the (7-4) band for ground-based applications. The atmospheric absorption is quite weak there, and the spontaneous lifetime of about 9 sec for this band is no longer than in existing satisfactory lasers.

If the trigger section of the transformer assembly does not provide a trigger wave at any of the exact wave-numbers of the atmospheric absorption lines -- perhaps because a chamber of concentrated CH_4 , H_2O , and CO_2 vapors within its cavity prevents lasing build-up at these wave-numbers -- then these locations will not be stimulated in the amplifying section and the transformer output beam energy will not be absorbable in the main parts of any of the spectrum lines of the atmosphere.

2.4 Collisional Energy Transfers

Carbon monoxide molecules initially in some of the rotational levels of ($v=0$) will absorb the Er glass laser light and be raised to corresponding rotational levels of ($v=3$). Thus, Table 4 shows that if the Er laser spectrum employed overlaps merely the R(6) to R(2) lines near 6370 cm^{-1} , about 64% of the molecules in ($v=0$) at any instant in which Boltzmann rotational equilibrium obtains will be in a position to absorb the pump light. Molecular collisions

TABLE 4

Distribution of the population of CO·X molecules in ($v=0$) among the rotational levels of that vibration state when the gas is in rotational thermal equilibrium at 100°K, (calculated from the standard formulas, as quoted by Herzberg (1950), for example.)

<u>J</u>	<u>F_J</u>	
0	2.74%	
1	7.79%	
2	11.6 %	} These sum to 64% of total molecules in ($v = 0$)
3	13.8 %	
4	14.2 %	
5	13.2 %	
6	11.2 %	
7	8.73%	
8	6.36%	
9	4.32%	
10	2.74%	
11	1.63%	
12	0.91%	
13	0.48%	
14	0.24%	
15	0.11%	
16	0.049%	
17	0.020%	
18	0.003%	
'	'	
'	'	
'	'	

will tend to maintain as close as possible to a Boltzmann rotational equilibrium in both ($v=0$) and ($v=3$) at all times -- since a carbon monoxide molecule in CO at 100 atm and 100°K experiences about 1.1×10^{12} collisions per sec (Gaydon and Wolfhard, 1960), and it is well established that practically every collision in CO causes changes in the rotational quantum numbers. (See, for example, Herzfeld and Litovitz, 1959).

As soon as an important fraction of the molecules have been moved up to ($v=3$) by intense pumping, some of the collisions will begin to cause "vibrational exchange" of excitation energy between colliding molecules. Thus, two ($v=3$) molecules may sometimes emerge from a collision as one ($v=2$) molecule and one ($v=4$) molecule, having transferred a vibrational quantum of energy from one of the molecules to the other. In this fashion the entire vibrational ladder will eventually get filled up, with the relative population distribution following fairly close to a general Boltzmann type of curve. This will approximately follow a formula in which the average number of vibrational quanta present in the vapor per molecule, \bar{v} , will replace the expression kT in the usual Boltzmann exponential equation (Shuler, 1960).

The probability of such vibrational exchanges upon collision depends on temperature and on the energy discrepancy between the different transitions made by the two colliding molecules. Table 1 shows that a CO·X molecule dropping from (v=3) to (v=2) will lose about 2091 cm^{-1} of vibrational energy, while the other molecule upon rising from (v=3) to (v=4) will take up only about 2064 cm^{-1} of vibrational energy. The difference will go into translational energy. The magnitude of the energy discrepancy ΔE cannot be fixed precisely, since one cannot tell what changes in rotational energy may also be occurring in the same collision, but the rotational steps are always fairly small. Callear (1962) surveyed the experimental and theoretical evidence on such exchanges in small diatomic molecules and decided that at room temperature one in every 1,000 to 10,000 collisions produces such an exchange of $\Delta v = \pm 1$ whenever the vibrational contribution to ΔE is less than about 100 cm^{-1} , and the rotational contribution to ΔE is not large. (Exchanges with greater Δv than ± 1 are more rare at every temperature and every region of ΔE .) From the theory of Schwartz, Slawsky, and Herzfeld (1952) -- a classic paper which is customarily referred to as SSH -- the probability of the process should be approximately proportional to the absolute temperature. Therefore, at

100°K at least $Z = 15,000$ collisions might be required per exchange process.

With the collision rate between all kinds of CO molecules being around 10^{12} under the conditions considered here, it follows that molecules will certainly be spread over many vibrational levels within less than a μsec after the first considerable number have been pumped up to ($v=3$). However, the very high levels will still remain sparsely populated in a Boltzmann distribution, unless intense pumping is continued *without* any lasing. If molecules are being lased downward from ($v=7$) just as rapidly as they are being pumped upward from ($v=0$), the equilibrium vibrational distribution at all but the most extreme power levels would doubtless contain negligible populations above about ($v=20$), say.

Simple arithmetic applied to the rotational and vibrational distributions will show that inversion occurs for high members of the P-branch of the (7-4) band, for example, long before the pumping transitions in the R-branch of (3-0) have been saturated. Conditions suitable for lasing can thus be attained by strong Er glass laser pumping. The pump-collide-lase-collide-pump cycle may be traversed by a given molecule repeatedly in the course of a 1 ms pulse, and this cycle is the basis of the transformer laser concept being studied under this contract.

2.5 Resistance of CO to Waste Heat Production

The rotation-shifting collisions and the vibration-exchanging collisions discussed in the last section will always involve transferring very small amounts of energy both into and out of the translational energy reservoir of the system -- the sensible heat content which determines the gas density behavior. However, preliminary analysis indicates that a good energy balance may be maintained in this respect, so that two types of collisions will not produce appreciable *net* waste heat.

A different type of collision, which is to be strongly avoided in this transformer design, is one which causes vibration-to-translation relaxation. Then, a whole vibrational quantum would be immediately converted to sensible heat. The greatest reason for special interest in CO laser transformers is that this type of collision is very rare in carbon monoxide, particularly at low temperatures. If τ_a be defined as the time for one eth of a quantity of vibrational energy to degrade to translational energy by collisions in a gas at 1 atm pressure, the SSH paper showed theoretically that, for any choice of gas, $\log \tau_a \sim T^{-1/3}$ at high absolute temperatures. At lower temperatures a curve of $\log \tau_a$ vs. $T^{-1/3}$ would be expected to have a decreasing slope away from the straight line. At other pressures than 1 atm, τ_a should be inversely proportional to P. Dickens and Ripamonti (1961)

collected data for a wide variety of molecular types and showed that SSH theory was quite well validated. Millikan and White (1963a) were also able to systematize a mass of experimental data with this one relation.

In the case of CO, Hooker and Millikan (1963) displayed a large amount of data which fit the high temperature SSH curve very nicely, as shown by Figure 3. When the straight line is extrapolated at decreasing slope through the recent *room temperature* values of $\tau_a = 0.8$ sec from Ferguson and Read (1965) and $\tau_a > 0.2$ sec from Millikan (1963), a very reasonable value for τ_a for CO at 100°K should be about 3 sec. It may be noted that experimental measurements of τ_a for CO are customarily found to be in error on the low side, if any, rather than being too high -- because it is hard to keep out impurities which relax much faster than CO. (See the survey of this matter by Cottrell and McCoubrey, 1961.)

At a pressure of 100 atm this would mean a vibration-to-translation relaxation time of about 30 ms.

The vibrational steps of CO are so large, $\sim 2100\text{ cm}^{-1}$, that in practically all the experiments which were used in drawing the SSH curve for this molecule only ($v=1$) and ($v=0$) had any appreciable population. That is, the experimental

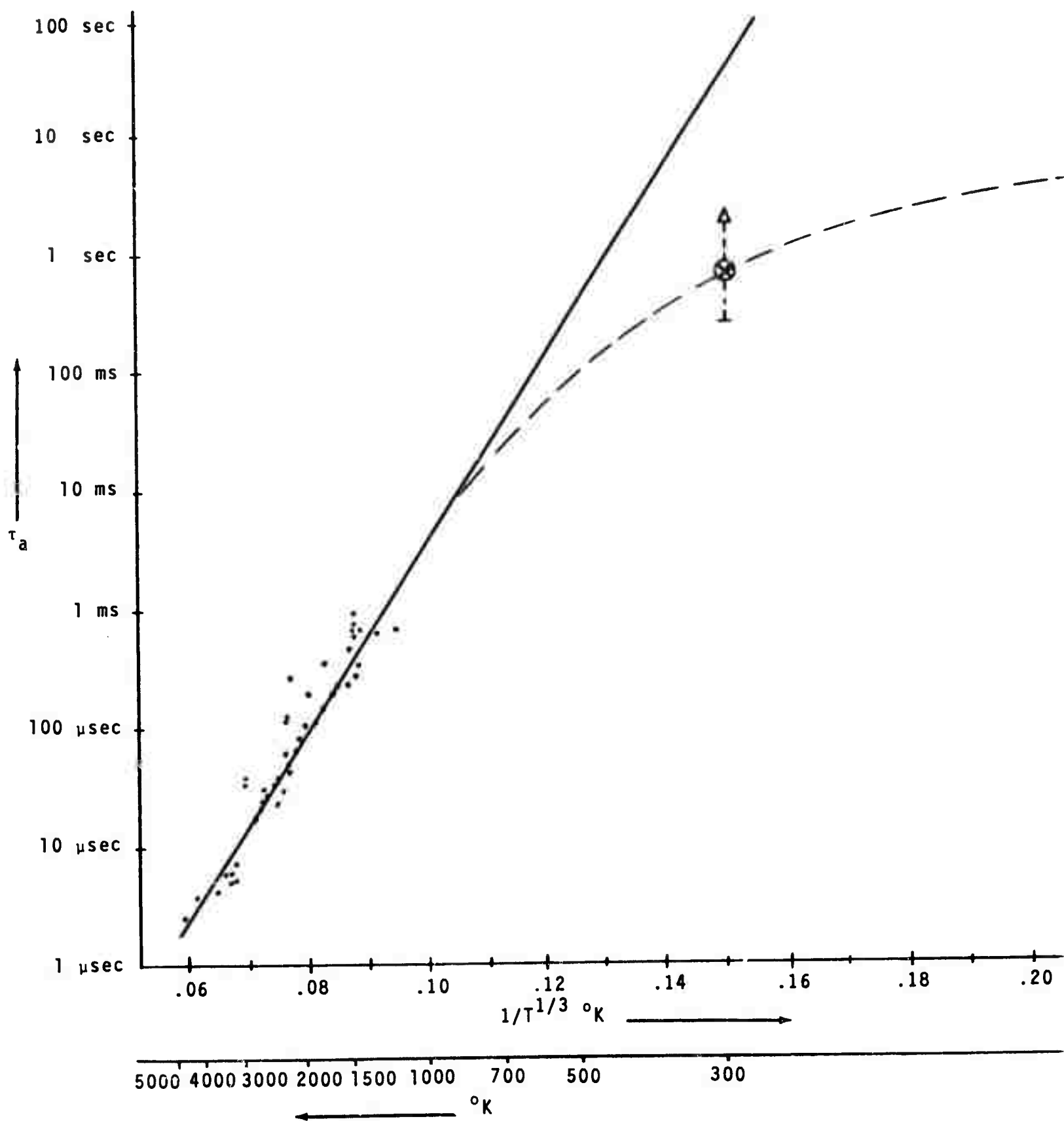
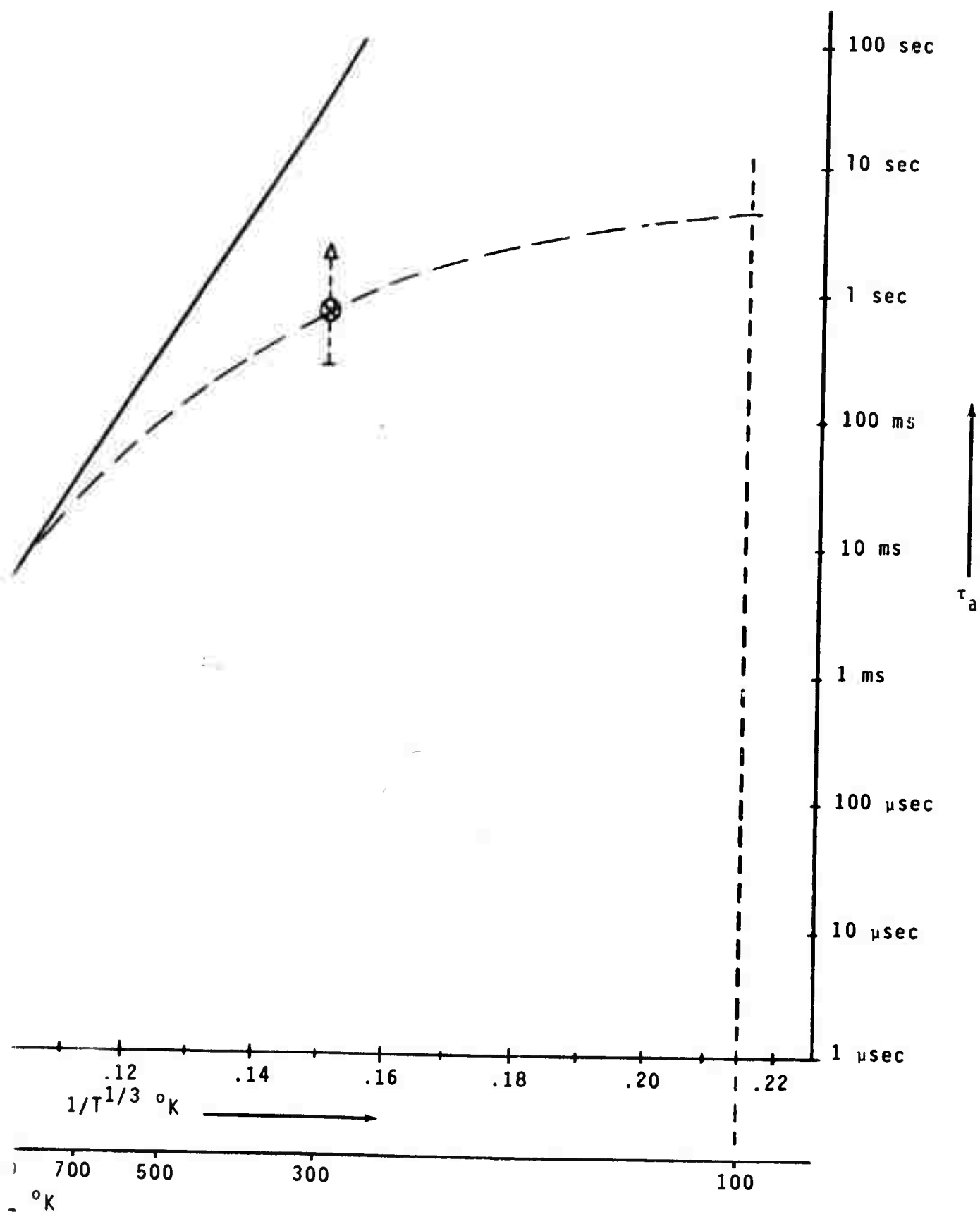


Figure 3. Vibration-to-translation energy relaxation time at one atmosphere pressure for diagram is adapted from Hooker and Millikan (1963b), with dashed line extrapolation sent author to pass through the room temperature data points of Millikan (1963) and Ferguson and Read (1965) (vertical arrow).

A



energy relaxation time at one atmosphere pressure for pure CO. This is from Miller and Millikan (1963b), with dashed line extrapolation added by present author (the room temperature data points of Millikan (1963) (cross) and (vertical arrow)).

relaxation time called τ_a was actually more nearly the time $\tau_{1 \rightarrow 0}$ for simply dropping down out of the ($v=1$) level. Such a process would then occur in only one out of about 3×10^{10} collisions under the conditions considered here.

According to SSH theory, collisional jumps of $\Delta v = 1$ should be more frequent among the higher vibrational levels, with the probability increasing roughly in a proportion to v . In a heavily pumped gas with high steps on the ladder populated by the vibrational exchange collisions which are expected in the transformer laser, one should inquire how high the molecules could climb before appreciable vibration-to-translation heat would appear because of high level collisions, within the time scale of a 1 ms pulse. If under the proposed conditions $\tau_{1 \rightarrow 0} \approx 30$ ms, then $\tau_{30 \rightarrow 29}$ would be about 1 ms. It would therefore seem that this transformer laser would not develop appreciable waste heat from such a cause until extremely high output energy density levels were reached.

2.6 The Molecular Heat Balance

Another important point regarding the sensible heat balance for any laser transformer design involves the inevitable discrepancy between the quantum energy of the pumping input and the quantum energy of the lasing output -- the latter

always being smaller since, as was demonstrated in report GPL A-31-2, inversion will occur only in transitions lying on the long wavelength side of the pumping transition. In the CO-Er case, if we pump near the R(4) line of the (3-0) band at about 6370 cm^{-1} and lase near the P(4) line of (7-4) near 6020 cm^{-1} , there is a 350 cm^{-1} energy discrepancy (or 5.5% of the input energy) which is left behind in the gas for each output quantum emitted.

The most obvious way to balance this out is by adjustment of the ratio between the output beam intensity and the *fluorescence* loss rate from the vapor -- through variation of the trigger flux intensity. The strongest fluorescence will always come from the $\Delta v = -1$ series of transitions, since $\tau_{\text{spont}} \approx 33 \text{ ms}$ for the (1-0) band and decreases approximately in inverse proportion to ν in such a series, reaching about 1 ms near the (30-29) band.

Each emergent fluorescent quantum of a line near the center of the (1-0) band, for example, will carry away about 2150 cm^{-1} of energy, or more than enough to compensate for the input-output discrepancy of six output quanta. When the fluorescence loss from the vapor equals 5.5% of the pumping input, no net sensible heat will be left behind in the vapor during the pulse from these processes. A planned efficiency loss for the entire system of 5.5% for this cause is not excessive.

It may be noted that radiation trapping will not slow down the escape from the vapor volume of fluorescence from the P-branch lines of the $\Delta v = -1$ bands. These will be inverted whenever the P-branch of the $\Delta v = -3$ bands are in a lasing condition, and so will actually be superradiant.

One other point on a slightly different subject: preliminary calculations show that no more than about 1% of the total expected input pump energy during a pulse will have gone into the initial process of filling up the vibrational ladder population, at the time when strong inversion first appears in the P-branch of (7-4). Such a 1% efficiency loss to the system from this cause can also be tolerated. The figure also indicates that not too much engineering trouble will be experienced in recirculating the gas and dumping this vibrationally stored energy into a heat exchanger, when it has converted itself into sensible heat through relaxing collisions long after the pulse is over.

The next section now shifts to a brief consideration of a *polyatomic* molecular gas medium, where the vibrational relaxation process is probably far less favorable than with CO.

3. POLYATOMIC MOLECULES IN IR TRANSFORMERS

The studies in this report series so far have been concerned with diatomic molecules as vapor media for transformer lasers. One of the simplest of the polyatomic possibilities will now be discussed.

3.1 The HCN-Er Glass Possibility

As mentioned before, the laser emission wavelength observed by Snitzer and Woodcock (1965) for erbium in a typical glass at room temperature is 1.5426μ , which is 6480.8 cm^{-1} . This is very close to the P(12) line of the (002 - 000) rotation-vibration absorption band of the HCN molecule, as may be calculated from the measurements of Rank, Guenther, Shearer, and Wiggins (1957). Exact coincidence could easily be obtained by pressurizing the HCN at about 2 atm to broaden its lines, as shown by the data of Pigott and Rank (1957), or by changing the Er laser temperature or the glass composition.

This 1.5μ absorption band is the second harmonic of the ν_3 fundamental vibration of HCN, whose frequency corresponds to 3312 cm^{-1} . Rank, Skorinko, Eastman, and Wiggins (1960). If this were the single vibration frequency of a diatomic molecule, it would be highly resistant to collisional vibration-to-translation relaxation at usual temperatures as is CO. However, as Rice (1964) remarks, in polyatomic molecules there is "little evidence of any hindrance to the free transfer of energy among all the vibrations". The HCN vibration of lowest energy

is one of the components of ν_2 near 714 cm^{-1} . In a possibly comparable case*, Yardley and Moore (1966) found that a CH_4 molecule excited to its 3018 cm^{-1} vibrational level transferred, probably by vibrational exchange processes, to its 1306 cm^{-1} vibrational mode after only 60 collisions of CH_4 against CH_4 .

If the transformer medium were to consist of HCN gas only somewhat above room temperature (the boiling point is 26°C), kT would be as large as about 250 cm^{-1} . Vibration-to-translation relaxation from the 714 cm^{-1} level would then have a fairly high probability. Molecular vibration states only become relatively immune to collisional relaxation when the energy to be transferred is many times kT , as is described by the SSH theory and found experimentally. Any major amount of sensible heat developed in the gas during the power pulse by a relaxation process would cause serious deterioration of the optical quality of the transformer medium.

One might consider dropping the vapor temperature to about -50°C , where kT is about 150 cm^{-1} . The relaxation rate from the 714 cm^{-1} HCN vibrational level would then be much reduced. However, at such a temperature the saturated pressure of HCN vapor over the solid is only about 1 cm Hg, and since the P(12) line originates from a rotational level about 245 cm^{-1} above the ground, not many molecules would

* Although, see the data on one level of CO_2 in the next section, for which vibrational transfer is very much slower than in CH_4 and most other hydrogenic molecules.

be available to absorb the pump light, in contrast to the 100 atm CO case of the last section. Since the spontaneous lifetime of this HCN band is also probably as long as a few seconds, attainment of high transformer pulse energy densities would seem to require excessive pumping and lasing radiation fluxes.

The situation is rendered even more doubtful by the existence of various polymers in HCN gas everywhere below about 400°C. Thus, Felsing and Drake (1936) found that near room temperature the HCN vapor pressure curve departed from that expected for an ideal monomer gas by about 7%. Simple dimers are probably occurring, but Pauling (1960) has shown that $(\text{HCN})_3$ should be even more stable than $(\text{HCN})_2$, and there has been considerable speculation that the tetramer may also be present -- as a square ring configuration. By comparison with the vibrational frequencies of other complex molecules (see, for example, Amer. Inst. of Phys. "Handbook of Physics"), it seems likely that all of these polymers would have at least one vibrational energy level as low as 300 cm^{-1} or less, and so be very susceptible to collisions producing waste heat.

3.2 The Polyatomic Situation in General

The above notes have by no means really disposed of HCN-Er as a transformer laser combination. They merely point up some of the intricate questions which will be involved with

any polyatomic molecules. A considerable amount of analysis and, of course, experimentation will be required to find out whether there is some molecule where vibration-to-translation relaxation, for example, will not be a problem.

Also, the contract work so far has dealt solely with the use of 1 ms pumping and lasing pulses. The applications for such a device do not exhaust the field. For applications which demand a 1 μ sec pulse or shorter, compromises might be made in the various parameters so that the relaxation heat did not get into the translational form until after the pulse was over. After the pulse the optical quality of the medium is of no importance, and the gas can simply be circulated through a heat exchanger and fresh isothermal gas brought in for the next pulse.

The possible use of an additive molecule in the gas medium, with which a simultaneous compensating molecular refrigeration process might be carried on, by means of an auxiliary laser pump, is another field which has not been explored.

It is sometimes mentioned that the CO_2 gas laser now operates nicely with a polyatomic molecule; and in fact with pure CO_2 the output power is actually limited by the slowness of relaxation of the lowest vibrational level -- so much so that H_2O is often added to cause more frequent relaxing collisions.

However, this medium is being operated at low pressure. If operated at pressures greater than 1 atm, as would be necessary for large enough populations to reach a high transformer energy pulse density range, the CO_2 relaxation rate would indeed produce too much sensible heat per millisecond to be tolerated. Thus, Wittman (1962) found from experiments that about 5×10^4 collisions in pure CO_2 near room temperature are needed to relax the vibrational energy to translation from a group of molecules placed in the first ν_2 level of CO_2 , which is the lower level of the lasing transition. And Herzfeld (1962) calculated theoretically that about 1.3×10^5 collisions at 300°K would suffice to relax molecules from the first ν_3 level, which is the upper level of the lasing transition. Slobodskaya (1948) measured 6×10^4 collisions for the latter figure, and Hurle and Gaydon (1959) found 8×10^4 , although both experiments are open to some question. These numbers are to be compared with the 10^7 collisions which a CO_2 molecule in pure gas at 15°C and 1 atm pressure experiences each millisecond (Kennard, 1938).

4. NOTES ON THE Na₂-RUBY TRANSFORMER COMBINATION

Previous to the initiation of the present contract, GPL Division with its own funds carried out considerable analysis of the possibilities for a sodium vapor laser transformer pumped in the Na₂·(A-X) band system by a battery of ruby primary lasers. The sodium vapor would be saturated at 500°C in 20 atm of He. A small amount of the information developed has been somewhat codified under this contract and is presented here for general information. The analysis, as based on all experimental information so far available in the scientific literature, indicates considerable likelihood that this combination could yield a very high power output beam in the range 7000Å-8000Å, with good optical quality. However, experimental checking at this laboratory of some of the still unknown factors in the behavior of sodium vapor under intense irradiation is not yet underway at this date.

4.1 Location of the (A-X) System and of Its Neighbors

The red band system Na₂·(A-X), which has been known for almost 100 years, lies in the range from around 5500Å to 8150Å, or from the vicinity of 18,200 cm⁻¹ to 12,300 cm⁻¹, being rather sharply bounded on both sides. It is a simple $1_{\Sigma}-1_{\Sigma}$ system with each band having one P and one R branch, degraded to the red, with a single head in the R branch very near the origin.*

*Loomis and Nile (1928) give reasons to expect the bands to change appearance and degrade to the violet near 8000Å, but no rotational structure near this infrared edge has yet been resolved.

The molecular constants are compiled in the Herzberg (1950) book. With the usual formulas, these constants should permit calculation of the wavenumber of any line in the known system. However, for very few of the bands have many rotation line positions actually been measured with much precision.

It has long been known that various individual rotation lines spread periodically throughout this system are associated with rotation of the plane of polarization of a light beam traversing the vapor at wavelengths immediately adjacent to them, when the vapor is in a strong magnetic field. Several suggestions were made that this "magnetic rotation spectrum" could be due to perturbations of certain of the upper rotational levels, arising from periodic close coincidences with the rotational levels of another otherwise invisible state threading through $\text{Na}_2 \cdot \text{A}$. This explanation was finally elaborated in some detail by Carroll (1937). A triplet electronic state ($a^3 \Pi_{0u}^+$) lying somewhat below state A has been indicated as the probable source of the perturbation. The selection rule forbidding single-triplet transitions in light molecules prevents observation in absorption of either this state or the other multiplet components $^3 \Pi_{0u}^-$, $^3 \Pi_{1u}$, and $^3 \Pi_{2u}$ which must lie adjacent to it. The individual perturbed levels would doubtless show small wavenumber shifts from their simple formula positions, but these have not yet been measured. From the effect upon

state A, molecular constants were deduced by Carroll for the state ($a^3\Pi_{0u}^+$) as $\omega_e \approx 145 \text{ cm}^{-1}$ and $B_e \approx 0.140 \text{ cm}^{-1}$.

Figure 4 displays the available information* on the potential energy curves, etc., as well as some additional speculations.

*Sources of data for Figure 4 in addition to the compilation in Herzberg's book, are the following:

State X potential curve - solid line: Davies, Mason, and Munn (1965)

" " " " - dashed line: Singh and Rai (1965)

States A, B, and C potential curves - solid line: Singh and Rai

" A and B " " - dashed line: King and Van Vleck (1939)

" X, A, and C " " - lines of circles: Extrapolations

by the present writer. Singh and Rai, and Barrow, Travis, and Wright (1960), disagree on the dissociation limit for state C.

State X dissociation energy: Barrow (1961)

Lower state $3\Sigma_u^+$ potential curve: Davies, Mason, and Munn.

Atomic level separations: Moore (1949)

States $3\Pi_u$, $3\Sigma_g^+$, $1\Pi_g$, $3\Sigma_u^+$, and $3\Pi_g$ arising from (3s + 3p):

Curves sketched roughly from the schematically suggested curves of Mulliken (1932). There is a certain amount of evidence deducible from experiment that the labels $3\Sigma_g^+$ and $3\Sigma_u^+$ might well be interchanged, but Mulliken's assignments seem more reasonable from the theoretical viewpoint.

Energy and classification of state E: Barrow, Travis and Wright.

Energy levels of states D, E, and F are known, but the potential curves shown are merely sketched schematically by the present writer.

The dashed line curves for all other states derived from (3s+4s), (3s+3d), and (3s+4p) are likewise merely schematic sketches.

The dashed curve shown for the state $1\Sigma_g^+$ has been somewhat arbitrarily drawn parallel to the lower $3\Sigma_u$ repulsive curve. However, this places three $1\Sigma_g^+$ states with curves near the region 3.5\AA and $28,000 \text{ cm}^{-1}$, and they will probably interact with each other. The lines of circles indicate a possible "repulsion" between those states, which will mix their properties, as suggested by Prof. D.R. Herschbach, a Consultant for this contract.

Population distributions for vibrational levels of states X and A in Boltzmann equilibrium at 500°C shown at lower left were calculated by the usual formula from the known level locations.

The line of crosses is plotted at $14,400 \text{ cm}^{-1}$ above the state A curve to show the first effect of absorption of a second ruby laser light quantum by a Na_2 molecule which had already been pumped up to state A.

The line of crosses plotted at ($X+16,960 \text{ cm}^{-1}$) shows the first effect of atomic D line absorption by a ground state molecule.

The region labelled "IR head of heads" indicates the probable range of closest approach of the X and A curves, which would produce the fairly sharp edge of the (A-X) system observed near $12,300 \text{ cm}^{-1}$ by Loomis and Niles (1928).

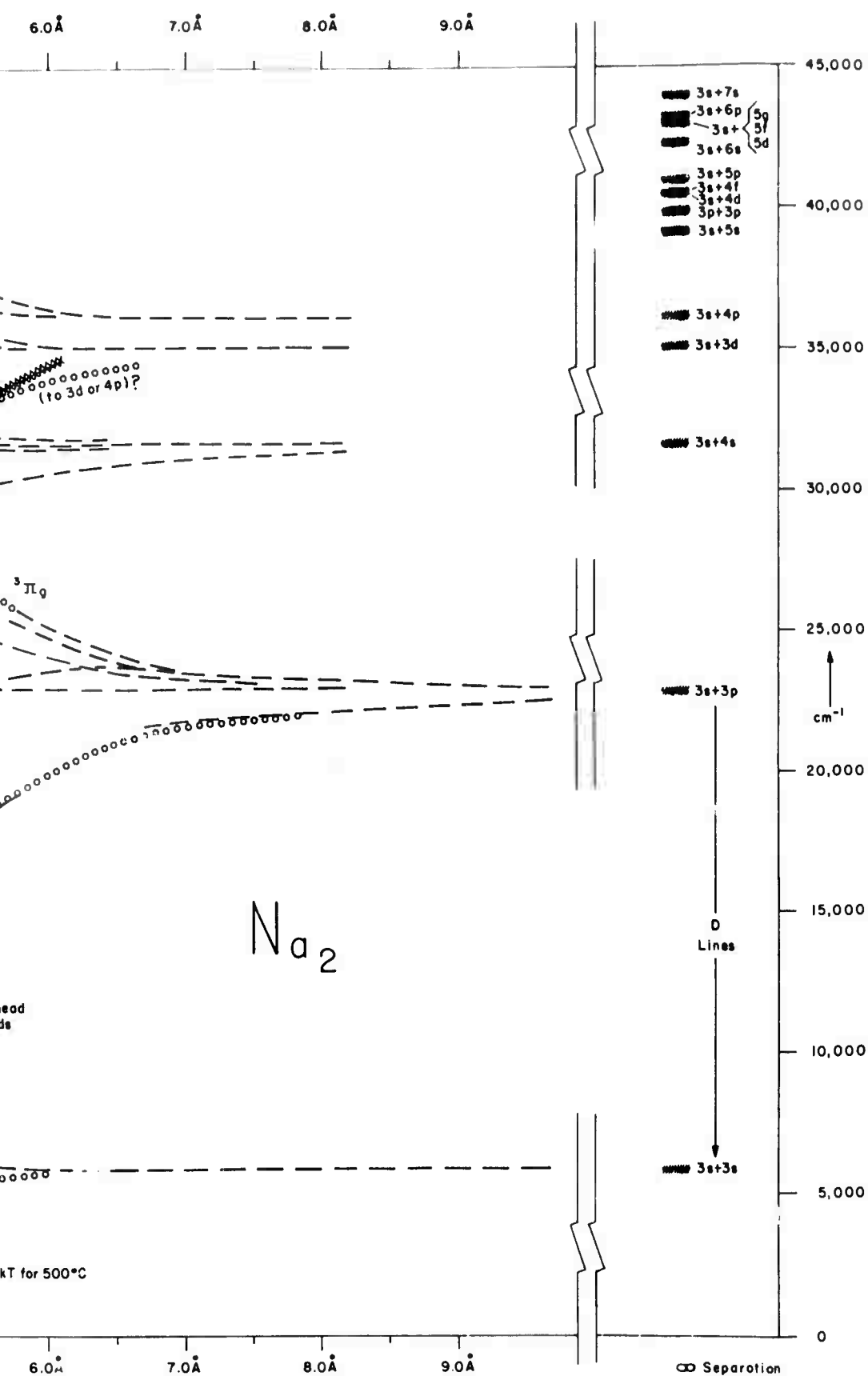


Fig. 4. Energy diagram for the Na_2 molecule. Sources of data, and explanations, are given in a footnote in the text.

The (B-X) band system lies in the blue-green region, $\sim 4450\text{\AA}$ to $\sim 5500\text{\AA}$, or $\sim 22,500\text{ cm}^{-1}$ to $\sim 18,200\text{ cm}^{-1}$. It has been investigated by numerous workers. Some 6000 lines are observable in this system.

The ultraviolet absorption band systems (C-X), (D-X), and higher, have been analyzed as to vibrational structure, but their assignment to the various dissociation limits is uncertain.

4.2 Calculated Band Origins for (A-X)

Table 5 gives a few experimental relative intensity estimates and lists the wavenumbers of band origins of the (A-X) system, as calculated from the molecular constants quoted by Herzberg, for all bands detected wholly or partly, either in absorption or emission or by their magnetic rotation effects, by Wood and Galt (1911) with identifications from Uchida (1932), by Fredrickson and Watson (1927), and/or by Fredrickson and Stannard (1933). The many other magnetic rotation lines measured by Wood and Hackett (1909) doubtless belong to a number of additional bands in the $17,000 - 14,000\text{ cm}^{-1}$ region, but their quantum numbers have not yet been identified. A further unresolved band group near $12,500\text{ cm}^{-1}$ was recorded in emission by Hamada (1933).

Wavenumbers of all band heads will be about $1-2\text{ cm}^{-1}$ greater than those of the band origins listed in Table 5.


Table 5. CALCULATED WAVENUMBERS OF ORIGINS FOR ALL OBSERVED (A-X) BANDS OF Na₂

ν_A	ν_X	0	1	2	3	4	5	6	7	8	9	10	11	12	13
0			14501.9	14345.6	14190.8	14037.5	13885.7	13735.5	3586.8	13439.7	13294.2		13008.1	12867.4	
1			14618.8	14462.5	14307.7	14154.4	14002.6	13852.4	13703.7	13556.6	13411.1	13267.2	13125.0	12984.3	1284
2			14734.8	14578.5	14423.7	14270.4	14118.6	13968.4	13819.7	13672.6	13527.1	13383.2	13241.0	13100.3	1296
3	15007.9 (3)	14850.1 (4)	14693.8 (4)							13787.9	13642.4	13495.5		13215.6	1307
4	15122.5 (4)	14964.7 (5)	14808.4 (5)	14653.6 (4)	14500.3	14348.5	14198.3	14049.6 (1)	13902.5 (1)	13757.1 (1)			13470.9		
5	15236.3 (5)	15078.5 (5)	14922.2 (4)	14767.4 (4)	14614.1 (3)	14462.3 (2)	14312.1 (2)	14163.4 (1)							
6	15349.3 (5)	15191.5 (3)		14880.4		14575.3 (2)	14425.1 (2)	14276.4		13983.8 (1)					
7	15461.6 (5)	15303.8	15147.5	14992.7											
8	15573.1 (5)	15415.3 (4)	15259.0		14950.9										
9	15683.9 (5)		15369.8	15215.0	15061.7										
10	15793.9 (3)	15636.1	15479.8	15325.0	15171.7										
11	15903.1 (4)	15745.3	15589.0	15434.2	15280.9										
12	16011.6 (3)	15853.8 (4)	15697.5	15542.7	15389.4	15237.6		14938.7							
13	16119.3 (2)	15961.5 (3)	15805.2	15650.4	15497.1										
14	16226.3 (2)	16068.5 (2)	15912.2												
15	16332.5 (3)	16174.7 (3)													
16	16438 (2)	16280 (2)	16123	15969											
17	16544 (1)	16386 (2)													
18	16648 (1)	16490 (2)	16333												
19		16592 (1)	(Lines from other bands have probably been seen here.)												
20															
21															
22		16898 WG	16741 WG	16587 WG	16433 WG	16282 WG									
23		16998 WG	16841 WG	16687 WG	16533 WG	16382 WG	16231 WG								
24		17097 WG	16940 WG	16786 WG	16632 WG	16481 WG	16330 WG								
25		17196 WG	17039 WG	16885 WG	16731 WG	16580 WG	16429 WG	16281 WG							
26		17293 WG	17136 WG	16982 WG	16828 WG	16677 WG	16526 WG	16378 WG							
27		17391 WG	17234 WG	17080 WG	16926 WG	16775 WG	16624 WG	16476 WG	16329 WG						
28		17487 WG	17330 WG	17176 WG	17022 WG	16871 WG	16720 WG	16572 WG	16425 WG	16279 WG					
29		17582 WG	17425 WG	17271 WG	17117 WG	16966 WG	16815 WG	16667 WG	16520 WG	16374 WG					
30		17677 WG	17520 WG	17366 WG	17212 WG	17061 WG	16910 WG	16762 WG	16615 WG	16469 WG	16325 WG				
31			17614 WG	17460 WG	17306 WG	17155 WG	17004 WG	16856 WG	16709 WG	16563 WG	16419 WG	16277 WG			
32				17554 WG	17400 WG	17249 WG	17098 WG	16950 WG	16803 WG	16657 WG	16513 WG	16371 WG	16225 WG		
33						17341 WG	17190 WG	17042 WG	16895 WG	16749 WG	16605 WG	16463 WG	16322 WG		

24

	11	12	13	14	15	16	17	18	19	20	21	22
	13008.1	12867.4										
2	13125.0	12984.3	12845.3		12572.4							
2	13241.0	13100.3	12961.3									
5		13215.6	13076.6	12939.3	12803.7	12669.8	12537.6					
	13470.9				12918.3	12784.4		12521.7				
						12898.2	12766.0		12506.8			
					13145.1	13011.2			12619.8			
						13123.5	12991.3	12860.8				
							13102.8		12843.6			
								13083.1	12954.4		12702.2	
										12937.5		12688.9
								13302.3				
									13282.1	13155.2	13029.9	

(Other bands seen in
emission are probably
near $\nu_A = 28$, $\nu_X = 40$)



16277
WG
16371
WG
16463
WG
16322
WG

NOTES: (1) Digits in parentheses below wavenumber entries are eye estimates of relative band intensities by Fredrickson and Watson (1927) from their photographic plates of absorption at fairly low temperature. (2) Entries without any notation are additional bands seen by Fredrickson and Stannard (1933) at somewhat higher temperature, in absorption and/or through magnetic rotation effects. (3) Portions of unresolved band groups near some or all of the spectrum locations labelled WG were seen by Wood and Galt (1911), and by several others, in emission from a discharge tube, and by Beutler, Bogdany, and Polyani (1926) in emission from a flame reaction. Uchida (1932) identified probable quantum numbers for these bands, at least approximately, up to $16,970 \text{ cm}^{-1}$. Higher WG wavenumbers indicate approximate quantum number assignments to Wood and Galt's groups by the present writer in analogy with Uchida's work. (4) Scattered lines seen in the magnetic rotation spectrum by Wood and Hackett (1909) doubtless belong to numerous additional bands in the $17,000\text{--}14,000 \text{ cm}^{-1}$ region, but their quantum numbers have not yet been assigned. (5) Loomis and Nile (1928) found strong absorption at wavenumbers as large as $18,200 \text{ cm}^{-1}$ with dense columns of vapor. (6) Loomis and Nile mentioned, and Hamada (1933) recorded, an unresolved group of bands near $12,500 \text{ cm}^{-1}$ in the emission from a discharge which probably arise from about $\nu_A=28$.

Figure 5 is a Franck-Condon diagram for the (A-X) system. To each band head corresponding to an entry in Table 5 there has been added a tail arbitrarily stretching 200 cm^{-1} toward smaller wavenumbers in the diagram. (Note that in this method of plotting the Franck-Condon diagram any line drawn downward from left to right at a 45° angle is a line of constant wavenumber). Actually, as discussed in report GPL-A-31-3, the position within each band where absorption lines in sodium vapor at 500°C have about 1% of the intensity of the strongest lines of the band will lie as much as 660 cm^{-1} away from the head. There will, therefore, be many experimental situations in which overlapping of bands will be even more extensive than Figure 5 indicates.

The relative population percentages listed along the axes in Figure 5 give a partial indication as to which bands should be strongest in absorption or in fluorescence whenever one is dealing with vapor in vibrational Boltzmann equilibrium at 500°C -- although intensities in Na_2 are always considerably affected by the exact degree of overlap of each pair of level wavefunctions involved in a transition. These intensities are likely to vary markedly among adjacent bands originating from the same initial level.

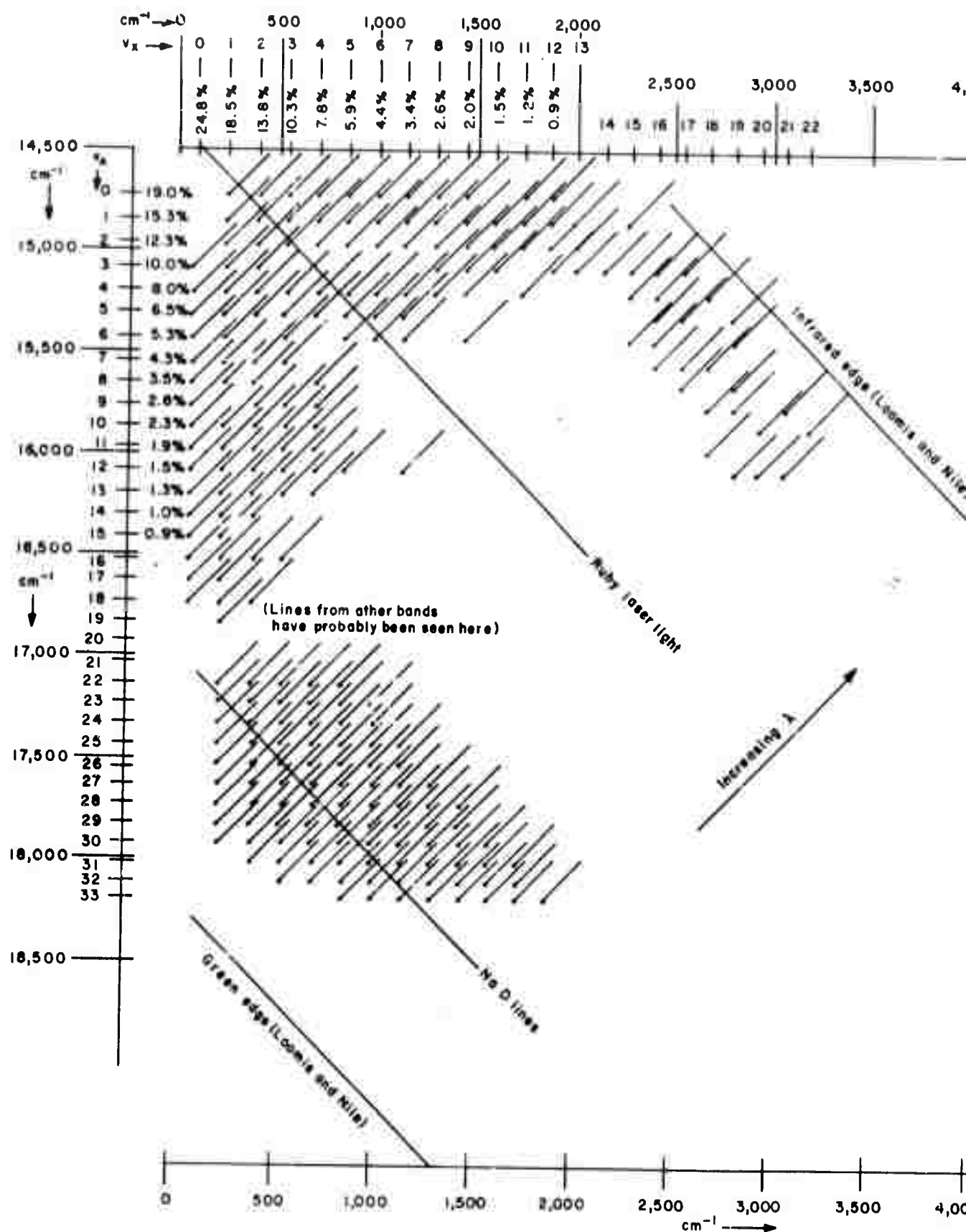
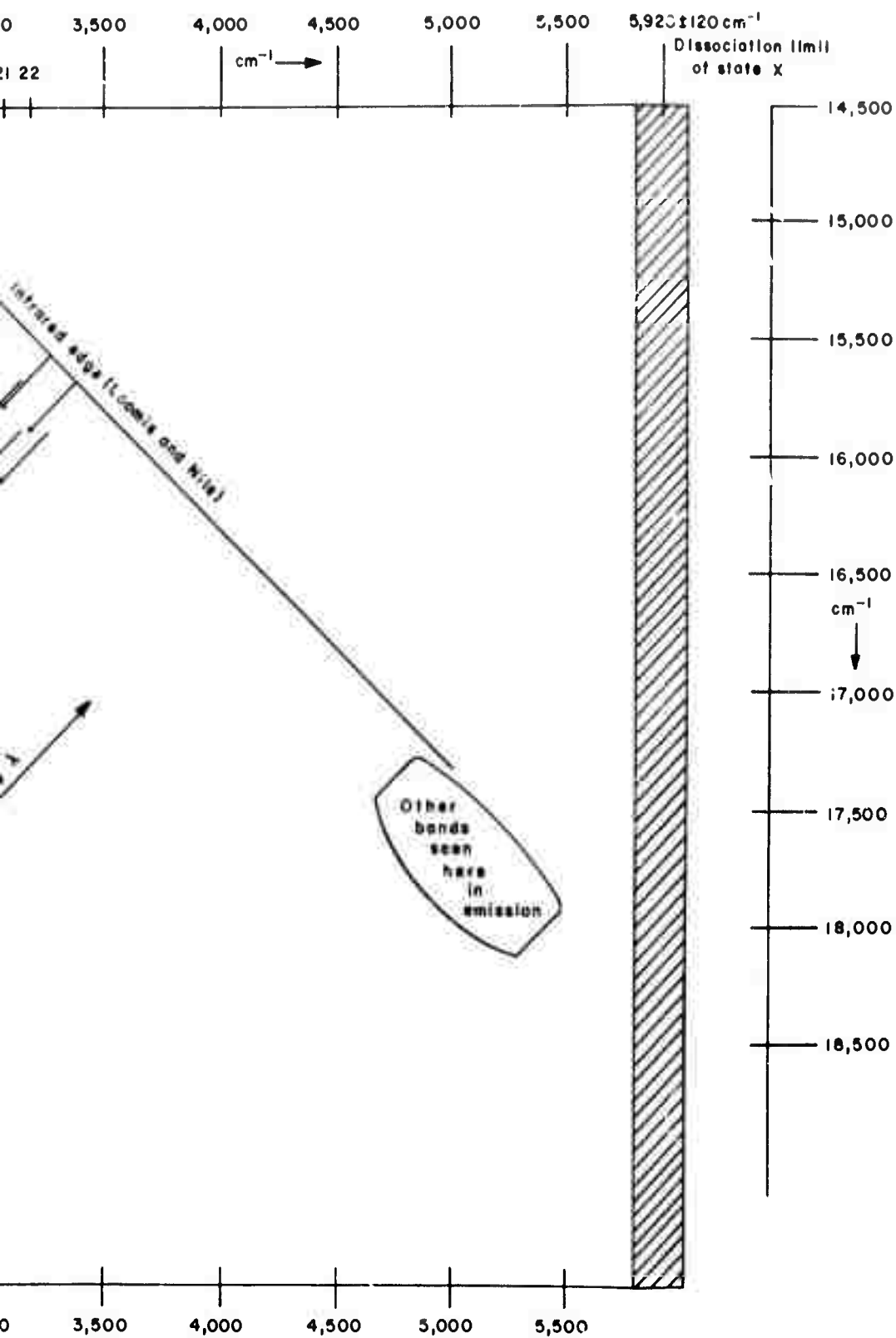


Figure 5. Franck-Condon diagram for the observed $\text{Na}_2^+(\text{A-X})$ band system. The energy difference from each band head is arbitrarily shown here as 200 cm^{-1} , actually stretch for a considerably greater distance from experimental conditions. Along the axes are also shown the vibrational levels that would occur in the first few vibrational levels, if those states were each, separately, to be in Boltzmann vibrational equilibrium.



(A-X) band system. The tails degrading to the red are as 200 cm^{-1} long. Lines of observable intensity are shown at various distances from each head, under most typical conditions. Also shown are the relative population densities, which are calculated for those molecules in state X and those in Boltzmann vibrational equilibrium at 500°C.

4.3 General Remarks on Na₂-Ruby

As may be seen from Figure 5, ruby lasers could be arranged to pump into the absorption lines near the heads of the (2,3) and the (6,6) bands, of which the former would be the more intense at 500°C. Weaker transitions of a number of other bands would also be pumped simultaneously. The addition of 20 atm He to the system provides numerous molecular collisions which will continually spread the molecules over the rotation levels of both the upper and lower vibrational states, to try to maintain Boltzmann rotational population distributions -- in the same fashion as described in detail for the CN-Nd transformer combination in report GPL A-31-1 and discussed in section 2 of the present report for CO-Er. Just as for these combinations, after intense pumping strong inversion will be present in transitions whose lines lie toward longer wavelengths than those of the pumped transitions.

Under heavy pumping and lasing conditions, the molecules will be carried repeatedly around a pump-collide-lase-collide-pump cycle, as described for the CN-Nd transformer. Large limiting output energy densities per pulse, at good optical quality of the beam, can be calculated *provided* about 40% of the Na₂ molecules can be maintained in the Na₂·A level without causing too much energy loss which would create excessive waste heat in the vapor volume.

The most common source of energy loss from a pumped upper electronic state which has been uncovered in the various media studied under this contract is escalation of the molecules from the pumped electronic state to higher excited states. This can be due to (a) absorption of a second quantum of pump light by a molecule already in state A, or (b) the type of collision of two molecules in state A which drops one of them to the ground state and uses the released energy to raise the other to a higher excited state.

The line of crosses at $(A + 14,400 \text{ cm}^{-1})$ among the potential curves of Figure 4 shows where absorption of a second quantum of Nd pump light would place a molecule already in state A. The only upper states which selection rules would permit the molecule to reach with good probability are the two suggested perturbed ${}^1\Sigma_g^+$ states. These are reasonably stable and so would not lead directly to waste heat production. Only absorption of a *third* pump quantum to some of the very high repulsive states could seem to constitute a possibly harmful heat source. Absorption of a second quantum to the one available repulsive ${}^1\Pi_g$ state, followed by dissociation of the molecule with the development of kinetic energy in the vapor, would have a low probability, *provided* its curve actually is located as shown in Figure 4, because of the large angle at which the two curves cross.

The possibilities for waste heat production by collision between two $\text{Na}_2\cdot\text{A}$ molecules are considerably more difficult to assess, but it is probably a very hopeful circumstance that only one repulsive curve, the $^1\text{II}_g$, seems likely to cross the $(\text{A} + 14,400 \text{ cm}^{-1})$ curve. This region is probably much more clear of repulsive potential curves than the corresponding two-quantum region of the Cs_2 energy level diagram.* One can only conclude that experiments are badly needed in which large numbers of sodium molecules are placed in the $\text{Na}_2\cdot\text{A}$ state.

Most of the remainder of this report will deal with the Cs-Nd transformer laser design. Reference is made to the report GPL-A-31-3 which was largely concerned with an estimation of many properties of cesium vapor and of the Cs_2 molecule. In the following section only such additional properties are discussed which bear directly on problems arising in the recent laboratory work under the contract.

*However, it should be kept in mind that chemical reactions are possible. For example, the processes $\text{Na} + \text{Na}_2\cdot\text{A} \rightarrow \text{Na}_2\cdot\text{X} + \text{Na}$ or $\text{Na}_2\cdot\text{A} + \text{Na}_2\cdot\text{A} \rightarrow \text{Na}_2\cdot\text{X} + 2\text{Na}$ are energetically allowed and could occur if the (unknown) potential energy surfaces for the transient polyatomic systems existing during collision had a suitable form. These possible chemical processes thus might provide other ways to lose the $\text{Na}_2\cdot\text{A}$ excitation and to transform it to heat via vibrational or rotational excitation of the $\text{Na}_2\cdot\text{X}$ produced and relative translational motion of the $\text{Na}_2\cdot\text{X}$ and Na . On the other hand, an example in which a similar chemical process involving the $\text{Na}_2\cdot\text{B}$ state is energetically allowed but has been found not to occur is discussed in GPL A-31-1, pp. 100-105. (D.R. Herschbach)

5. SOME PROPERTIES OF CESIUM MOLECULES

As will be elaborated in the experimental sections of this report, irradiation of hot cesium vapor with a beam of 1.06μ Nd glass laser light in a lms pulse was found to cause an apparent bleaching of the absorbing transitions at an unexpectedly low beam intensity level. Numerous possibilities for explanation of this behavior could be suggested, and several of these will be discussed in connection with the experiments themselves. However, in this section some information will be collected with a particular bearing on three of these possibilities.

- (a) There might be fewer diatomic cesium molecules actually present in this vapor volume than would be expected from previous reports in the literature. If there were very few molecules present the transitions would be easy to bleach.
- (b) Molecules present at the expected equilibrium concentration at the beginning of a pulse might be dissociated early, as a result of some energy absorption process, and then the recombination processes in the vapor might not proceed fast enough to restore the equilibrium concentration before the pulse was over.

- (c) Dissipative processes resulting from absorption of light early in the pulse might be creating enough waste heat in the initially saturated vapor that this considerably superheated the volume -- to such a point that a very low molecular concentration would then normally be expected in the remainder of the pulse, for equilibrium at the superheated temperature and pressure.

An approximate calculation on possibility (b) indicates that recovery times of less than one μsec will probably prevail. An investigation of possibility (a) can be combined with a survey of information on the probable spontaneous radiative lifetime of a molecule in the excited Cs_2^*A state, as described in the following section.

5.1 Expected Intensity of the Cs_2^* (A-X) Band System

Only one attempt at quantitative measurement of the intensity of the Cs_2^* (A-X) band has been published -- that of Wechsler (1966), at Arthur D. Little, Inc., who carried out a two year study of the absorption bands in sodium, potassium, and cesium vapors (all mixed with one atom of argon) at low dispersion, over a broad range of the spectrum. Lapp and Harris (1966), at the General Electric Research Laboratory, similarly measured potassium and cesium vapor absorption in the visible region, where their results agreed with those of Wechsler within about a factor of three (including substitution of other noble gases as the additive at pressures from 0.05 atm to 1.1 atm), but they did not extend their cesium studies into the infrared as far as the (A-X) band.

Wechsler reduced his data to a smoothed molecular absorption cross section curve, giving σ in $(\text{\AA})^2$ extending over each of his experimental wavelength intervals. The calculation involved the assumption of curves of molecular concentration vs. temperature which, in the case of Na_2 and K_2 , were the same as those presented in Figure 3 of report GPL-A-31-3. However, the molecular concentration curve given in that Figure for Cs_2 lies a factor of 1.4 higher than the one assumed by Wechsler -- although it may be questioned whether the difference is meaningful, in view of the probable uncertainty by a factor of at least 3 quoted for the Cs_2 curve in the Figure. Table 6 lists the cross sections obtained by Wechsler at the strongest parts of the (B-X) and (A-X) bands for each of the three molecules, with his Cs_2 values having been reduced by the factor 1.4.

The relation between the Einstein coefficients A and B for spontaneous emission and for absorption, respectively, in a given transition at wavelength λ is

$$A \sim \frac{B}{\lambda^3}$$

Table 6 shows the quantity $\left[\left(\frac{\lambda^3}{\sigma} \right) / \left(\frac{\lambda^3}{\sigma} \right)_{\text{Na}_2} \right]$ as calculated from Wechsler's data, which should be proportional to the *relative spontaneous emission lifetimes* of the excited molecular states.

GPL Division's qualitative measurements on the Cs_2 (A-X) band were shown in Figure 12 of Report GPL A-31-2. The intensity observed was at least as great as that seen by Wechsler. He found about 25% average absorption in the range 9400 \AA to 1μ , with a nominal path length of 6" in slightly unsaturated vapor, obtained

Table 6
Molecular Radiative Cross Sections

	Maximum molecular absorption cross sections, σ (Wechsler, 1966).		$\left[\frac{\lambda^3}{\sigma} \left(\frac{\lambda}{\sigma} \right)_{\text{Na}_2} \right]$	Experimental molecular emission, τ spont (Hupfeld, 1929)		Theoretical molecular emission, τ spont (Stephenson 1950) and Davies, 1958).
	(B-X) Bands	(A-X) Bands		Bands (B-X)	Bands (A-X)	
Sodium	3.5 Å ²	2.0 Å ²	1	1	1.0 x 10 ⁻⁸ sec.	1.7 x 10 ⁻⁸ sec.
Potassium	11.0 "	4.0 "	0.8	0.9	0.8 "	_____
Cesium	21.5 " (amended)	3.6 " (amended)	0.6	0.5	_____	_____

from 99.93% pure cesium plus one atm of argon, at somewhat varying temperatures near 297°C , using a spectrometer of fairly low resolution. With an instrument giving a little more spectral resolution, GPL Division found about 22% average absorption in this region for a path length of about 1" in presumably saturated, undiluted, reasonably pure cesium vapor, somewhere in the neighborhood of 280°C . No really close comparison between the two observations is possible, since differences in many of these experimental parameters are known to affect measurements within an unresolved molecular band in a complex manner.

Hupfeld (1929) has measured the actual fluorescent decay rates in the (B-X) bands of Na_2 and K_2 , and Stephenson (1950) has calculated theoretically the τ_{spont} to be expected for the A state of Na_2 , his value later being given some corroboration by the much more detailed theoretical treatment of Davies (1958). These results are also shown in Table 6.

Although the numbers in Table 6 are not so very precise, (in particular, the K_2 absorption cross sections might actually be a factor of two or three smaller, and the Cs_2 cross sections might be altered by a factor of about three either way, because of the uncertainty in the molecular concentration curves as described in the report GPL-A-31-3; furthermore, Wechsler's light beams traversed a somewhat uncertain effective path length

and also contained slightly unsaturated vapors, which are known to show some reduction in molecular concentration from the saturation values*) still, it may probably be assumed from a consideration of all the relative numbers that τ_{spont} for a $\text{Cs}_2\cdot\text{A}$ molecule is in the general neighborhood of 10^{-8} sec.

It may be noted that the analogous $(n^2\text{P} - n^2\text{S})$ transitions in the corresponding alkali metal atoms have upper states with τ_{spont} for all three in the neighborhood of 2×10^{-8} sec. (The most recent experiments are by Link, (1966)).

From the above evidence, it appears that the cesium vapor conditions in the experiments of GPL Division must have produced saturated equilibrium molecular concentrations at least in the general neighborhood of those to be expected theoretically, which were described in Figure 3 of Report GPL-A-31-3.

The next section will consider possibility (c) listed above -- that the population density of molecules in correct thermodynamic equilibrium with the atoms might actually be decreasing during the pumping pulse, because of superheating of the vapor.

*Calculations on this matter are given in Section 5.3. Also, Minkowski and Mühlenbruch (1930) have experimentally observed the decreases in cesium molecular absorption band strength which accompany superheating of the vapor.

5.2 Molecular Concentrations in Superheated Vapors

The equilibrium constant for the gas reaction



can be expressed in terms of the partial pressures at any equilibrium point as

$$K_p = \frac{P_{\text{molecules}}}{(P_{\text{atoms}})^2}.$$

It is well known* that K_p as so defined for this reaction is a function of absolute temperature T only, and is independent (a) of total ambient pressure, (b) of the pressure of any additional inert gas, and (c) of whether the volume is saturated or superheated -- provided both the above reacting entities can be approximated as ideal gases, and provided neither is involved at the same time in any reaction other than the above.

In the case of cesium in the temperature range $700^\circ\text{--}1400^\circ\text{C}$, Ewing, et al (1965b) found that values of K_p deduced from their vapor pressure measurements were *not* independent of pressure at a given temperature. They interpreted this as the effect of additional competing reactions involving higher polymers, such as Cs_4 and perhaps Cs_6 . However, in the range $300^\circ\text{--}400^\circ\text{C}$ where the experiments of GPL Division were performed,

*Further discussion of the thermodynamic quantities used in this section can be found in such texts as W.J. Moore, "Physical Chemistry", Prentice-Hall, 3rd Ed., 1962.

the concentration of these higher polymers is doubtless so small that their effects can be ignored, and K_p can be taken as a function only of T , to an approximation adequate for the present purpose.*

Furthermore, in the present problem we are interested only in temperature and pressure ranges where the diatomic molecules constitute less than 3% of the mixture, as indicated by Figure 2 of report GPL-A-31-3, so that it is an adequate approximation to set $P_{\text{atoms}} \approx P$, the total sodium pressure. This means that $P_{\text{molecules}} \approx P^2 K_p$. A comparison between (a) the equilibrium molecular partial pressure in superheated vapor at any chosen temperature and chosen total pressure, and (b) the equilibrium molecular partial pressure in *saturated vapor at the same temperature* is then given simply by

$$\left[\frac{P_{\text{molecules}}}{(P_{\text{molecules}})_{\text{sat.}}} \approx \frac{P^2}{(P_{\text{sat.}})^2} \right]_{\text{const. } T.}$$

At various points along the saturated vapor pressure curve of cesium in a P - T graph, one can mark the expected equilibrium molecular concentrations (as taken from Figure 3 of GPL A-31-3, with the reservations as to accuracy expressed therein) and then

*Figure 4 of report GPL-A-31-3 was partially in error. The curves for the estimated K_4 and Na_4 fractions were incorrectly plotted. Figure 6 of the present report is a corrected version.

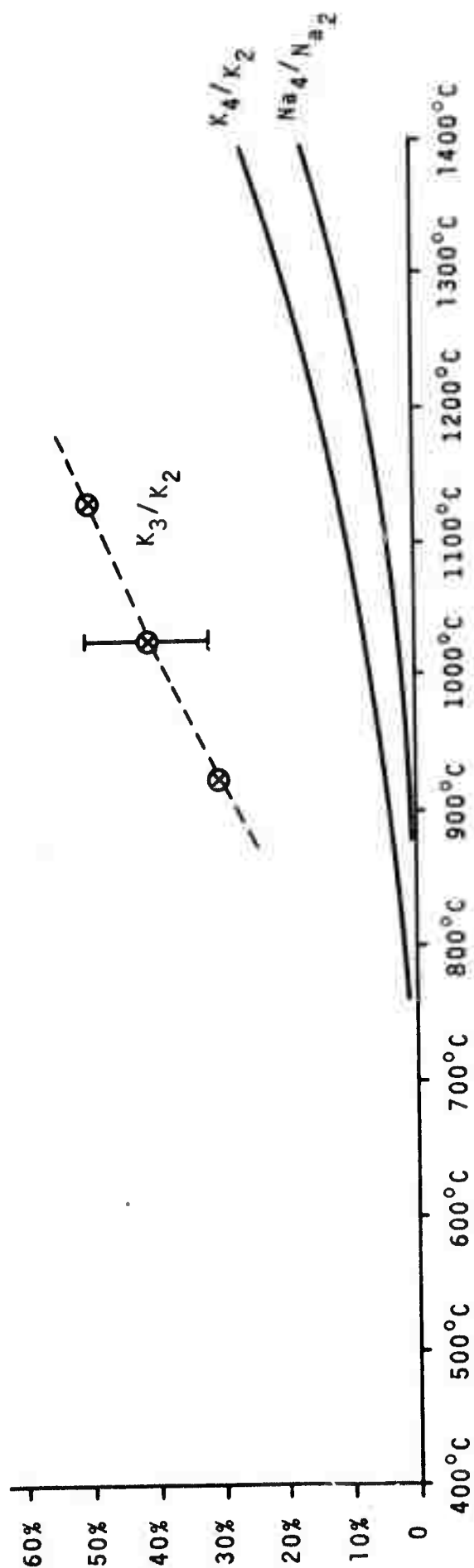


Figure 6. Equilibrium concentration ratios of higher polymers to dimers, as postulated from one type of analysis of vapor pressure curves for pure saturated alkali metals at high temperatures. Data from Stone, et al (1965) for the Na_4 assumption, and Ewing, et al (1965) for the K_4 assumption. Alternative assumption of K_3 from Walling (1963).

Note: This is a corrected version of Figure 4 of report GPL A-31-3. Some of the curves in that Figure were incorrectly plotted.

find the equilibrium molecular concentrations at any point in the superheated region by simple proportion between the squared pressures along vertical lines of constant T. Figure 7 has been constructed in this manner, with *solid* lines being drawn through points of constant predicted molecular equilibrium concentration in the superheated region.

If one begins with a volume of vapor in a saturated condition at some chosen temperature, and then dumps heat into this vapor, the particular point in the superheated region which will be reached will depend on the exact manner in which the experiment is performed. In an effort to approximate the conditions of the GPL Division experiment, which will be more thoroughly described in a later section, let us make the following assumptions:

- (a) a definite quantity of sensible heat is dumped into the vapor within a small fraction of a millisecond;
- (b) the vapor volume is constant, because it is in a closed container;
- (c) during the heat dumping period there is no time for any additional mass of cesium to be evaporated from the small area of liquid reservoir which is in contact with the saturated vapor; and

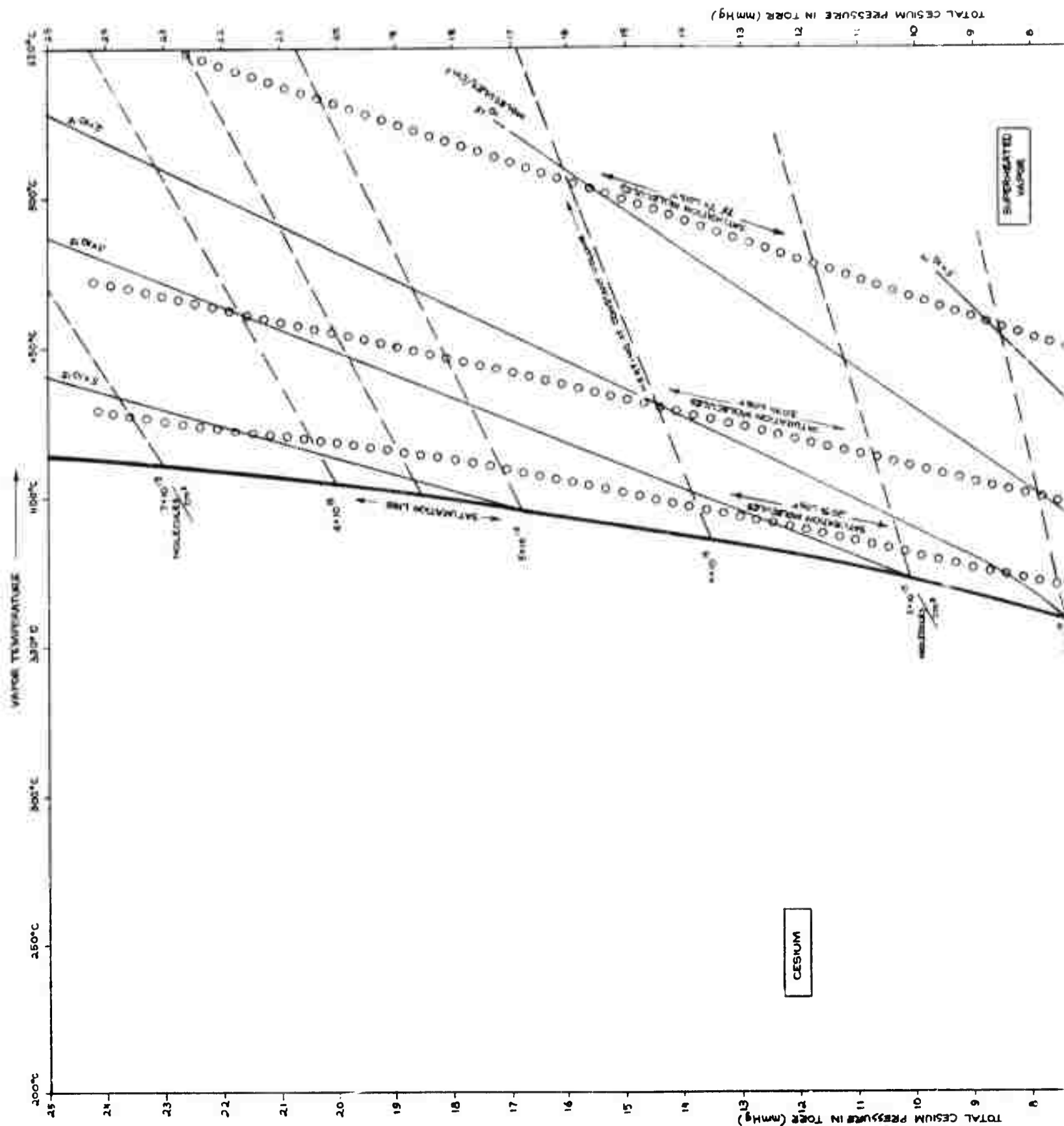
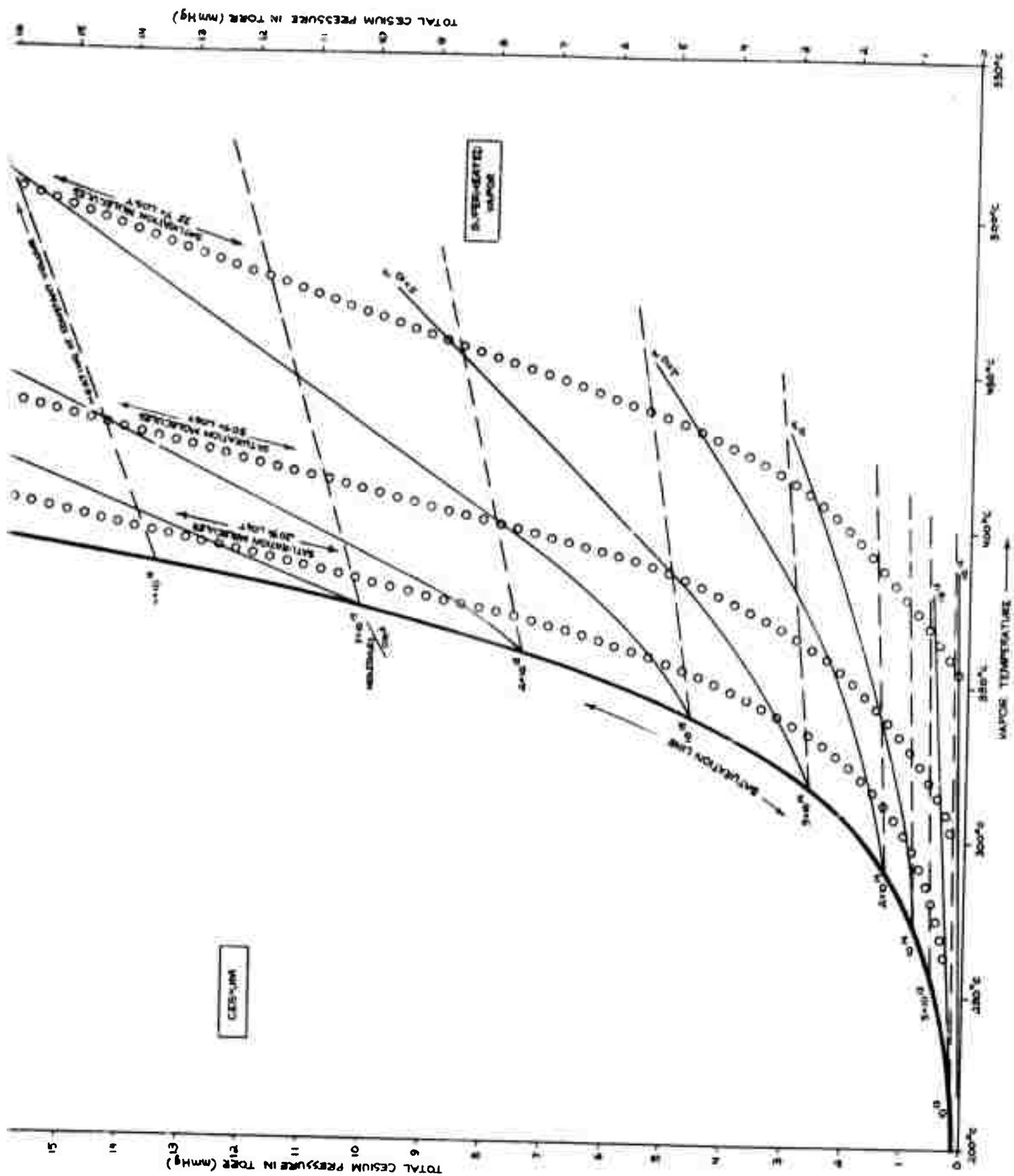


Figure 7. Approximate equilibrium concentra to be expected in cesium vapor at along the saturated vapor line an The lines of circles show the app cular concentrations reached afte of heat to the saturated vapor at



e 7. Approximate equilibrium concentrations of Cs_2 molecules to be expected in cesium vapor at temperatures and pressures along the saturated vapor line and in the superheated region. The lines of circles show the approximate equilibrium molecular concentrations reached after applying very quick pulses of heat to the saturated vapor at constant volume.

- (d) during the heat dumping period there is no time for any appreciable amount of the additional heat to be lost from the vapor by thermal radiation, or by conduction or convection to the walls.

In such an assumed situation, by the end of the heat dumping period the added sensible heat will have raised the temperature and pressure of the vapor under the conditions of constant mass and constant volume. On the approximation that the vapor behaves like a perfect gas, and the further rough approximation that the effect on pressure of changes in average molecular weight can be neglected in this temperature region, every constant-mass-constant-volume line on the P-T graph would be a straight line whose extension passes through the origin -- the latter lying at zero pressure and zero degrees absolute. Such straight *dashed* lines are shown in Figure 7 extending into the superheated region away from a number of chosen starting points along the saturated vapor curve.

Starting from any given saturation point, progress along one of the constant volume lines, because of very quick addition of heat, will carry the vapor to points of smaller and smaller equilibrium molecular concentrations. The lines of circles in Figure 7 show the end points where 20%, 50%, and 75% of the initial saturated molecular concentration will have been lost*. As a rough generalization it appears that for any starting

* If the heat was to have been added extremely quickly, in a time much shorter than the $\sim 1 \mu\text{sec}$ molecular recovery time estimated previously, the vapor would not actually follow the graph as shown since the atom-molecule equilibrium would not obtain at every instant, as was assumed in constructing Figure 7. However, as soon as atom-molecule equilibrium was regained once more, the graph would properly describe the endpoint reached.

temperature in the 200°-400°C range, saturated cesium vapor will lose about 20%, 50%, or 75% of its initial molecular concentration upon quick application of enough energy to cause temperature rises of about 15°C, 50°C, or 130°C, respectively.

In a case where the volume contains only pure cesium, the amount of energy which must be absorbed from the Nd laser beam per cm³ of vapor in order to cause 75% of the saturation molecular content to disappear, for example, will be given in rough approximation by the following expression:

$$\begin{aligned}
 \left(\text{Joules/cm}^3 \text{ to cause 75\% Cs}_2 \text{ disappearance from pure cesium vapor saturated at } T^\circ\text{K} \right) \approx & \left[(0.75) \times (\text{molecules/cm}^3 \text{ at saturation}) \right. \\
 & \times (3600 \text{ cm}^{-1}, \text{Cs}_2 \text{ diss. energy to make two 6s}^2 \text{ atoms}) \\
 & \left. \times (2 \times 10^{-23} \text{ joules/cm}^{-1}) \right] \\
 & + \left[(3 \text{ cal/mole per } ^\circ\text{C}, C_v \text{ for monatomic ideal gas}) \right. \\
 & \times (\Delta T, ^\circ\text{C}) \\
 & \times \left(\frac{P_{\text{sat}} \times 273}{760 \times T_{\text{sat}} (^{\circ}\text{K}) \times 22,400} \text{ moles/cm}^3 \text{ ideal gas density} \right) \\
 & \left. \times (4.2 \text{ joules/cal}) \right]
 \end{aligned}$$

Using data from Figure 7, the absorbed energy density required for this purpose is listed in Table 7 for several saturation starting temperatures. The amount turns out to be no greater than about one millijoule/cm³ under these conditions.

Table 7

Energy Required for Suppressing the Molecules

Starting Temperature	Joules/cm ³ for 75% Mol. Loss in Pure Cesium		Joules/cm ³ Required in Cs Plus 1 atm He	
	For Dissociation	For Sensible Heat Total	For 20% Mol. Loss	For 50% Mol. Loss
250°C	2.0 x 10 ⁻⁶	2.0 x 10 ⁻⁵	2.2 x 10 ⁻⁵	1.8 x 10 ⁻²
300°C	1.4 x 10 ⁻⁵	5.8 x 10 ⁻⁵	7.2 x 10 ⁻⁵	1.4 x 10 ⁻²
350°C	8.1 x 10 ⁻⁵	1.9 x 10 ⁻⁴	2.7 x 10 ⁻⁴	1.1 x 10 ⁻²
400°C	3.1 x 10 ⁻⁴	8.2 x 10 ⁻⁴	1.1 x 10 ⁻³	1.3 x 10 ⁻²

In a case where the saturated cesium vapor is mixed with 1 atm of helium gas, since the molar density of the Cs will always be less than 1/40th that of the He in this temperature range, both of the above contributions from Cs to the total enthalpy change can be neglected in an approximate calculation. The energy which must be absorbed is roughly that needed to heat up the helium alone, which is given simply by $(3 \times \Delta T \times 273 \times 4.2) / (T_{\text{sat}} \times 22,400)$ joules/cm³. The temperature data from Figure 7 lead to the energy absorptions listed in Table 7 for causing 20% or 50% loss of the Cs₂ molecules in this mixture.

Taking the largest of all these numbers, 1.8×10^{-2} joules/cm³ for 50% loss of the molecules present in saturated Cs plus 1 atm He at 250°C, let us now try to envisage some molecular process which could cause the supposed effect. According to Table 7, to dissociate 50% of the molecules present in saturated vapor at 250°C requires about 1.7×10^{-6} joules/cm³. Therefore, the postulated process must be putting roughly 10,000 times as much sensible heat into the volume as the energy required to dissociate enough Cs₂ to cause the observed *net* decrease in molecular population.

This additional factor of 10^4 is probably to be related to the ratio of the experimental disappearance time of the absorption

spectrum ($\sim 100\mu\text{sec}$) to the population recovery time ($< 1\mu\text{sec}$).

Of course, the net equilibrium decrease of 50% in the molecular density is accomplished only as a result of dissociating a much larger quantity of molecules than this, since the recombination collisions are continuously re-creating molecules in an effort to maintain the original equilibrium until the vapor has become thoroughly heated. There is not enough evidence at this time to show whether or not the superheating phenomenon postulated here would suffice as a complete explanation for the disappearance of the molecular absorption spectrum during the pumping pulse. There might well be a mixture of several other processes involved at the same time.

The remainder of this report will consist of a survey of the experimental work performed by GPL Division during the last six months of this contract period.

6. INTRODUCTION TO EXPERIMENTAL WORK

The purpose of the experimental program has been to test molecular cesium as a suitable material for use in a laser transformer. The program also included supplementary tests and measurements on materials and components to be used in the transformer laser experiments.

During the previous phase of the experimental program (Technical Report GPL A-31-3), the existence of Cs_2 molecules in the absorption cells had been established by the presence of a strong absorption band between 0.90 and 1.15μ that appeared with increasing temperature. Laser-excited fluorescence in this region had also been found and its general features found to correspond with those of the absorption spectrum. The preparation of Corning 1720 glass cells filled with cesium had been established and repeated. Perhaps the most important finding reported previously was the apparent "bleaching" of the cesium cell at the laser wavelength (1.06μ) for laser pulses above certain intensities. One interpretation of this was the saturation of the molecular transitions at 1.06μ by the laser light. Apparatus for the transformer laser experiment, pumping Cs with Nd^{3+} light, had been designed and construction begun.

During this report period the apparatus for the laser transformer experiment was completed and operated. In these experiments no transformer laser action was found for the conditions under which the experiment was conducted and the observations made. A large portion of the effort was given over to a study, of a supplementary nature, whose aim was to provide an understanding of why no lasing was observed. The study was primarily concerned with the

observation of changes in the optical properties of the hot cesium vapor during and after an intense laser pulse. This also involved a detailed determination of the pump-laser characteristics.

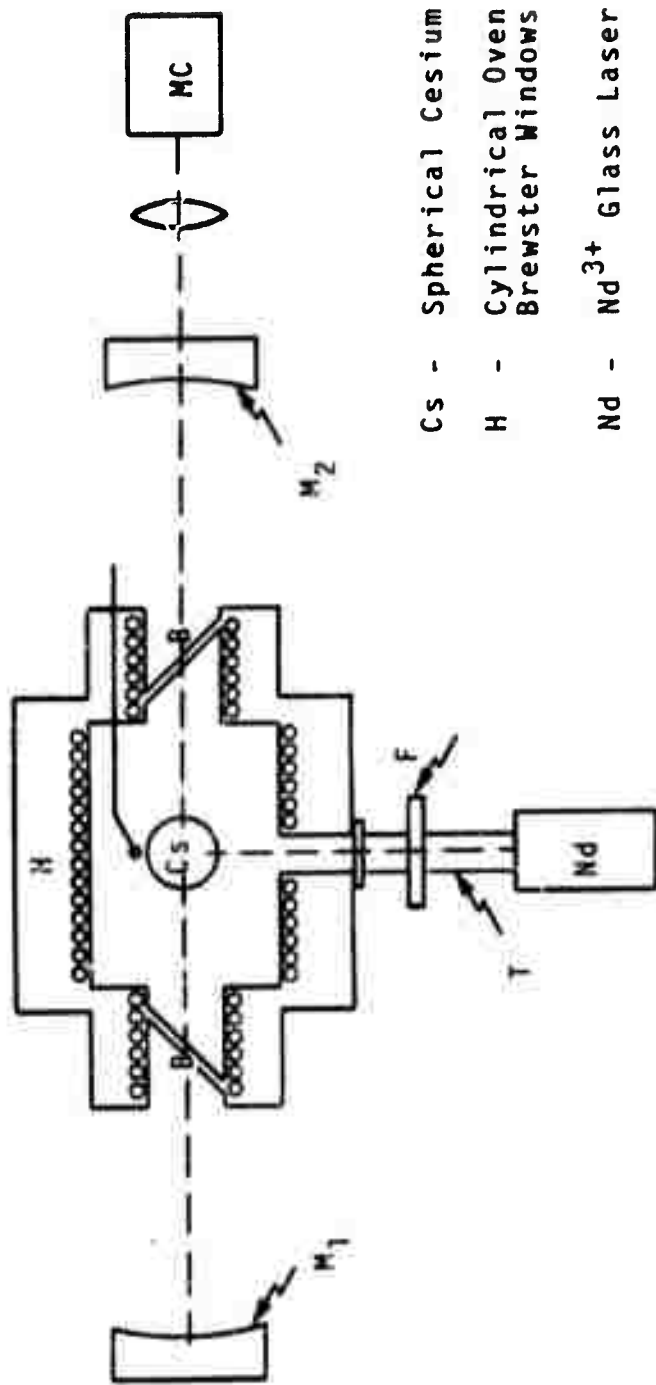
The organization of this section of the report begins with a description of the experiments that were performed in the search for laser transformer action. Analysis of some of these conditions is given in the sections that follow on the studies of cesium vapor and its interaction with the intense pumping laser beams. A general discussion of the significance of the experiments is then given.

7. TRANSFORMER LASER EXPERIMENT

In the transformer laser experiment an attempt was made to pump hot cesium vapor with the 1.06μ output of a Nd^{3+} glass laser and obtain a laser output at adjacent wavelengths corresponding to transitions in the Cs_2 molecular spectrum.

7.1 Experimental Arrangement

The experimental arrangement of the essential components is shown in Figure 8. The laser medium, hot cesium vapor, was contained in a spherical glass bulb about 1.2" in diameter. The bulb was hand blown from Corning 1720 glass. It was positioned inside a cylindrical oven provided with a side port to admit the pumping flux from the Nd^{3+} glass laser. The oven was also equipped with heated Brewster angle windows along the direction of the Cs lasing cavity.



Cs - Spherical Cesium Bulb

H - Cylindrical Oven with Brewster Windows (B)

Nd - Nd^{3+} Glass Laser

M_1, M_2 , Spherical, Dielectric Coated Mirrors Mounted in Confocal Geometry

MC - Grating Monochromator with Photoelectric Monitoring

F - Glass Filter

TC- Thermocouple

T - Light Tube

Figure 8. Schematic Drawing of Transformer Laser Experiment

A red glass filter (Corning #2-64) was placed in the light pipe between the Nd^{3+} glass laser and the cesium bulb to prevent the Nd exciter flash light to the blue of 6200\AA from getting into the oven.

The cesium laser cavity was completed by means of two spherical mirrors (focal length 67.6 cm) with dielectric coatings. The reflectivities of the two mirrors were about 70 and 80% at 1.00μ . The mirrors were mounted in the confocal arrangement centered about the cesium cell. The alignment of the spherical mirrors was accomplished by illuminating them with a narrow beam from a He-Ne laser and bringing the images formed by the reflecting surfaces into coincidence at some distance from the cavity. A photograph of the cesium laser cavity is shown in Figure 9.

The pump laser light was obtained from the rod described in Section 8. Its characteristics and their determination are described in more detail in this section. Briefly, an output of up to 8 joules in a 1 msec pulse could be obtained at 1.062μ in a band of 60\AA .

The output of the Cs laser cavity was focused on the input slit of a grating monochromator. The output of the monochromator was monitored photoelectrically.

The search for lasing was made by examining the output of the laser cavity for changes in the time- and frequency-dependence of the fluorescence during the pumping pulse. This was done as a function of the cavity being aligned or not aligned. Alignment of the cavity was destroyed by insertion of a beam deflector between the confocal mirrors. The spectrum between 1.0565 and 1.2225μ

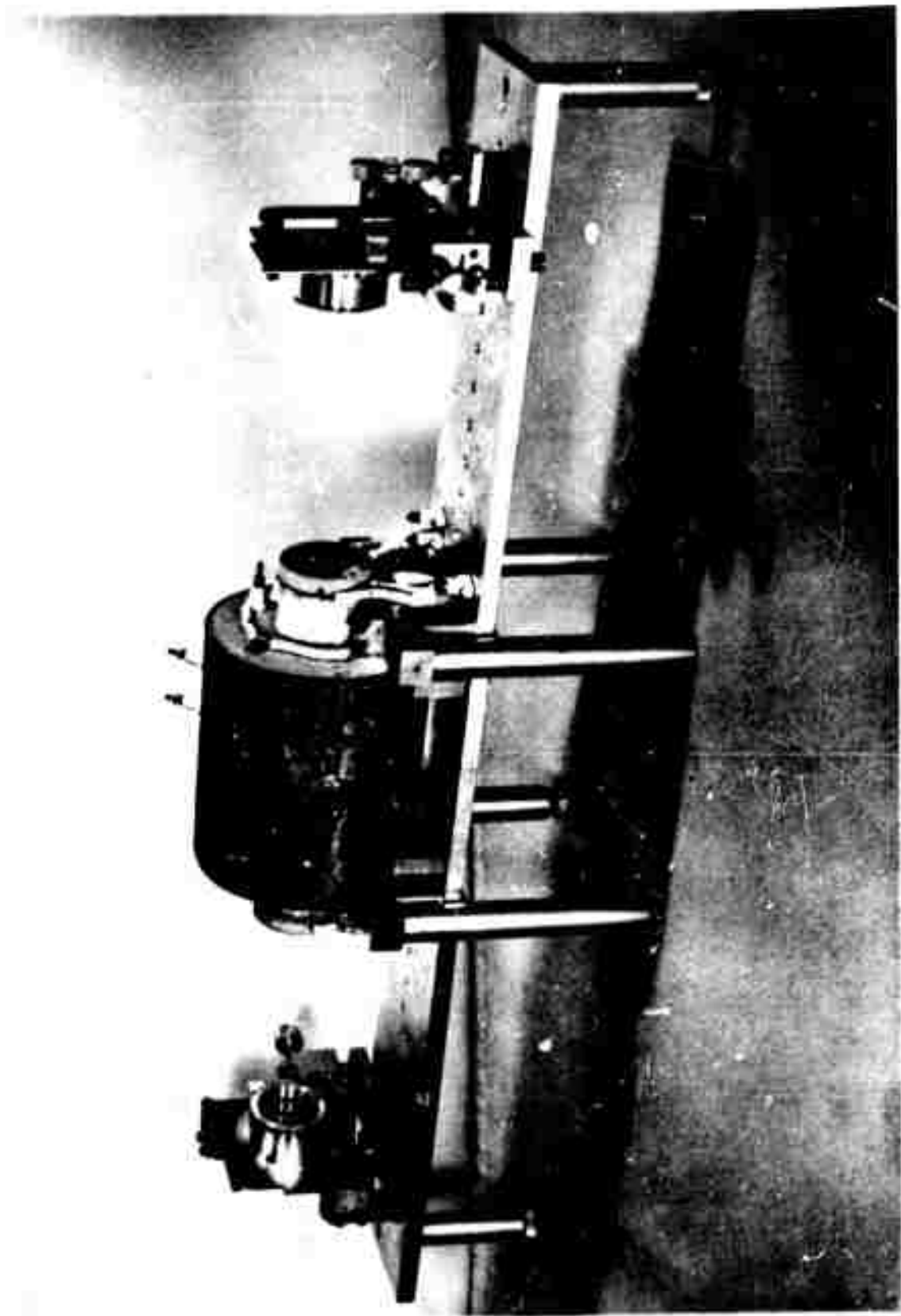


Figure 9. Photograph of Portion of Apparatus for Transformer Laser Experiment Showing Optical Cavity and Oven.

was explored. The region about the Cs D-lines was also examined in the same way. No changes in the time- and frequency-dependence of the fluorescence were observed on changing the cavity from the aligned to unaligned condition. A search was also made for the appearance of some threshold phenomenon near 1.2075μ as the pump laser power was increased and the alignment of the cavity changed. Again, no changes were noted between the aligned and not aligned conditions of the cavity.

7.2 Discussion of Results

No transformer laser action was observed in the experiments performed. A review of the experimental arrangement and procedures brought about the recognition of several factors which could have prevented the lasing from taking place or, if it had occurred, from its being detected. These factors can be grouped generally into three categories: absence or disappearance of Cs_2 molecules, low or variable Q of the optical cavity, and lasing in a manner that could not be seen.

In the first group concerned with the absence of Cs_2 molecules, one difficulty may have been that there were never enough Cs_2 molecules in the absorption cell. Comparison of low intensity absorption curves with absorption data in the literature showed this not to be the case; the molecular density at the temperatures used was about that to be expected. This is discussed in more detail in Section 5.1. Another phenomenon that belongs with this group is the possible disappearance of the cesium molecules during the pumping pulse. This could come about through the destruction of cesium molecules or their polymerization during the intense

light pulse. A separate experiment was performed to detect changes in the concentration of the cesium molecules during the laser pulse. A reduction in the absorption in the (X→A) and (X→B) regions during the laser pulse was found. The experiments and results are described in Section 11 and their interpretation in 12.

Of course, even though a certain percentage of the cesium molecules capable of absorbing from the ground state disappear during the laser pulse, it may still be possible to lase by means of the transformer pump cycle on the remaining molecules. If this be the case, then the remaining effects listed above could prevent the lasing or prevent its detection.

The poor optical quality of the glass bulb limited the precision of the alignment of the laser cavity mirrors; the turbulence in the air between the mirrors, due to the hot base plate, contributed a random variation to the tuning that remained.

An alternate explanation to the apparent absence of lasing in the direction of the laser cavity is that lasing was taking place only in the direction of the pump laser beam. A brief examination of the forward beam (in the direction of the pumping beam) gave no indication of changes in the spectrum with increasing laser pump power. This experiment was performed without the optical resonator mirrors in place.

The lack of success in obtaining lasing from the hot cesium vapor pumped with the Nd^{3+} light led to further studies of the interaction between cesium and the light.

8 . INVESTIGATION OF NEODYMIUM AND RUBY LASER CHARACTERISTICS

Prior to the beginning of the present report period, all Nd-pumped cesium studies had been conducted with relatively low laser outputs, in the neighborhood of 0.035 joules. In order to be able to investigate the neodymium-cesium system at much higher laser flux densities, a new laser cavity was constructed and several large neodymium glass rods were purchased. In anticipation of the eventual inclusion of the ruby-pumped sodium system in the laser transformer program, a large ruby crystal was also purchased. All rods were 6-5/8 to 7" long by 10 mm or 1/2" in diameter, and could be used interchangeably in the same laser cavity. The output characteristics of two of the rods were investigated in detail. These rods were:

- (a) Eastman Kodak Co. neodymium glass - TIR (total internal reflection) prism on one end; reflecting dielectric coating, optimized for maximum output power, on the other end.
- (b) A. Meller Co. ruby crystal (0.04% chromium) - 100% reflecting dielectric coating on one end; anti-reflection dielectric coating on the other end.

The new laser cavity consisted of a 6" diameter cylindrical reflecting shell surrounding a linear xenon flash tube (EG&G FX 47B-6.5) mounted parallel to and about 2" away from the laser rod. The power supply for the flash tube had sufficient capacity to provide up to 4500 joules in an approximately one millisecond pulse. In the case of the ruby crystal which had an anti-reflection coating on its output end, an external dielectric mirror, 55% reflecting at 6943Å, completed the laser cavity.

8.1 Experimental Methods

The investigation of the output characteristics of the neodymium and ruby rods included the following measurements:

- (a) Calorimetric: A commercial liquid calorimeter was used to measure the total energy per laser pulse as a function of several operating variables, primarily the energy furnished to the flash lamp.
- (b) Photoelectric: Oscilloscope traces of the laser pulses, as detected by an S-1 multiplier phototube, were photographed simultaneously with the calorimeter measurements. These traces provided pulse duration and peak power data.
- (c) Spectrographic: Spectra of the laser beams were obtained photographically with the 3/4 meter grating spectrograph, at a dispersion of $22\text{\AA}/\text{mm}$.

Simultaneous calorimetric and photoelectric measurements were made with the experimental set-up shown in Figure 10. The output of the laser was focused on the entrance window of the calorimeter absorption cell. A portion of the laser beam was deflected toward the phototube by means of a glass plate used as a beam-splitter. Pulse energies measured by the calorimeter were corrected for Fresnel reflection losses at the several glass surfaces between the laser and the calorimeter.

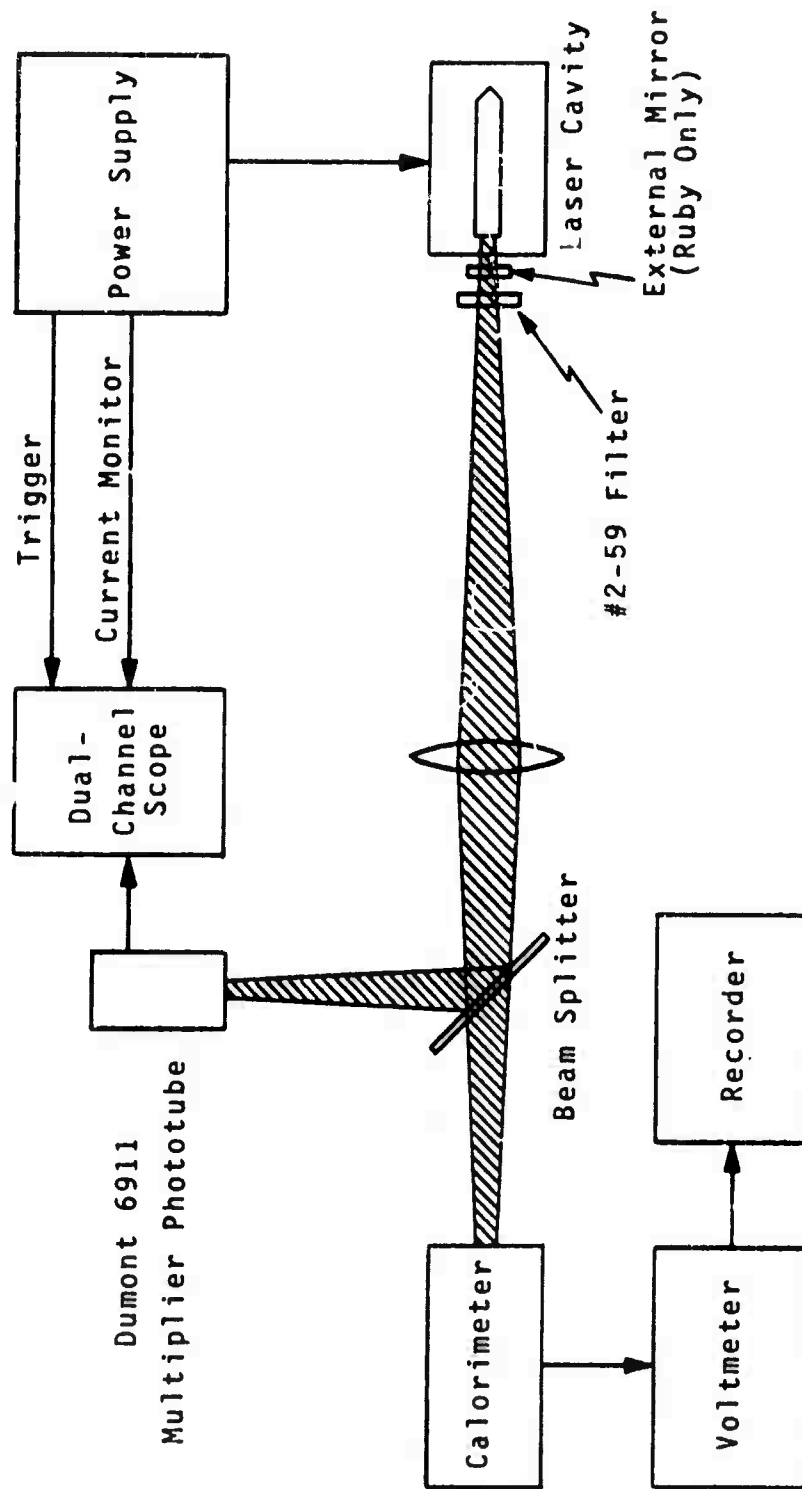


Figure 10. Experimental Arrangement for Investigation of Neodymium and Ruby Laser Outputs

For the spectrographic analyses the outputs from the neodymium and ruby lasers, unfocused and suitably attenuated, were directed at the entrance slit of the spectrograph. Correct photographic plate exposures were obtained by varying the slit opening (between 5 and 20 μ) and the beam attenuation. Either one or two glass plates, each deflecting 8-10% of the incident beam toward the spectrograph, were found to be the most suitable attenuators. Eastman Kodak I-2 spectroscopic plates were used for the neodymium spectra at 1.06 μ and I-N plates, for ruby at 6943 \AA .

8.2 Summary of Results

A summary of the output characteristics of both the neodymium and ruby lasers is presented in Table 8. The laser energies are taken from a plot of calorimeter readings, suitably corrected, versus flash lamp energy. Laser efficiencies are represented by the slopes of these essentially linear plots. For the calculation of peak powers, a triangular pulse shape was assumed; thus:

$$\text{peak power} = 2 (\text{total energy} / \text{pulse width}).$$

This was a very close approximation in the case of the ruby laser, and slightly less accurate for the neodymium rod.

Wavelength positions (for neodymium) and band widths were determined from spectroscopic plates of the neodymium and ruby outputs obtained with low (close to threshold) and high flash lamp energies. As shown in Figure 11, the neodymium spectrum appears as a series of well-defined lines spaced at $\sim 2\text{\AA}$ intervals.

TABLL 8

Summary of Neodymium and Ruby Laser Characteristics

laser	flash lamp energy, joules	laser energy, joules	flash lamp energy at threshold, joules	laser efficiency, percent	laser pulse width, msec	laser peak power, kw	spectral output λ , Å	$\Delta\lambda$, Å
neodymium	1000	0.8	550	0.49	0.46	3.7	10617 10619	28 59
	1250	2.0			0.57	6.9		
	1500	3.2			0.63	10.2		
	1750	4.4			0.67	13.4		
	2000	5.6			0.69	16.6		
	2250	6.9			0.70	19.9		
	2500	8.1			0.70	23.2		
	868	0.2						
	2276	7.0						
ruby	3000	*	3000	0.47	0.23	---	(6943) (6943)	<1.8 <1.8
	3250	*			0.41	---		
	3500	0.3			0.54	1.6		
	3750	1.5			0.62	4.6		
	4000	2.6			0.67	7.6		
	4250	3.8			0.71	10.7		
	4500	5.0			0.73	13.7		
	3310	<0.1						
	4030	2.8						

* Energy too low to be measured with calorimeter
 ** Nominal wavelength; exact wavelength not measured
 *** Output broadened slightly because of plate overexposure

10617Å



Neodymium: flash lamp energy = 868 joules

10619Å



Neodymium: flash lamp energy = 2276 joules
(replicate exposures)

(6943Å)



Ruby: flash lamp energy = 4030 joules

Figure 11. Neodymium and Ruby Laser Spectra Obtained with
3/4 Meter Grating Spectrograph. Entrance Slit = 10μ.

Replicate exposures indicate that the exact positions and relative intensities of these lines are random. The ruby output appears as a single sharp line.

9. PHOTOELECTRIC ABSORPTION SPECTRA

9.1 Experimental Arrangement

Additional measurements of the absorption of white light by cesium vapor have been carried out to supplement the data included in Technical Report GPL A-31-3. The new spectra were obtained with the 3/4 meter Czerny-Turner grating spectrograph used for the earlier photographic absorption studies. In order to extend the region investigated beyond 1.1μ , the region in which Eastman Kodak I-Z spectroscopic plates begin to decrease sharply in sensitivity (even when hypersensitized with ammonia), photoelectric rather than photographic detection was employed in the present work. An automatic scanning and recording system recently put into operation greatly facilitated the acquisition of the absorption data. The amplified output from a lead sulfide photocell at the spectrograph exit slit was fed to the Y axis of a Houston Model HR-97 11x17" X-Y recorder. The X axis was driven by a signal proportional to the wavelength setting of the spectrograph.

Details of the experimental arrangement are shown in Figure 12. A tungsten bulb was used as a source for the absorption measurements, and a low pressure mercury lamp as a calibration standard to check the accuracy of the spectrograph wavelength drive and recorder response. A #2-64 Corning filter which transmits only above 6400 \AA prevented light from entering the spectrograph that could be detected in second and third order by the photocell. Entrance and exit slit openings were each 40μ and the 600 grooves/mm grating gave a dispersion of 22 \AA/mm .

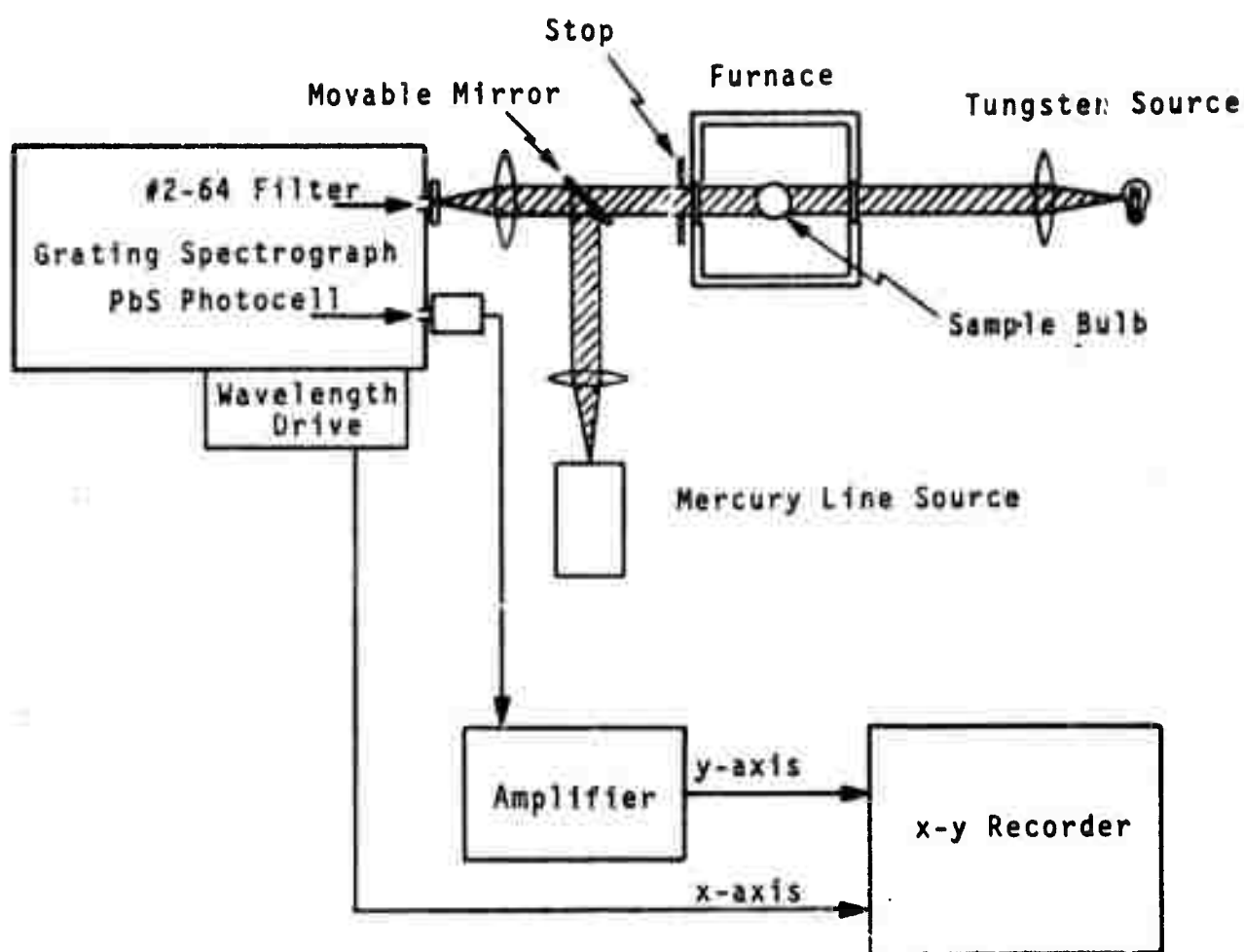


Figure 12. Arrangement of Apparatus For Photoelectric Absorption Spectra Measurements

Since "single-beam" operation was used for obtaining the absorption data, reference curves were first run at room temperature with the cesium bulb in the furnace (negligible vapor absorption occurs at 25°C). These curves served to establish the light levels effectively measured by the recorder throughout the region of interest (7000-13000 Å in the case of cesium). The variations with wavelength of the tungsten lamp output, grating efficiency (grating blazed for maximum efficiency at 1μ), and lead sulfide detector response could thus be eliminated from the cesium absorption curves by comparisons with the reference curves. The reference curves also helped to establish the position and magnitude of atmospheric absorption bands which, although greatly reduced by purging the spectrograph with dry nitrogen, could not be eliminated altogether.

9.2 Presentation of Cesium Results

Traces of the absorption curves (photographically reduced by 60%) for a sample bulb containing cesium and helium, the latter at a pressure of one atmosphere at room temperature, are shown in Figures 13-a, 13-b, and 13-c.

9.3 Discussion of Cesium Results

Comparison of the details of this cesium-helium spectrum run at 320°C with the spectrum of cesium alone obtained under the same conditions indicates that, apart from slight pressure broadening of the D-line absorption bands and the appearance of a new band in the vicinity of 8300 Å, the presence of a buffer gas has little effect on the absorption of cesium.

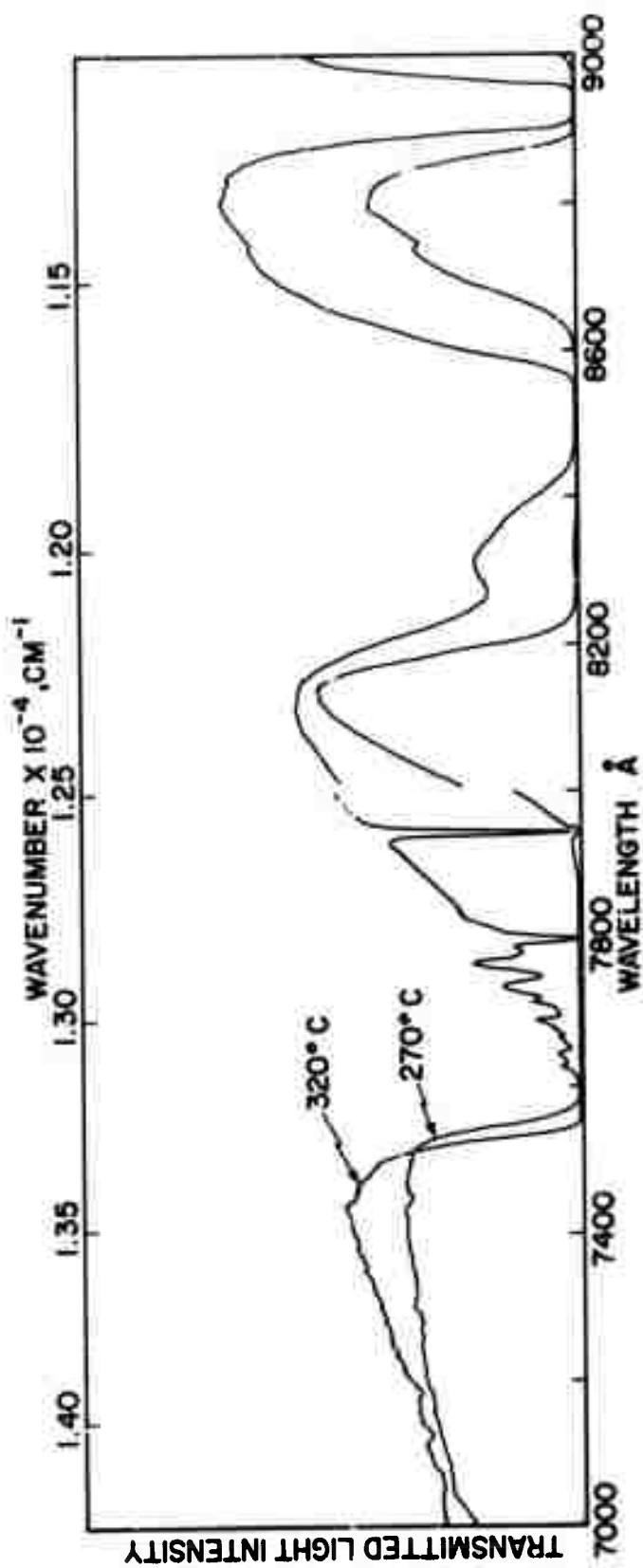


Figure 13-a. Absorption Spectrum of Cesium Vapor with Helium Buffer Gas Between 7000 and 9000 Å; Furnace Temperature = 270 and 320°C. (Bands at 7800 and 7948 Å Are Due To Trace Amounts of Rubidium).

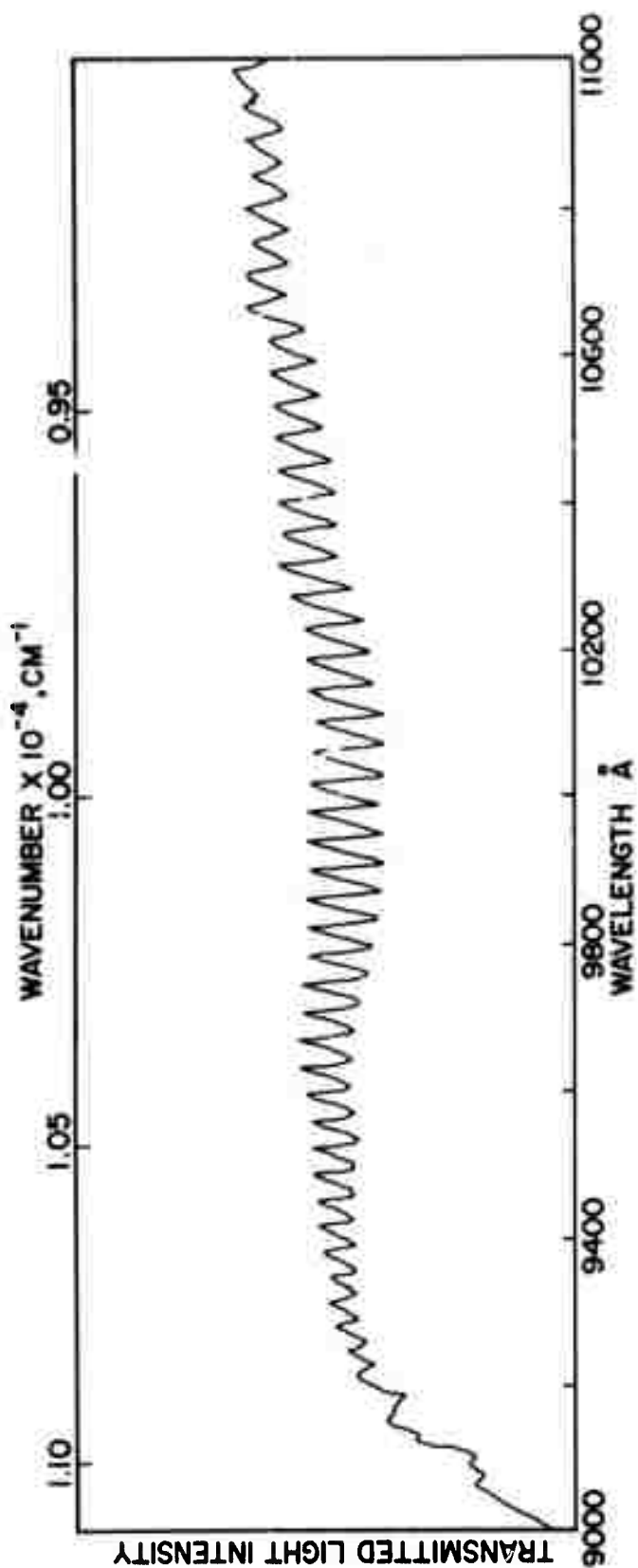


Figure 13-b. Absorption Spectrum of Cesium Vapor With Helium Buffer Gas Between 9000 and 11000 Å; Furnace Temperature = 320°C.

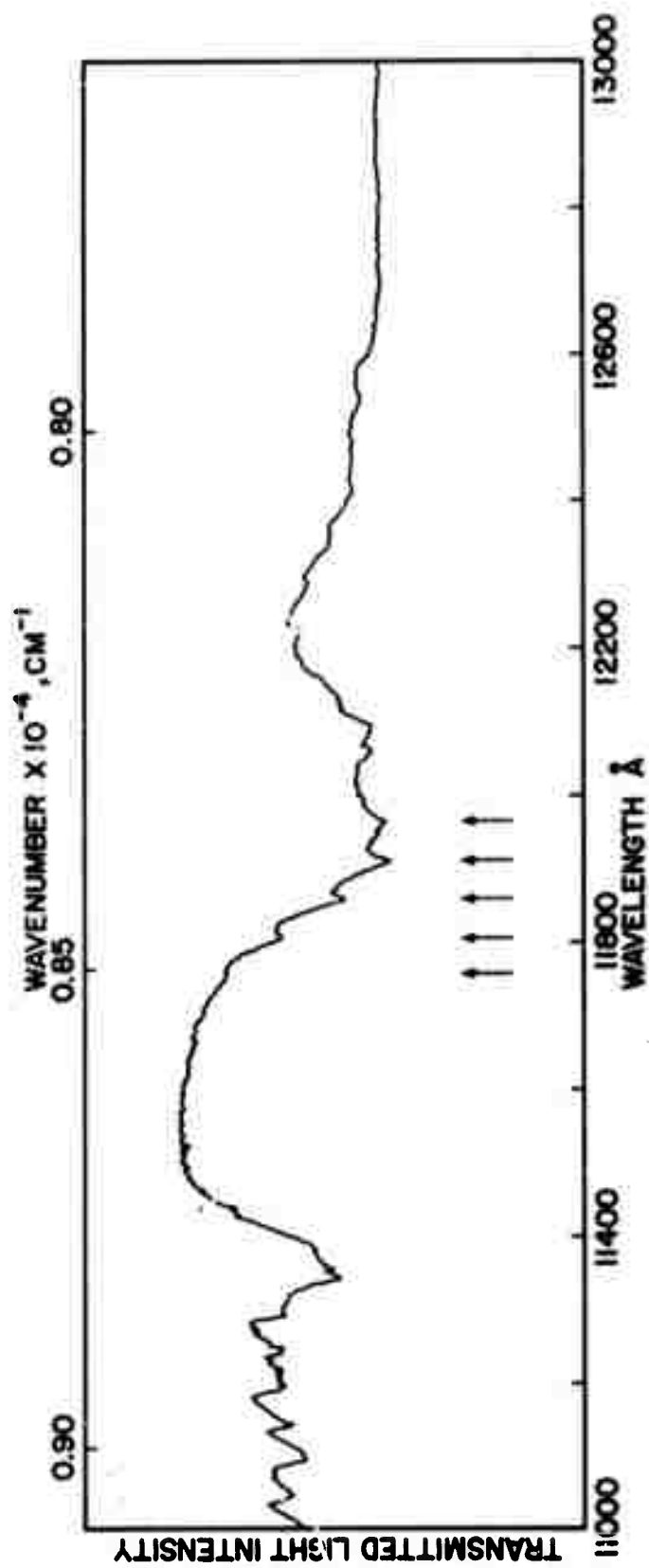


Figure 13-c. Absorption Spectrum of Cesium Vapor With Helium Buffer Gas Between 11000 and 13000Å; Furnace Temperature = 320°C.

The 8300Å band is probably of little consequence in respect to the ultimate question of the effect of neodymium pumping on cesium vapor since it occurs so far below the 1.06μ pumping region.

With the relatively high resolution available with the grating spectrograph, the approximately 40 cm⁻¹ periodicity is easily seen in the X+A absorption region between 9000 and 11500Å. Details of this structure are more apparent in the photoelectric results than in the previously reported photographic spectrum. A significant result of these current studies is the fact that this same 40 cm⁻¹ band structure is also present in the region of 1.18 to 1.22μ. Earlier low resolution photoelectric data, although showing the presence of an absorption band at 1.2μ, had not been able to detect the superimposed 40 cm⁻¹ structure. The appearance of the spectrum in this region is the same for both cesium alone and cesium with helium. The approximate coincidence between sub-band spacings in these new features and in the known Cs₂ bands is at least preliminary evidence that these bands may also belong to Cs₂.

9.4 Rubidium Absorption Spectra

In order to check on the appearance of a spectrum quite analogous to Cs₂, some quick measurements were made on the absorption spectrum of rubidium vapor. The vapor was contained in a 1.2" diameter Corning 1720 glass bulb and maintained at 370-385°C.

Entrance and exit slit openings for the spectrograph were 40 μ each, except in the region 6000-7000 \AA where the lower grating efficiency required settings of 60 μ .

The rubidium spectra, photographically reduced by 60%, are shown in Figures 14-a, 14-b, 14-c, and 14-d.

10. LASER-EXCITED FLUORESCENCE

During the previous report period (Technical Report GPL A-31-3) measurements were made of the fluorescence spectrum of cesium vapor when pumped with a low energy (~ 0.035 joule) neodymium laser. Data were obtained using a low resolution prism monochromator with the cesium vapor maintained at temperatures up to 400°C. These measurements have been extended during the past six months to include an investigation of (a) the effect of pumping with a laser operated at much higher outputs (up to 8 joules) and (b) the effect of the presence of a buffer gas on the cesium fluorescence spectrum.

10.1 Experimental Procedures

Both photographic and photoelectric methods of detecting the fluorescence were attempted. Preliminary efforts using Eastman Kodak I-2 plates, hypersensitized with ammonia solution, were abandoned, however, when it was found that more than fifty laser flashes were required to produce sufficient plate exposure to show the cesium fluorescence in the 1 μ region.

Instead, photoelectric data were taken in a manner comparable to that used previously with the low resolution monochromator. It was not found necessary, however, to monitor

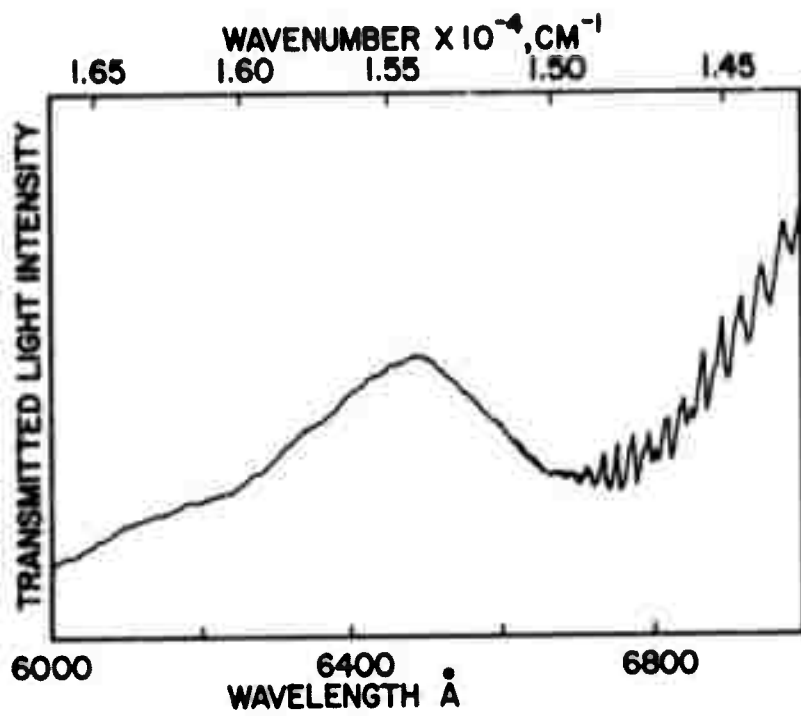


Figure 14-a. Absorption Spectrum of Rubidium Vapor Between 6000 and 7000 \AA ; Furnace Temperature = 385°C.

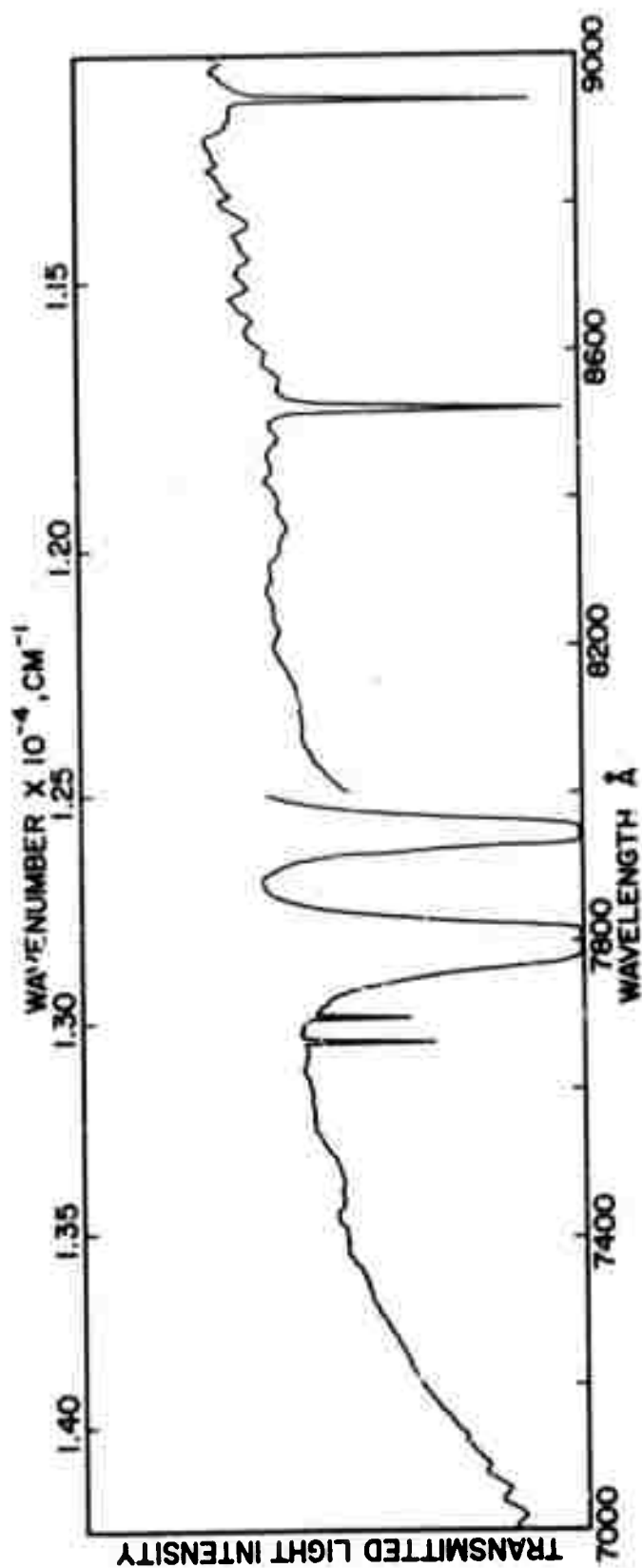


Figure 14-b. Absorption Spectrum of Rubidium Vapor Between 7000 and 9000 Å; Furnace Temperature = 385°C. (Bands at 7665, 7699, 8521 and 8943 Å Are Due to Trace Amounts of Potassium and Cesium).

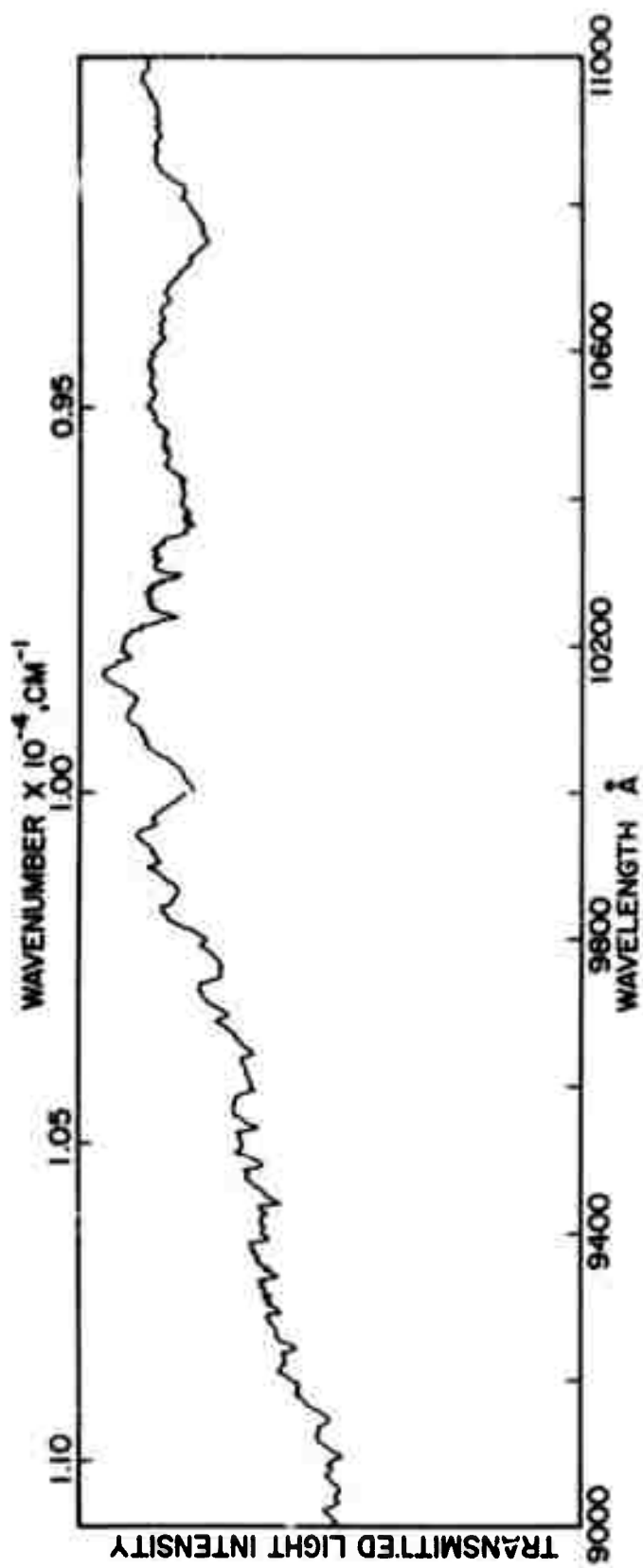


Figure 14-c. Absorption Spectrum of Rubidium Vapor Between 9000 and 11000 Å; Furnace Temperature = 385°C.

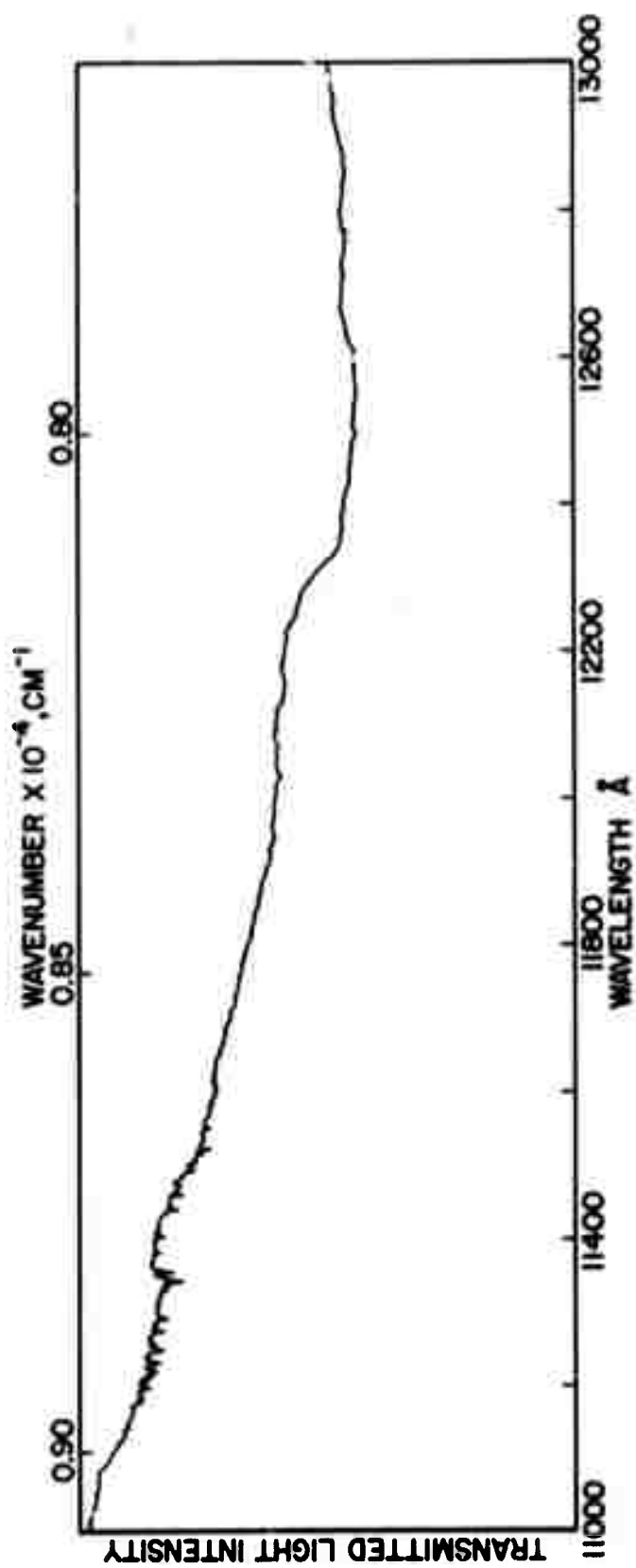


Figure 14-d. Absorption Spectrum of Rubidium Vapor Between 11000 and 13000 Å; Furnace Temperature = 385°C.

the output of the new high power neodymium laser in order to obtain reproducible data. The intensities of successive pulses, when the laser was flashed at one minute intervals, were essentially constant within the accuracy of the measurements. Elimination of the monitor made it possible to read fluorescence peak heights directly from the oscilloscope rather than from photographs of the traces as was necessary when both fluorescence and monitor pulses were recorded simultaneously.

Figure 15 shows the experimental arrangement used for obtaining the fluorescence spectra. The output from the Nd laser was focused on the sample contained in the same Corning 1720 glass used for earlier measurements. The sample bulb was located in a furnace having windows arranged to permit viewing of the light emitted from the vapor at right angles to the pumping beam. A #2-59 Corning filter which transmits only to the red of 6200\AA was used to eliminate much of the extraneous xenon flash lamp radiation from the laser output beam. Measurements made at room temperature indicated that any flash lamp light above 6200\AA reaching the sample bulb and scattered by it to the spectrograph was negligible.

The fluorescence emitted by the cesium when excited by the Nd pump laser was focused on the entrance slit of the $3/4$ meter grating spectrograph. The #2-64 Corning filter at the entrance slit prevented any light below 6400\AA from being detected by the PbS photocell in second and third orders up to 12800\AA , the upper limit of the region of interest in the fluorescence spectra. Measurements were made at 25\AA intervals with both entrance and exit slit openings set at one millimeter and a dispersion of

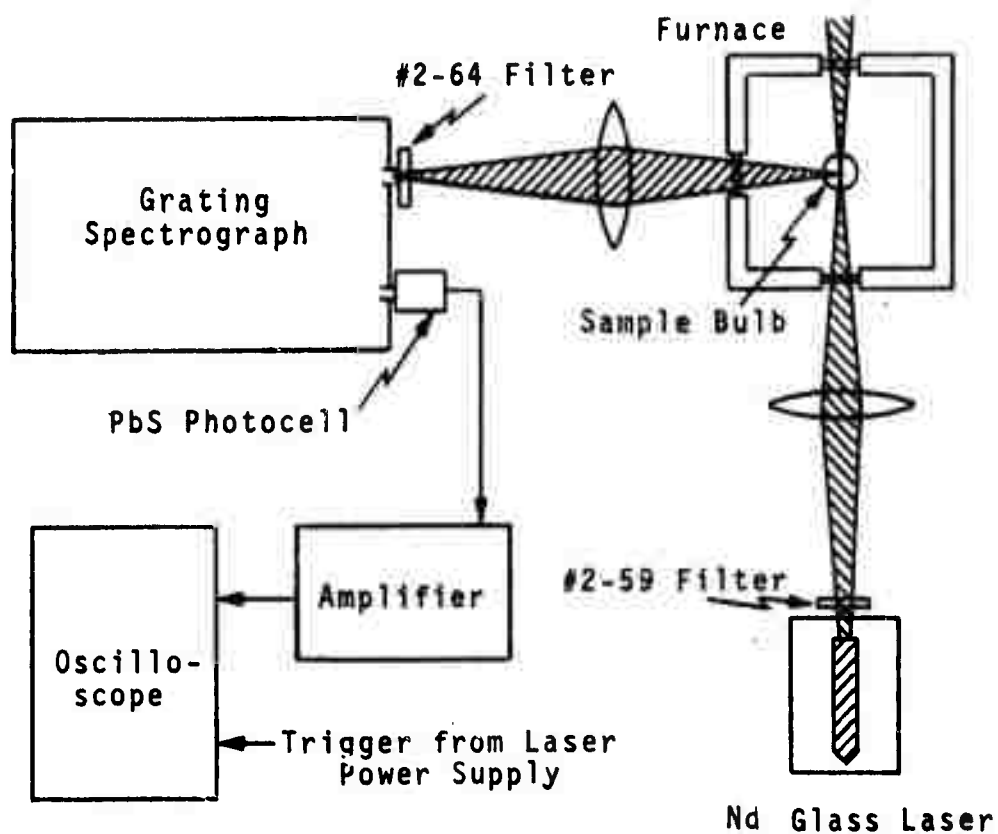


Figure 15. Arrangement of Apparatus for Photoelectric Fluorescence Measurements

22Å/mm. High resolution was thus sacrificed for the convenience of more rapid data taking.

10.2 Presentation of Results

The fluorescence spectra shown in the accompanying figures were obtained by pumping (a) cesium vapor with no buffer gas (Figures 16-a, 16-b, and 16-d) and (b) cesium vapor with helium added to a pressure of approximately one atmosphere at room temperature (Figures 16-c and 16-d.) The neodymium laser was operated at 6 joules output throughout and the cesium bulbs were maintained between 363 and 380°C. It should be pointed out that because both the spectrograph grating efficiency and the PbS photocell response vary with wavelength, the intensities of the fluorescence peaks shown in the above figures are only semi-quantitative. Since the grating efficiency reaches a maximum at 1μ and the detector response at about 2μ , the intensities of the fluorescence peaks below 1μ are actually somewhat greater, relative to those above, than shown.

10.3 Discussion of Results

Several conclusions are apparent from these fluorescence curves. The intense peak in the vicinity of 1μ is simply the instrumentally scattered Nd pump light, that is, light scattered primarily by the walls of the glass sample bulb. A peak of comparable intensity was observed at 25°C; at this temperature the cesium vapor density is well below that necessary for fluorescence to be detected. The width of this scattered light peak,

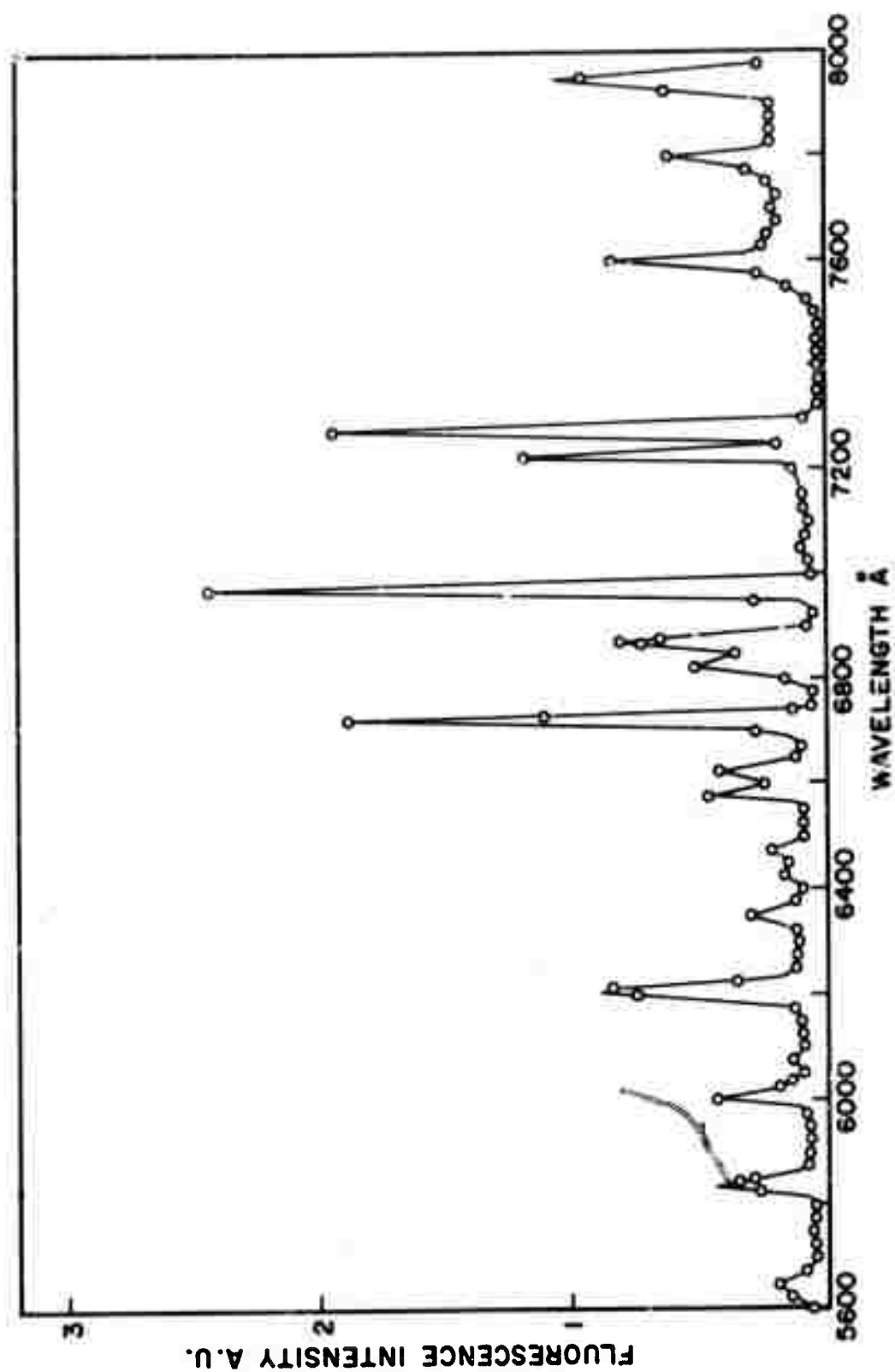


Figure 16-a. Fluorescence Spectrum Between 5600 and 8000Å of Neodymium Laser-Excited Cesium Vapor (Without Helium Buffer Gas); Furnace Temperature = 375°C.

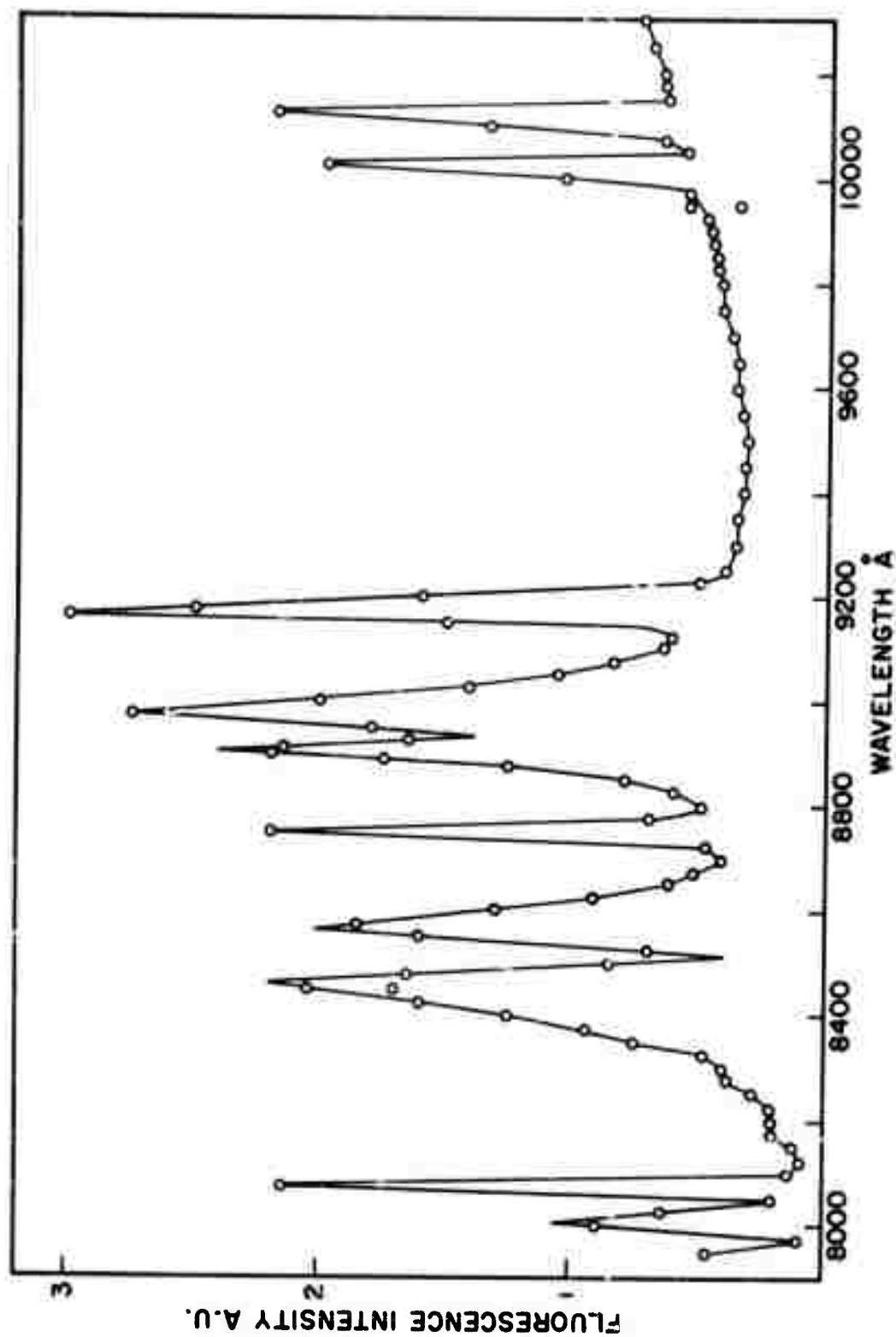


Figure 16-b. Fluorescence Spectrum Between 7900 and 10300Å of Neodymium Laser-Excited Cesium Vapor (Without Helium Buffer Gas); Furnace Temperature = 375°C.

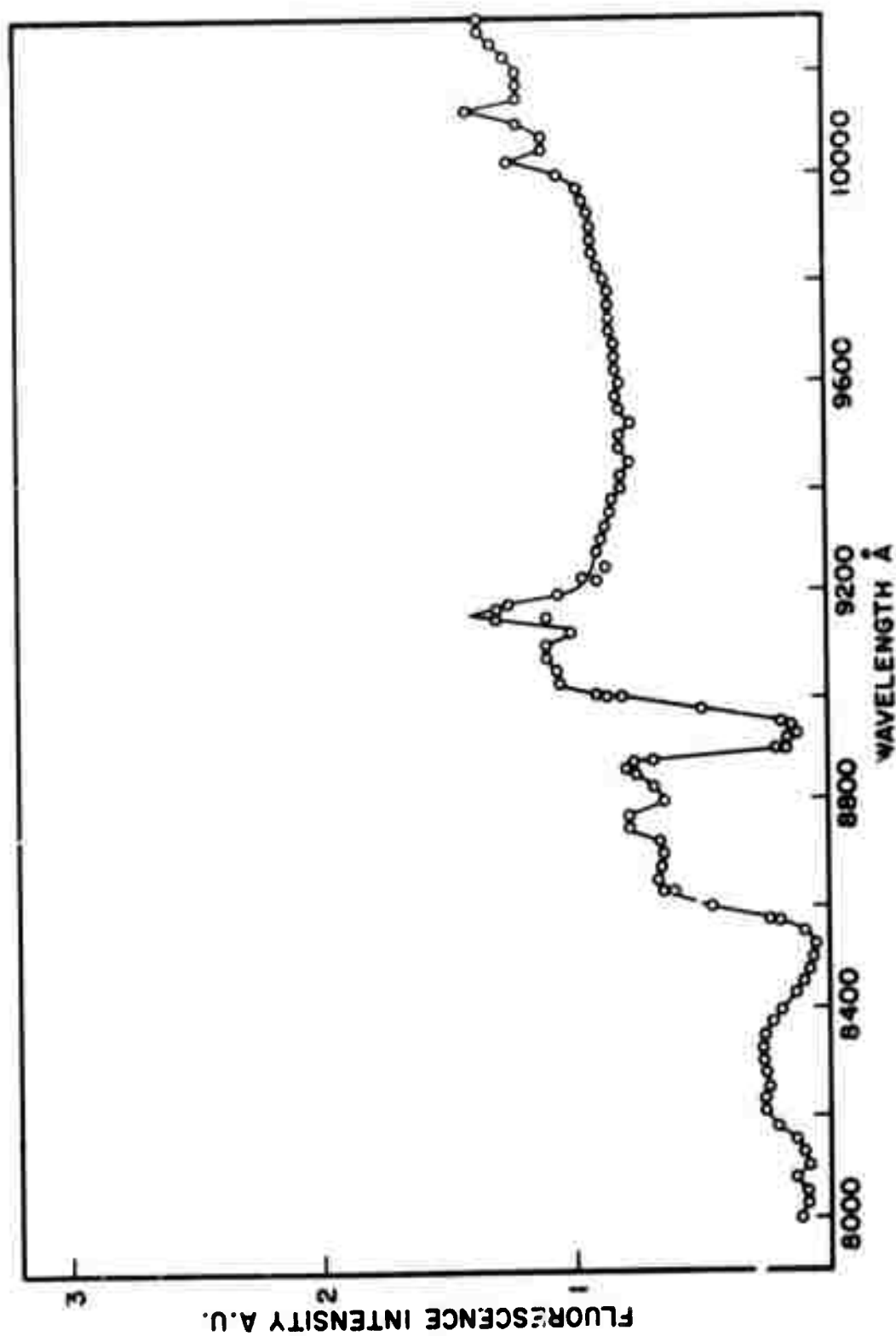


Figure 16-c. Fluorescence Spectrum Between 7900 and 10300Å of Neodymium Laser-Excited Cesium Vapor (With Helium Buffer Gas); Furnace Temperature = 375°C.

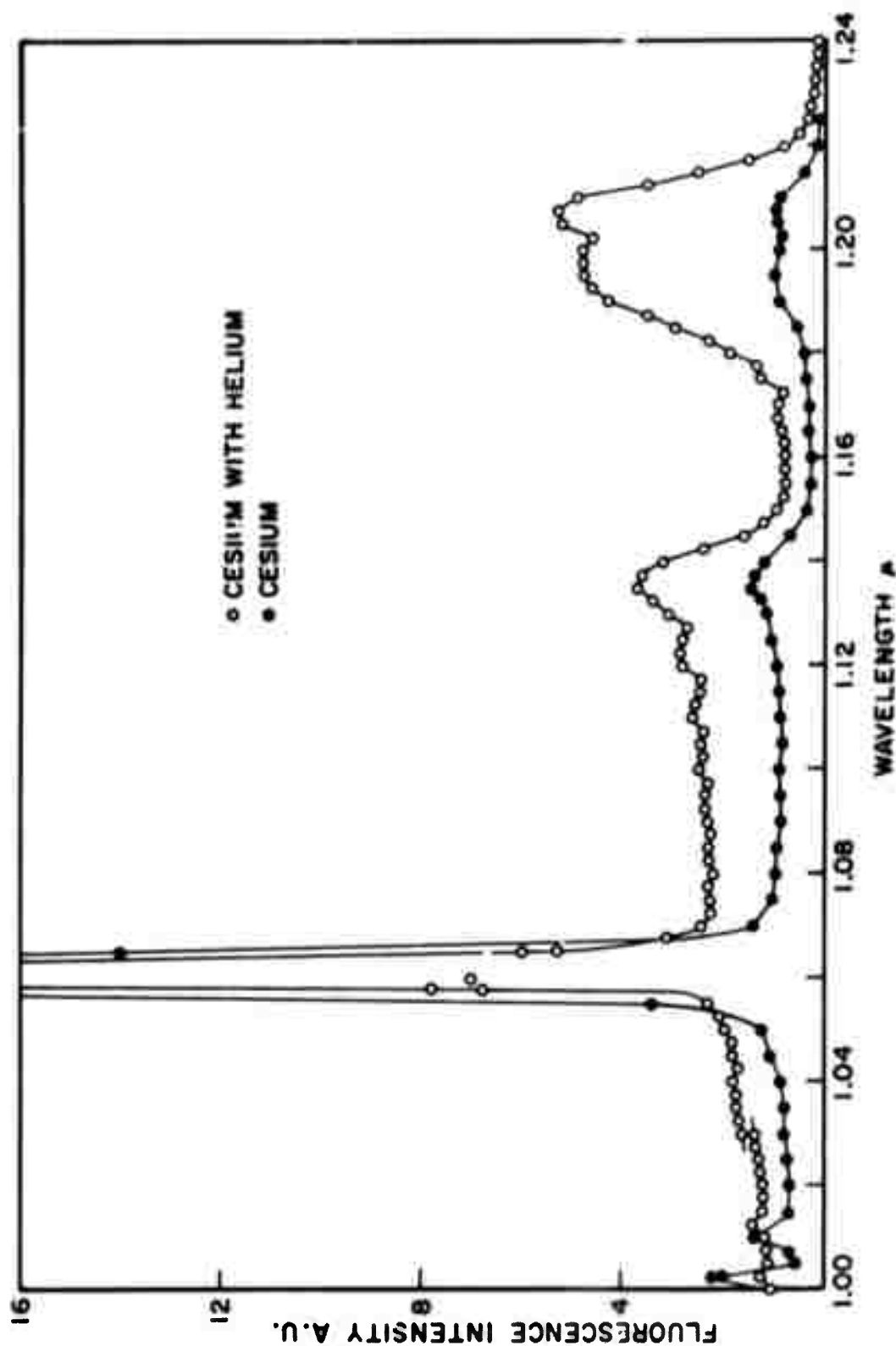


Figure 16-d. Fluorescence Spectrum Between 1.00 and 1.24 μ of Neodymium Laser-Excited Cesium Vapor (With and Without Helium Buffer Gas); Furnace Temperature = 375°C.

$\sim 75 \text{ \AA}$, compared with the actual width of the laser output (60 \AA) determined under high resolution conditions with the grating spectrograph, provides a measure of the resolution obtained with the spectrograph slit widths used in this experiment.

Above and below the 1μ region there is a general background fluorescence of very low intensity. Two distinct peaks appear at 1.135 and 1.20μ , somewhat stronger, relative to the background fluorescence, with helium than without. These peaks are apparently the same as those reported previously (Technical Report GPL A-31-3) although the contours are somewhat different because of the increased resolution in the present work. The positions of these peaks correspond to regions in which molecular absorption occurs (Figure 13-c).

Of particular significance is the absence of any strong emission in the immediate vicinity of the pumping light. It might have been expected that the most likely region for fluorescence to occur would be adjacent to 1.06μ . The resolution of the earlier measurements was not sufficient to distinguish between the strongly scattered laser light and possible nearby fluorescence. It now appears certain that except for the weak background fluorescence mentioned above, no strong emission occurs between 1.06 and 1.12μ .

Perhaps the most striking feature of the fluorescence spectra is the presence of the sharp lines below 1μ in the case of cesium without a buffer gas. A few of the stronger lines are also observed with the bulb containing helium. In both cases the sharp lines appear in a broad continuum. No fluorescence of

of any kind had been detected previously below 9000\AA when cesium was pumped with a 0.035 joule laser. Comparison of this line structure with the known emission lines of atomic cesium shows excellent correspondence both in the positions and relative strengths of the lines. The atomic resonance lines at 8521 and 8944\AA are observed with their centers "burned-out" because of self-reversal, more so in the case of buffered cesium than with cesium alone.

10.4 Effect of Varying Laser Power

The effect of varying the laser pump energy was briefly investigated in the region of the strong fluorescence band at 1.2μ . The data in Figure 17 show that as the laser output is increased from approximately 0.5 to 8 joules, the fluorescence at 1.205μ , the position of the band maximum, evidently approaches a limiting value at laser energies of 8 to 10 joules. This may be simply due to the decrease in molecular density during the more intense laser pulses as discussed in Section 11. It is also apparent that the strengths of the two peaks which make up the band (at 1.1925 and 1.205μ) change, relative to each other, as the pump power is varied.

10.5 Fluorescence with Ruby Excitation

In order to understand better the mechanism by which the cesium fluorescence was produced in the case of the neodymium-pumped vapor, the effect of exciting unbuffered cesium with the output of a ruby laser was briefly investigated. The characteristics of this laser are described in Section 8. In contrast

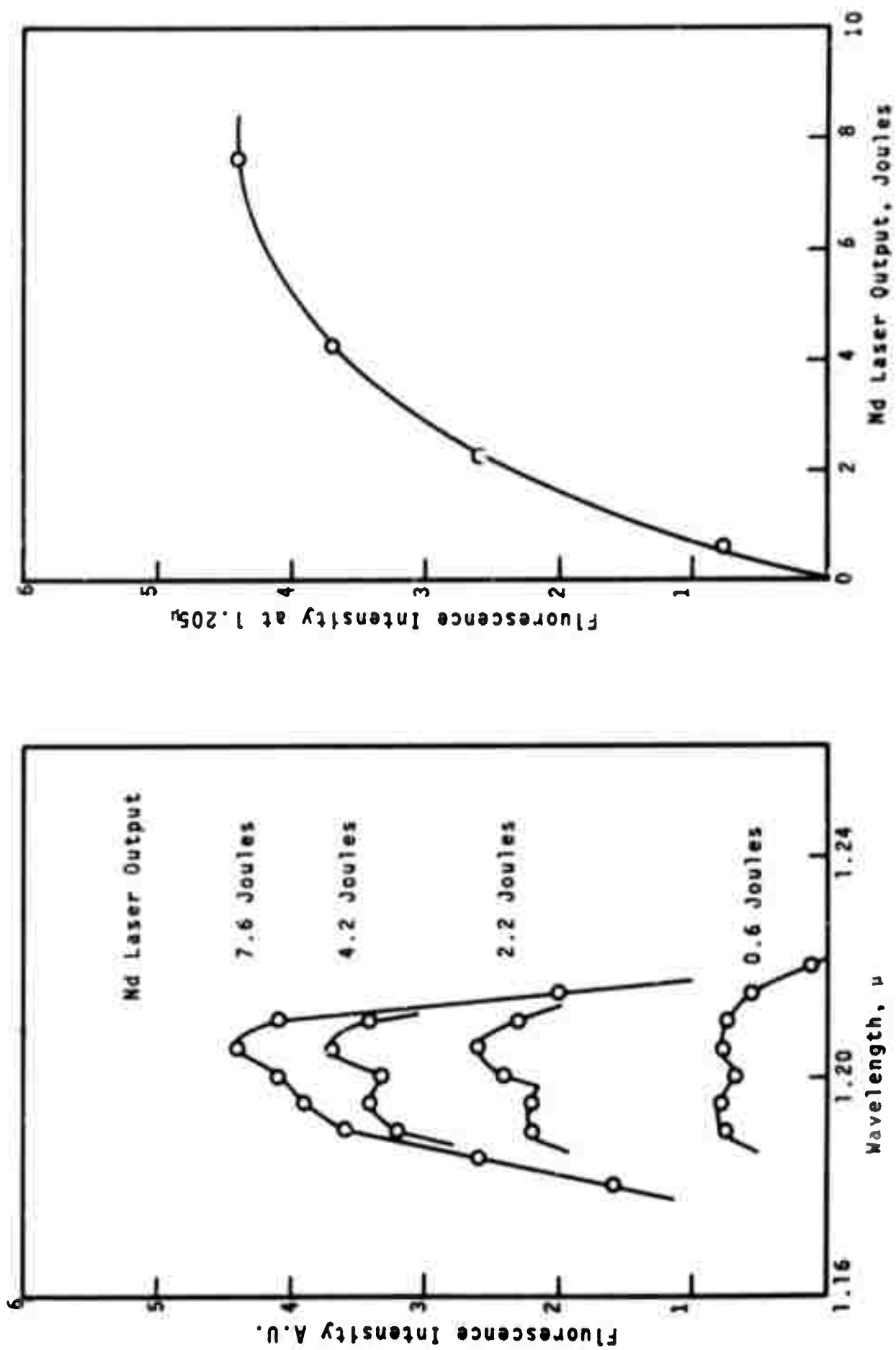


Figure 17. Cesium Fluorescence as a Function of Neodymium Laser Energy.

to the case of the Nd laser whose output falls in a region of strong cesium absorption, the ruby output is in a region in which no measurable absorption occurs.

Fluorescence data were obtained for the ruby-cesium combination at 370°C between 8000 and 9400Å in the same manner used for the Nd - cesium studies. As in the case of neodymium pumping, strong atomic emission lines were observed in this wavelength region. The self-absorbed D-lines were similar in appearance to those shown in Figure 16 for Nd excitation. Weak emission lines also appeared at 8750 and 9175Å; the 8075Å peak, however, was not present.

From these results it is apparent that the mechanism responsible for the excitation of atomic cesium fluorescence does not require that the vapor be pumped in a region of strong, single-quantum absorption.

11. TIME-DEPENDENT ABSORPTION STUDIES OF CESIUM VAPOR

An experiment was conducted for the purpose of determining the relative number of cesium molecules before, during, and after an intense Nd^{3+} laser pulse. In this experiment a probe beam of "white" light was directed through the cesium cell, and its absorption at a selected wavelength was monitored during the time of the pulse. The changes in intensity of the transmitted probe beam provided a measure of the number of absorbers as a function of time. These observations were repeated at several wavelengths.

11.1 Experimental Arrangement and Procedures

The arrangement of the apparatus for observing the time dependence of the absorption is shown schematically in Figure 18. The cell to be studied was placed in an oven with windows that provided access to the cell from several directions. The light from the Nd^{3+} glass laser was focused on the cell to be studied. A Corning #2-64 filter was placed in the beam to keep the short wavelength components of the flash lamp from getting into the cesium cell. A second beam of light was directed through the cell in a direction perpendicular to the laser beam direction. This beam, from a tungsten lamp operated from a regulated source, was approximately parallel and was restricted by means of stops so as to travel through only the central portions of the cesium cell. This second beam could be chopped by means of a slotted disk mounted on the shaft of a variable speed motor. When turned by hand the slotted

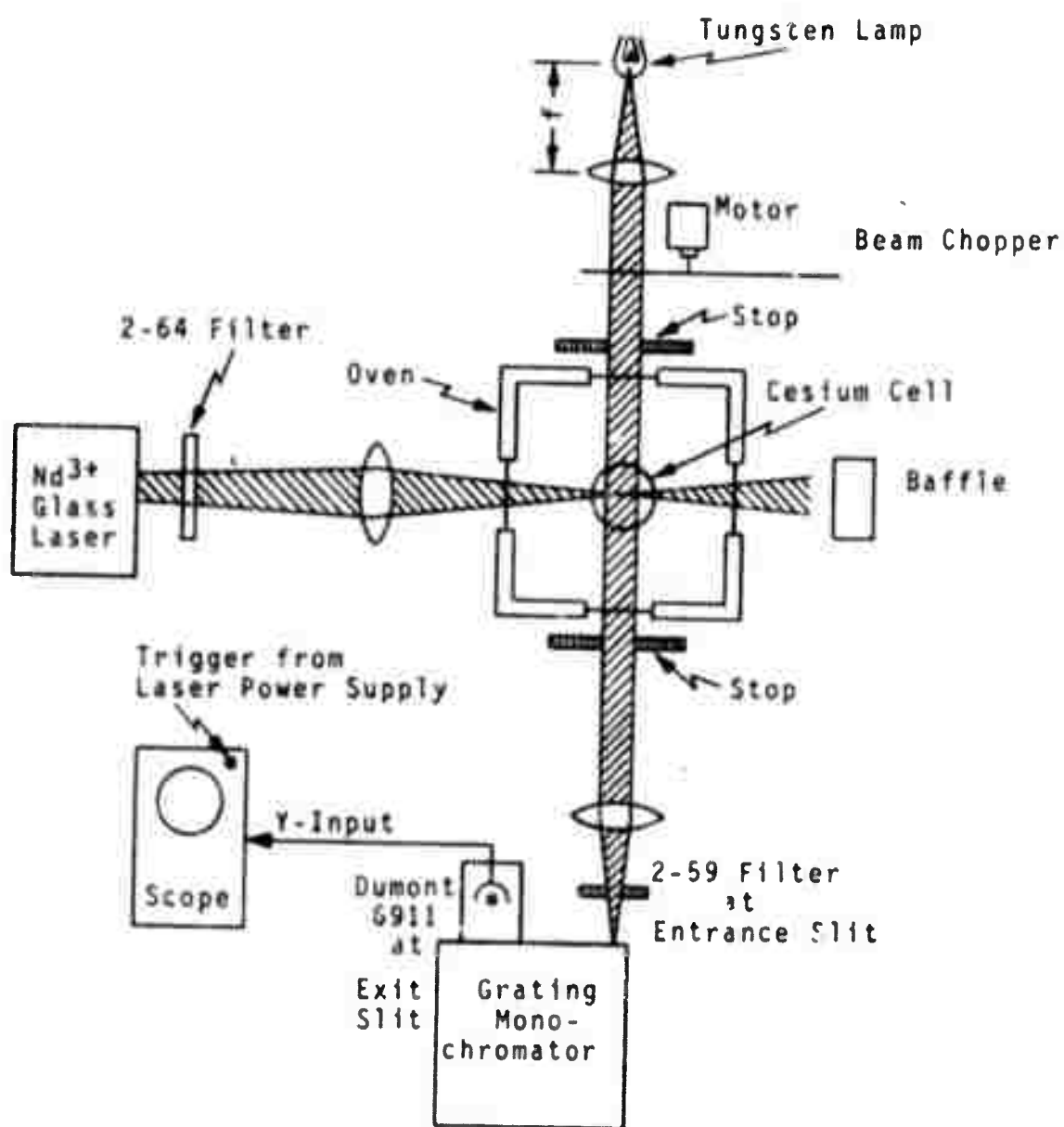


Figure 18. Experimental Arrangement for Observing Time Dependent Absorption Spectrum

disk also served as a shutter to block permanently or pass the beam. The beam from the tungsten lamp after leaving the oven was focused on the entrance slit of the 3/4-meter grating monochromator. All measurements were made in first order with a 600 grooves/mm grating blazed for 1μ . The output of the monochromator was monitored with a multiplier phototube (Dumont 6911-S-1 response) connected directly to the input terminals of an oscilloscope.

The following procedure was used for observing the time dependent absorption. With the cesium cell at room temperature, the intensity of the probe beam transmitted through the cell was measured at several wavelengths. These observations provide a reference level of the unattenuated beam. Then with the cesium cell at about 355°C , the intensity of the transmitted probe beam was observed as a continuous function of time beginning shortly before the rise of the laser pulse. The transient signals thus generated were photographed from the screen of an oscilloscope. With the cell still at 355°C , the intensity of the radiation from the cell excited by the laser was recorded while the probe beam was blocked. This gave a measure of the fluorescence radiation. The slow recovery of the absorption of the cell was also studied with the probe beam chopped. This provided a measure of the total light intensity during the transient behavior of the absorption.

Two cesium cells were used in these experiments: one contained saturated cesium vapor and the other, one atmosphere of helium in addition to the saturated vapor. Both cells were about 1.2 inches in diameter and were hand-blown from Corning 1720 glass.

11.2 Presentation of Results

Typical photographic records of the time-dependent absorption are shown in Figures 19, 20, and 21. The coordinates in these pictures are: time running left to right and light intensity increasing downward. In trace *a* Figure 19, taken at 9800\AA with the probe beam through the saturated cesium vapor cell, the changes of light levels relative to that before the laser pulse can be seen. At the onset of the laser pulse the light level increases to a maximum and then decays rapidly to a value greater than that which existed before the laser pulse, as shown by the increased transmitted intensity of the probe beam. That this is not some long-time fluorescence can be seen by comparison with trace *b* which was taken with the probe beam blocked. In this case, the light level immediately before and after the laser pulse is the same. The rise in intensity is just the molecular fluorescence excited by the laser.

The slow recovery of the absorption of the cell following the laser pulse can be seen in trace *c* which was again taken with the probe beam through the cell but at a sweep rate of 20 msec/div. Trace *d* provides the comparison with the probe beam blocked. The fluorescence pulse does not show in these photographs because the photographic exposure was chosen to show the slow recovery rather than the initial short (on this time scale) pulse at the very beginning of the trace.

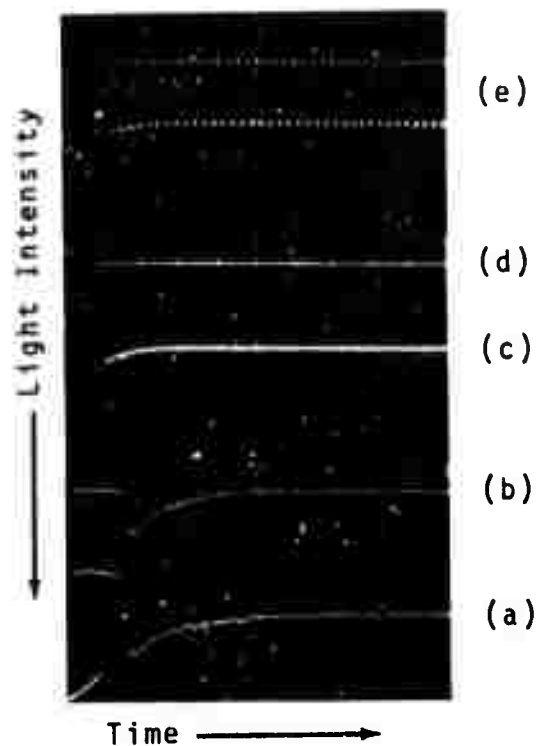


Figure 19. Time Dependent Absorption Curves for Saturated Cesium Vapor at 355°C ($\lambda = 9800\text{\AA}$).

- (a) Transmitted Probe Beam Intensity Plus Fluorescence, Sweep Rate: $200\mu\text{s}/\text{div}$.
- (b) Probe Beam Blocked - Fluorescence Only Sweep Rate: $200\mu\text{s}/\text{div}$.
- (c) Transmitted Probe Beam Intensity* Sweep Rate: $20\text{ms}/\text{div}$.
- (d) Probe Beam Blocked* Sweep Rate: $20\text{ ms}/\text{div}$.
- (e) Transmitted Probe Beam Intensity (Chopped)* Sweep Rate: $20\text{ ms}/\text{div}$.

*Fluorescence pulse does not show in photographic exposure chosen.

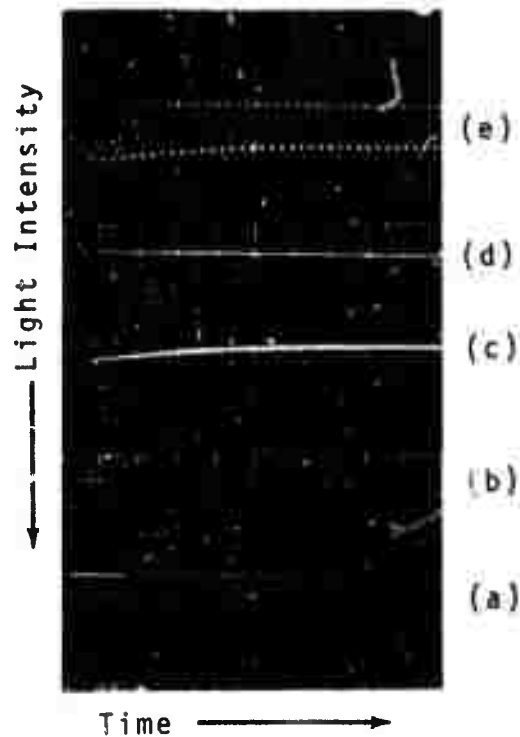


Figure 20. Time Dependent Absorption Curves for Saturated Cesium Vapor with One Atmosphere of Helium at 355°C ($\lambda = 7530\text{\AA}$)

- (a) Transmitted Probe Beam Intensity Plus Fluorescence, Sweep Rate: 200 $\mu\text{s}/\text{div}$.
- (b) Probe Beam Blocked - Fluorescence Only Sweep Rate: 200 $\mu\text{s}/\text{div}$.
- (c) Transmitted Probe Beam Intensity* Sweep Rate: 20ms/div.
- (d) Probe Beam Blocked* Sweep Rate: 20ms/div.
- (e) Transmitted Probe Beam Intensity (Chopped)* Sweep Rate: 20ms/div.

*Fluorescence pulse does not show in photographic exposure chosen.

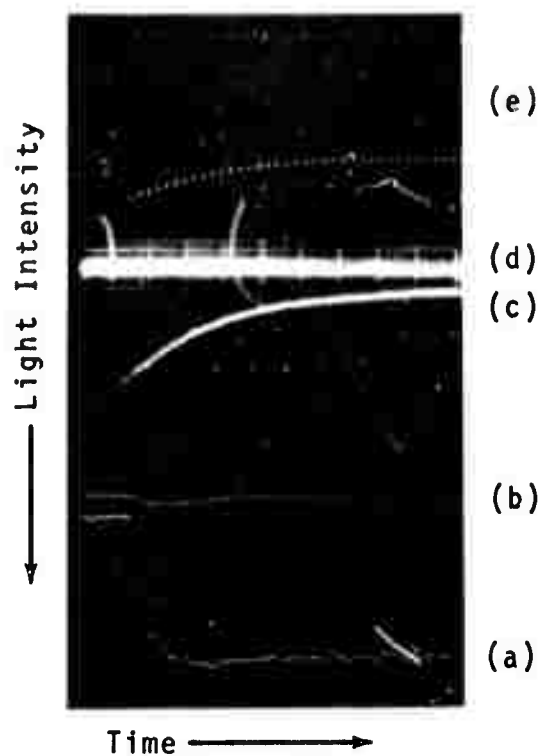


Figure 21. Time Dependent Absorption Curves for Saturated Cesium Vapor with One Atmosphere of Helium at 355°C ($\lambda = 9800\text{\AA}$).

- (a) Transmitted Probe Beam Intensity Plus Fluorescence, Sweep Rate: 200 $\mu\text{s}/\text{div}$.
- (b) Probe Beam Blocked - Fluorescence Only Sweep Rate: 200 $\mu\text{s}/\text{div}$.
- (c) Transmitted Probe Beam Intensity* Sweep Rate: 20ms/div.
- (d) Probe Beam Blocked* Sweep Rate: 20 ms/div.
- (e) Transmitted Probe Beam Intensity (Chopped)* Sweep Rate: 20 ms/div.

*Fluorescence pulse does not show in photographic exposure chosen.

Curve *e* was obtained with the tungsten light chopped in order to give a measure of the light intensity above the zero light level. The similar set of curves in Figure 20 was obtained with the Cs + He bulb at 9800Å. In Figure 21 the same set of observations was made on the Cs + He bulb at 7530Å. This wavelength is on the blue side of the (X+B) absorption band. Similar observations were made several times under these conditions and at several other wavelengths. In one set of measurements the energy of the laser was varied. The results of these observations are summarized in Table 9.

11.3 Discussion of Results

A comparison of the data at different wavelengths obtained directly from the pictures provides only a qualitative picture, since the output of the multiplier phototube is a complex, undetermined function of the grating response, output of the tungsten bulb, and response of the photocathode surface. A comparison can be made, however, of the relative transmission at the various wavelengths by normalizing the curves to the intensity of the incident light. The data reduced in this way are shown in Table 9. In the table are included the wavelengths at which the observations were made, the temperatures of the cesium cell, the ratios I_L/I_0 , I_T/I_0 , and f , where

I_L/I_0 is the ratio of intensity of the light immediately after the laser pulse to the incident intensity

TABLE 9

Summary of Time-Dependent Absorption Measurements
on Cesium-Helium Cell

Wavelength, Å	Temperature, °C	Energy of Laser Pulse, Joules	I_T/I_O	I_L/I_O	f
9800	359	4.7	.38*	.61*	.48*
9800	355	1.4	.38**	.57**	.39**
9800	355	0.5	.38+	.48+	.21+
9775	355	4.7	.33	.59	.52
9750	355	4.7	.31	.59	.54
7600	355	4.7	.0054**	.053**	.45**
7530	356	4.7	.34	.54	.43

* Average of 7 readings

+ Average of 3 readings

** Average of 2 readings

I_O is the transmitted light intensity with the cell at room temperature.

I_T is the transmitted light intensity with the cell at temperature T.

I_L is the transmitted light intensity immediately after the laser pulse.

I_T/I_0 is the ratio of intensity of light before the laser pulse to the incident intensity

f is the fractional decrease in average absorption coefficient immediately after the pulse.

The fractional decrease of the average absorption coefficient of the cell can be obtained from the simple consideration of linear absorption, i.e., that the transmitted intensity is $I = I_0 e^{-\bar{a}l}$ where \bar{a} is the average absorption coefficient and l is the length of the container. The incident intensity I_0 was taken to be that transmitted through the cell at room temperature.

In the case of the cesium cell with an atmosphere of helium added, the average absorption coefficient was about 50% less immediately after the laser pulse. The increase in transmission was found to be directly related to the laser energy.

In the case of the cell that contained only cesium, the average absorption coefficient decreased by more than the 50% observed in the Cs + He cell. A quantitative comparison between these data is not significant since the position and quality of the focus of the laser beam in the cells was not controlled and the ability to reproduce results after moving the cells was not tested.

Along this same line, since the laser light does not illuminate the entire path of the probe beam, the absorption

coefficient may vary considerably along this path. Therefore, the average coefficient is the quantity determined.

The rate at which the average absorption recovers after the laser pulse can be estimated by fitting an exponential curve to the data. For the curve in Figure 19 obtained with the bulb containing only cesium, the time constant is 17 ± 4 ms. This time constant, determined for the curve at 9800\AA , is the same for observations at other wavelengths. For the curves in Figures 20 and 21 obtained with the cesium-helium bulb, the time constant is approximately 57 ms. The decay curves in Figures 20 and 21 are similar.

Another observation can be made from these pictures: the rate at which the average absorption of the cell *decreases*. This is best seen in the bottom trace of Figure 21. In the other curves the fluorescence tends to obscure this rate. Within $200\ \mu\text{s}$ the absorption is at its lowest value. The absorption decreases most rapidly at the beginning of the laser pulse.

If the absorption is assumed to be due to transitions upward in the molecular spectrum, then the data indicate a decrease of at least 50% in the number of molecules in the ground state during the laser pulse. Possible mechanisms for this are discussed in Section 12.

12. DISCUSSION OF EXPERIMENTAL RESULTS

The objective of the experimental program was to evaluate molecular cesium as a transformer laser medium. It was expected that part of the energy delivered by the pump laser would be re-emitted as coherent light along the axis of the cesium laser cavity. Preliminary calculations gave a theoretical prediction of sufficiently high gain for lasing to occur in even a very low Q cavity.

No lasing action was observed. This may have been due to a lower gain in the laser medium than had been predicted. If this were the case, improvements in the design of the cavity and particularly in the optical quality of the cesium cell conceivably could have led to lasing. Because of the practical difficulties of obtaining high optical quality in Corning 1720 glass, all attempts to produce lasing were made with bulbs simply blown from this glass. It may also have been that the correct time, optical frequency, and direction were not chosen for looking for the laser radiation. However, it is most probable in light of the following discussion that the Cs_2 molecules in these experiments were dissipated early in the pulse.

An important observation was that very little of the 1.06μ radiation incident on the cesium cell was absorbed, although measurements of the absorption spectrum of the hot cesium cell throughout this spectral region showed the bulb to be a very strong absorber for white light. In Technical Report GPL A-31-2 the hot cesium vapor was shown to be a good absorber of very

low intensity 1.06 μ laser light. The study of the time-dependent absorption of the cesium vapor at wavelengths other than 1.06 μ during and after the laser pulse showed that, indeed, the absorption of the hot cesium vapor decreased at all wavelengths tested. The most likely reason for this is the disappearance of the cesium molecules during the laser pulse. If such were the case, this could also account for the low attenuation of the laser beam itself on passing through the hot cesium vapor. During the initial rise of the laser pulse, most of the diatomic cesium molecules are destroyed. Some of the laser energy would be absorbed during this time. The remainder of the pulse would then be transmitted unattenuated by transitions in diatomic cesium molecules.

Any process that is proposed to describe the removal of the cesium molecules must also fit the observations of the relatively slow regrowth of the absorption following the pulse. As order of magnitude numbers: the molecules disappear in about 100 μ s and reform at a rate of about $(17 \text{ ms})^{-1}$ in the case of the cell containing saturated cesium vapor and about $(57 \text{ ms})^{-1}$ in the cell containing an atmosphere of helium in addition to the saturated cesium vapor. The process in addition should also provide the mechanism for exciting the atomic fluorescence.

First consider a mechanism that does not destroy the molecules but only places them in states which are connected

to excited states by transitions outside the region of wavelengths that were examined. Such a mechanism would require that thermal processes tending to restore thermal equilibrium do not fill the ground state X of Cs_2 . This does not seem likely.

Among the processes which could cause the Cs_2 molecules to disappear are included formation of higher cesium polymers, decrease in atomic density, and dissociation of the cesium diatomic molecules. The first can be eliminated as unlikely. The thermal dissociation of the polymers would compete with the formation of them.

If the atomic density were to decrease during the laser pulse, the molecular density would also decrease. The formation of minute cesium metal droplets during the laser pulse would account for this. A quick search for this fog did not show any to be detectable (using scattering techniques). Also the appearance of strong atomic fluorescence during the pulse does not fit well with this hypothesis.

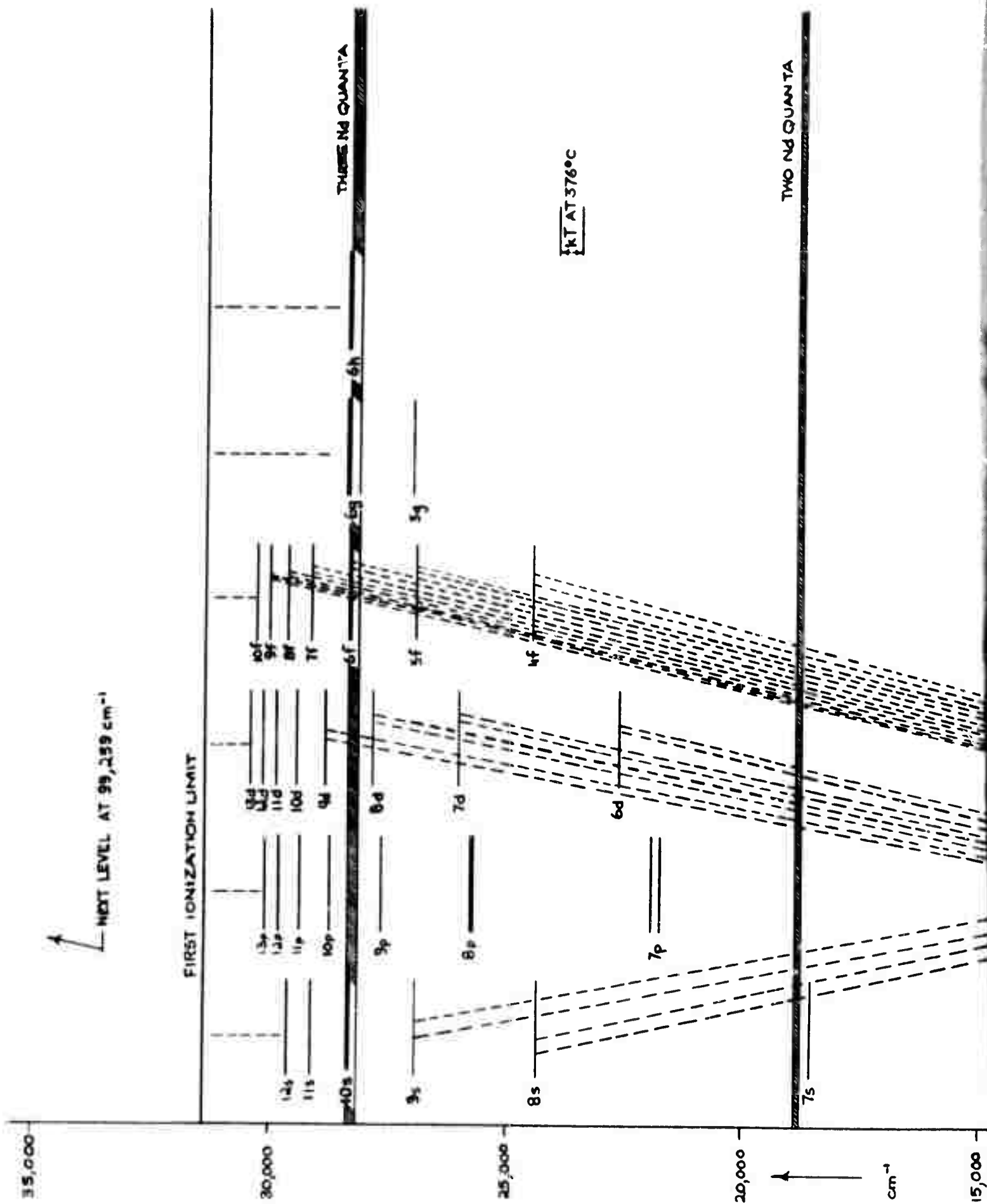
The cesium diatomic molecules may be directly broken up by photodissociation or indirectly by a rise in the temperature of the vapor. The final explanation of this phenomenon will probably include both direct and indirect dissociation as playing important roles. Direct photodissociation of the Cs_2 molecules can easily be seen to require a much greater energy than is available from the laser that was used. If photodissociation

were the only process, the number of photons required to destroy the molecules is not just a factor of two or three times the number of molecules present (the order of 10^{16}) but many times this, since thermal processes would continuously be remaking the molecules. The rate of formation of Cs_2 under normal conditions is probably less than a microsecond.

The change in molecular density due to a temperature rise through an isovolumic, constant density process was discussed in Section 5.3. An input of 1.8×10^{-2} joules/cm³ is required for a loss of 50% of the molecules at 250°C in the case of cesium plus one atmosphere of helium. An input of 1.7×10^{-6} joules/cm³ for the saturated cesium would result in 50% of the molecules being dissociated.

Dissociation of the molecules due to the sudden shift in temperature of the vapor brought about by the absorption of a small amount of the energy in the laser pulse would seem to fit the experimental observations.

The energy delivered to the vapor could be that left behind after multiple photon absorption either by the atomic or the molecular systems. For example, as shown in Figure 22, the energy of three photons comes within a few kT at 350°C of the 6f level in atomic cesium. Any non-radiative transitions made by an atom that has absorbed three photons would go into thermal energy to heat up the gas. The absorption of three photons by a Cs_2 molecule would lead to the ionization of the molecule. (The ionization threshold for Cs_2 is about $26,000 \text{ cm}^{-1}$;



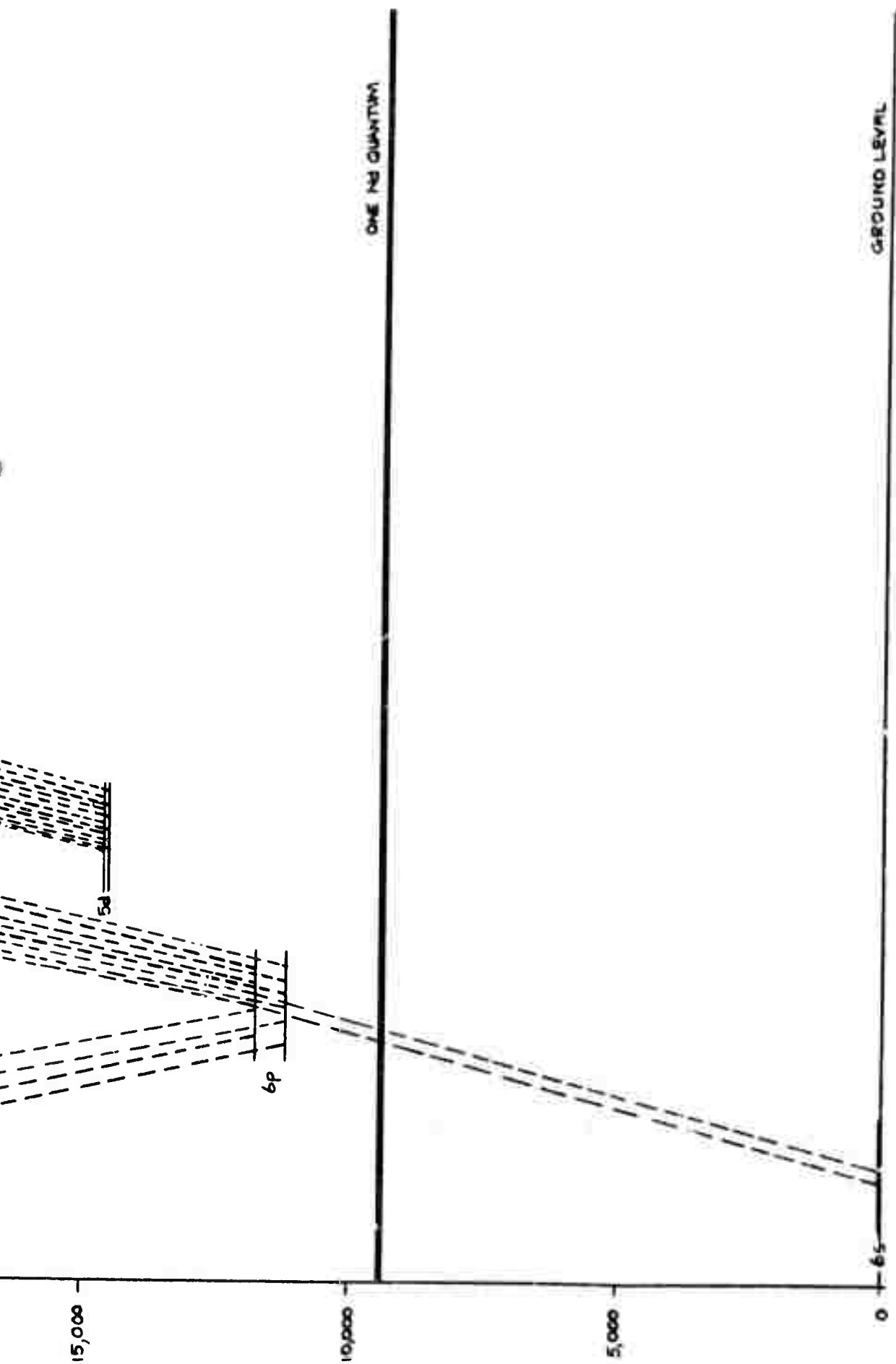


Figure 22. Energy Level Diagram for Cesium Showing Coincidences with Neodymium Laser Quanta.

the energy of three 1.06μ photons is $28,300\text{ cm}^{-1}$.) The probability of molecular ionization by three photon absorption is most likely greater than the raising of a Cs atom to the 6f level since no resonance energy conditions need be satisfied on reaching the final state in the case of ionization.

The ionization, or breakdown of gases due to focused, intense laser beams has been reported and analyzed by many authors, Tomlinson et al (1966), Haught et al (1966), and Bebb (1966). Most of these works were concerned with Q switched beams in which the powers used or assumed were much greater than those used in the present work. Although the details of the breakdown have not yet been found, it seems that multiple photon ionization provides the initial free electrons which then interact with the intense light beam to couple energy to the gas. Damon and Tomlinson (1963) reported comparable photo-ionization produced by either conventional or Q switched ruby laser pulses.

One process proposed for the heating of the cesium vapor is the coupling of the laser energy to the molecules and atoms via electrons that have been released by non-linear processes during the initial part of the pulse. Energetic electrons colliding with the atoms would be capable of exciting them to higher levels and thus account for the atomic fluorescence that was observed.

The results of the experiment performed with ruby light on cesium tend to agree with this. The cesium molecular spectrum shows no detectable absorption from the ground state at the ruby

wavelength. Two-photon absorption by the cesium atom (from 6s to 9d) is not likely with the ruby laser operated at room temperature (Abella 1962). However, two photon absorption in the Cs_2 molecule is quite likely to produce molecular ions and free electrons.

In the case of the cesium being illuminated by the Nd laser light another process may be proposed to account for the heating of the gas. Since the Cs_2 molecule can absorb 1.06μ light directly, a sizable population of excited Cs_2 molecules would be created during the beginning of the laser pulse. In a collision between two excited molecules one may as a result drop to the ground state, and the other be excited to a higher unstable energy level. The molecule thus excited could dissociate with some heat released. In a similar fashion a molecule may absorb a succession of single photons and thus escalate in energy. One somewhat different process that may add heat to the vapor is the absorption of a Nd laser photon (1.06μ) by a molecule with the subsequent reradiation at a longer wavelength (e.g., 1.2μ). The molecule can give up the energy difference as thermal energy through rotational and vibrational relaxation processes.

A detailed study of these phenomena would be required to establish the relative importance of these and other possible processes that result in a rapid heating of the vapor.

The destruction of the cesium molecules due to heating of the vapor during the laser pulse is probably the cause of the poor absorption of the high power Nd laser light. Identification and elimination of the process for the heat generation in the

cesium vapor would be necessary for the use of diatomic cesium molecules as the medium of a high power transformer laser.

13. CONCLUSIONS

At this date the transformer laser concept has been explored only to a preliminary degree.

Numerous possible gas media have been considered analytically, on the basis of their molecular properties as known from the existing scientific literature, for pumping over a 1 msec pulse length with a battery of either ruby or glass primary lasers. The coverage in this respect has been rather thorough for diatomic molecule gases, but less so for polyatomic molecule gases. No other pulse lengths or other primary laser types have been considered. The most emphasis has been placed on systems whose output wavelength would lie in one of the windows of the atmospheric absorption spectrum. These would be most suitable for ground based applications.

In the laboratory, experimentation so far has dealt exclusively with the system utilizing cesium vapor saturated at about 400°C in at least one atm of helium.

The analyses based on previously existing information indicated that the highest output pulse energy densities should be achievable by the following systems, provided experimental research does not establish any unfavorable new properties of the molecules under intense irradiation.

<u>Transformer Gas Molecules</u>	<u>Pumping Lasers</u>	<u>Output Wavelengths</u>
Cs_2	Nd Glass	1.1 - 1.2 μ
Na_2	Ruby	7000-8000 \AA
CO	Er Glass	$\sim 1.66\mu$
CO	Dy^{++} in CaF_2	$\sim 2.36\mu; \sim 4.74\mu^*$
CN	Nd Glass	$\sim 1.08\mu$

The experiments on Cs_2 -Nd so far indicate a probability of serious trouble from some dissipative reaction occurring in the vapor at high pumping fluxes. However, the origin of the trouble has not yet been definitely settled.

All of the above combinations of materials appear worthy of careful experimentation for their possible use in producing very intense laser outputs of good wavefront shape.

* The CO-Dy system was not studied under this contract, but was previously analyzed with GPL Division funds. It is mentioned here as a matter of information.

14. BIBLIOGRAPHY

I.D. Abella, Phys. Rev. Letters 9, 453 (1962).

"American Institute of Physics Handbook", ed. by D.E. Gray, McGraw-Hill, 1957.

R.F. Barrow, Article in "Mellor's ... Chemistry, Vol. II, Suppl. II, The Alkali Metals", Pt. I, 1961, John Wiley.

R.F. Barrow, N. Travis, and C.V. Wright, Nature 187, 141 (1960).

H.B. Bebb, Phys. Rev. 149, 25 (1966).

H. Beutler, St. v. Bogdandy, and M. Polyani, Naturwiss. 14, 164 (1926).

A.B. Callear, Discussions Faraday Soc. 1962, No. 33, p. 28.

T. Carroll, Phys. Rev. 52, 822 (1937).

T.L. Cottrell and J.C. McCoubrey, "Molecular Energy Transfer in Gases", London, 1961.

E.K. Damon and R.G. Tomlinson, Article in "Lasers and Applications", ed. by W.S.C. Chang, Ohio State Univ. Eng. Exp. Station, Columbus, 1963, p. 187.

D.W. Davies, Trans. Faraday Soc. 54, 1429 (1958).

R.H. Davies, E.A. Mason, and R.J. Munn, Phys. Fluids 8, 444 (1965).

P.G. Dickens and A. Ripamonti, Trans. Faraday Soc. 57, 735 (1961).

G.H. Dieke, H.M. Crosswhite, and B. Dunn, J. Opt. Soc. Am. 51, 820 (1961).

C.T. Ewing, J.P. Stone, J.R. Spann, E.W. Steinkuller, D.D. Williams, and R.R. Miller (a), Dept. of Def. Doc. AD-622190, Sept. 1965.

C.T. Ewing, J.P. Stone, J.R. Spann, E.W. Steinkuller, D.D. Williams, and R.R. Miller (b), Dept. of Def. Doc. AD-622227, Sept. 1965.

W.A. Felsing and G.W. Drake, J. Am. Chem. Soc. 58, 1714 (1936).

M.G. Ferguson and A.W. Read, Trans. Faraday Soc. 61, 1559 (1965).

- W.R. Fredrickson and C.R. Stannard, Phys. Rev. 44, 632 (1933).
- W.R. Fredrickson and W.W. Watson, Phys. Rev. 30, 429 (1927).
- H.W. Gandy, R.J. Ginther, and J.F. Weller, Phys. Letters 16, 266 (1965).
- A.G. Gaydon and H.G. Wolfhard, "Flames", Macmillan, 2nd Ed., 1960.
- H. Hamada, Phil. Mag., Series 7, 15, 574 (1933).
- A.F. Haught, R.G. Meyerand, Jr., and D.C. Smith, Article in "Physics of Quantum Electronics", ed. by P.L. Kelley, et al, McGraw-Hill, 1966, p. 509.
- G. Herzberg, "Molecular Spectra and Molecular Structure, I. Spectra of Diatomic Molecules", Van Nostrand, 2nd Ed., 1950.
- K.F. Herzfeld, Discussions Faraday Soc. 1962, No. 33, p. 22.
- K.F. Herzfeld and T.A. Litovitz, "Absorption and Dispersion of Ultrasonic Waves", Acad. Press, 1959.
- L.O. Hocker, M.A. Kovacs, C.K. Rhodes, G.W. Flynn, and A. Javan, Phys. Rev. Letters 17, 233 (1966).
- W.J. Hooker and R.C. Millikan, J. Chem. Phys. 38, 214 (1963).
- H.H. Hupfeld, Z. Physik 54, 484 (1929).
- I.R. Hurle and A.G. Gaydon, Nature 184, 1858 (1959).
- E.H. Kennard, "Kinetic Theory of Gases", McGraw-Hill, 1938.
- G.W. King and J.H. Van Vleck, Phys. Rev. 55, 1165 (1939).
- M. Lapp and L.P. Harris, J. Quant. Spec. & Rad. Transf. 6, 169 (1966).
- J.K. Link, J. Opt. Soc. Am. 56, 1195 (1966).
- F.W. Loomis and S.W. Nile, Phys. Rev. 32, 873 (1928).
- R.D. Maurer, Article in "Optical Masers", ed. by J. Fox, Polytech. Inst., Brooklyn, 1963.
- R.C. Millikan, J. Chem. Phys. 38, 2855 (1963).

- R.C. Millikan and D.R. White (a), J. Chem. Phys. 39, 3209 (1963).
- R.C. Millikan and D.R. White (b), J. Chem. Phys. 39, 98 (1963).
- R. Minkowski and W. Muhlenbruch, Z. Physik 63, 198 (1930).
- O.C. Mohler, "A Table of Solar Spectrum Wavelengths, 11984A to 25578A", Univ. Mich. Press, Ann Arbor, 1955.
- C.E. Moore, "Atomic Energy Levels ...", Vol. 1, U.S. Nat. Bur. Stand. Circ. 467, Wash. D.C., 1949.
- W.J. Moore, "Physical Chemistry", Prentice-Hall, 3rd Ed., 1962.
- R.S. Mulliken, Rev. Mod. Phys. 4, 1 (1932).
- C.K. N. Patel, Appl. Phys. Letters 7, 246 (1965).
- L. Pauling, "The Nature of the Chemical Bond," Cornell Univ. Press, Ithaca, 3rd Ed., 1960.
- S.S. Penner, "Quantitative Molecular Spectroscopy and Gas Emissivities", Addison-Wesley, Reading, Mass., 1959.
- G.T. Petrovskii, M.N. Tolstoi, P.P. Feofilov, G.A. Tsurikova, and V.N. Shapovalov, Opt. Spectry. (USSR) 21, 72 (1966).
- M.T. Pigott and D.H. Rank, J. Chem. Phys. 26, 384 (1957).
- D.H. Rank, A.H. Guenther, J.N. Shearer, and T.A. Wiggins, J. Opt. Soc. Am. 47, 148 (1957).
- D.H. Rank, G. Skorinko, D.P. Eastman, and T.A. Wiggins, J. Opt. Soc. Am. 50, 421 (1960).
- O.K. Rice, Article in "Energy Transfer in Gases", Inst. Int. de Chimie, Intersci. Publ., N.Y., 1964.
- R.N. Schwartz, Z.I. Slawsky, and K.F. Herzfeld, J. Chem. Phys. 20, 1591 (1952).
- K. Shuler, J. Chem. Phys. 32, 1692 (1960).
- R.B. Singh and D.K. Rai, Indian Jour. Pure & Appl. Phys. 3, 475 (1965).
- P.V. Slobodskaya, Izvest. Akad. Nauk SSSR (ser. Fiz.) 12, 656 (1948).

E. Snitzer, Dept. of Def. Doc. AD-454480, May 1965.

E. Snitzer and R. Woodcock, Appl. Phys. Letters 6, 45 (1965).

G. Stephenson, Nature 166, 191 (1950).

J.P. Stone, C.T. Ewing, J.R. Spann, E.W. Steinkuller, D.D. Williams, and R.R. Miller, Dept. of Def. Doc. AD-622191, Sept. 1965.

R.G. Tomlinson, E.K. Damon and H.T. Buscher, Article in "Physics of Quantum Electronics". ed. by P.L. Kelley, et al. McGraw-Hill, 1966, p. 520.

Y. Uchida, Japan. J. Phys. 8, 25 (1932).

J.F. Walling, J. Phys. Chem. 67, 1380 (1963).

A.E. Wechsler, Dept. of Def. Doc. AD-631469, Jan. 1966.

W.J. Witteman, J. Chem. Phys. 37, 655 (1962).

R.W. Wood and R.H. Galt, Astrophys. J. 33, 72 (1911).

R.W. Wood and F.E. Hackett, Astrophys. J. 30, 339 (1909).

J.T. Yardley and C.B. Moore, J. Chem. Phys. 45, 1066 (1966).

L.A. Young, Dept. of Def. Doc. AD-483866, May 1966.

L.A. Young and W.J. Eachus, J. Chem. Phys. 44, 4195 (1966).

E. Snitzer, Dept. of Def. Doc. AD-464480, May 1965.

E. Snitzer and R. Woodcock, Appl. Phys. Letters 6, 45 (1965).

G. Stephenson, Nature 166, 191 (1950).

J.P. Stone, C.T. Ewing, J.R. Spann, E.W. Steinkuller, D.D. Williams, and R.R. Miller, Dept. of Def. Doc. AD-622191, Sept. 1965.

R.G. Tomlinson, E.K. Damon and H.T. Buscher, Article in "Physics of Quantum Electronics". ed. by P.L. Kelley, et al, McGraw-Hill, 1966, p. 520.

Y. Uchida, Japan. J. Phys. 8, 25 (1932).

J.F. Walling, J. Phys. Chem. 67, 1380 (1963).

A.E. Wechsler, Dept. of Def. Doc. AD-631469, Jan. 1966.

W.J. Witteman, J. Chem. Phys. 37, 655 (1962).

R.W. Wood and R.H. Galt, Astrophys. J. 33, 72 (1911).

R.W. Wood and F.E. Hackett, Astrophys. J. 30, 339 (1909).

J.T. Yardley and C.B. Moore, J. Chem. Phys. 45, 1066 (1966).

L.A. Young, Dept. of Def. Doc. AD-483866, May 1966.

L.A. Young and W.J. Eachus, J. Chem. Phys. 44, 4195 (1966).

BLANK PAGE

Unclassified

Security Classification

DOCUMENT CONTROL DATA - R&D		
(Security classification of title, body of abstract and indexing annotation must be entered when the overall report is classified)		
1. ORIGINATING ACTIVITY (Corporate author) GPL Division, Aerospace Group, General Precision, Inc.		2a. REPORT SECURITY CLASSIFICATION Unclassified
		2b. GROUP
3. REPORT TITLE PUMPED TRANSFORMER LASERS		
4. DESCRIPTIVE NOTES (Type of report and inclusive dates) Final Report, 1 November 1964 to 31 October 1966		
5. AUTHOR(S) (Last name, first name, initial) Ellis, C.B., Simpson, J.H., Eberlin, E.C., and Greenwood, I.A.		
6. REPORT DATE 28 November 1966	7a. TOTAL NO. OF PAGES 122	7b. NO. OF REFS 70
8a. CONTRACT OR GRANT NO. Nonr-4718(00)	8a. ORIGINATOR'S REPORT NUMBER(S) GPL A-31-4	
b. PROJECT NO ARPA Number 306		
c. Project DEFENDER	8b. OTHER REPORT NO(S) (Any other numbers that may be assigned this report)	
d.		
10. AVAILABILITY/LIMITATION NOTICES		
11. SUPPLEMENTARY NOTES	12. SPONSORING MILITARY ACTIVITY Office of Naval Research, Dep't. of the Navy, Washington, D.C. 20360	
13. ABSTRACT A number of laser-pumped-laser systems have been studied which offer promise of development into sources for very high intensity beams of excellent parallelism. The arrangement proposed is to pump a vapor volume from many directions simultaneously with the output light from a large number of primary lasers -- which do not have to be of good optical quality. Absorption of the pump light by molecules of the vapor produces inversion in some of the molecular transitions, in such a manner that the vapor volume can lase out most of the total absorbed energy as a single output beam. Analysis based on molecular properties recorded in the existing literature pointed to at least five combinations of materials, with outputs between 7000Å and 5μ, which look potentially useful for such a system, provided no new unfavorable properties of the gas molecules under intense irradiation are established. All of these combinations appeared deserving of serious experimental investigation. Laboratory work under the contract has dealt entirely with one of these possible combinations: saturated cesium vapor near 400°C in a helium atmosphere, pumped at 1.06μ with Nd glass lasers. The experiments so far indicate a strong probability of serious trouble from some dissipative reaction occurring in the cesium vapor at high pumping fluxes. However, the origin of the trouble has not yet been definitely settled.		

Unclassified

Security Classification

14.	KEY WORDS	LINK A		LINK B		LINK C	
		ROLE	WT	ROLE	WT	ROLE	WT

Lasers, Transformer
Lasers, Molecular Gas
Lasers, Nd-glass-laser-pumped
Lasers, Er-glass-laser-pumped
Lasers, CaF₂:Dy⁺⁺-laser-pumped
Lasers, Ruby-pumped
Lasers, N₂Gas
Lasers, CN Gas
Lasers, Cesium Vapor
Lasers, Sodium Vapor
Lasers, CO Gas
Cesium Vapor, Molecular Properties
Cesium Molecules, Spectra
Carbon Monoxide Lasers

INSTRUCTIONS

1. ORIGINATING ACTIVITY: Enter the name and address of the contractor, subcontractor, grantee, Department of Defense activity or other organization (corporate author) issuing the report.

2a. REPORT SECURITY CLASSIFICATION: Enter the overall security classification of the report. Indicate whether "Restricted Data" is included. Marking is to be in accordance with appropriate security regulations.

2b. GROUP: Automatic downgrading is specified in DoD Directive 5200.10 and Armed Forces Industrial Manual. Enter the group number. Also, when applicable, show that optional markings have been used for Group 3 and Group 4 as authorized.

3. REPORT TITLE: Enter the complete report title in all capital letters. Titles in all cases should be unclassified. If a meaningful title cannot be selected without classification, show title classification in all capitals in parentheses immediately following the title.

4. DESCRIPTIVE NOTES: If appropriate, enter the type of report, e.g., interim, progress, summary, annual, or final. Give the inclusive dates when a specific reporting period is covered.

5. AUTHOR(S): Enter the name(s) of author(s) as shown on or in the report. Enter last name, first name, middle initial. If military, show rank and branch of service. The name of the principal author is an absolute minimum requirement.

6. REPORT DATE: Enter the date of the report as day, month, year, or month, year. If more than one date appears on the report, use date of publication.

7a. TOTAL NUMBER OF PAGES: The total page count should follow normal pagination procedures, i.e., enter the number of pages containing information.

7b. NUMBER OF REFERENCES: Enter the total number of references cited in the report.

8a. CONTRACT OR GRANT NUMBER: If appropriate, enter the applicable number of the contract or grant under which the report was written.

8b, 8c, & 8d. PROJECT NUMBER: Enter the appropriate military department identification, such as project number, subproject number, system numbers, task number, etc.

9a. ORIGINATOR'S REPORT NUMBER(S): Enter the official report number by which the document will be identified and controlled by the originating activity. This number must be unique to this report.

9b. OTHER REPORT NUMBER(S): If the report has been assigned any other report numbers (either by the originator or by the sponsor), also enter this number(s).

10. AVAILABILITY/LIMITATION NOTICES: Enter any limitations on further dissemination of the report, other than those

imposed by security classification, using standard statements such as:

- "Qualified requesters may obtain copies of this report from DDC."
- "Foreign announcement and dissemination of this report by DDC is not authorized."
- "U. S. Government agencies may obtain copies of this report directly from DDC. Other qualified DDC users shall request through _____."
- "U. S. military agencies may obtain copies of this report directly from DDC. Other qualified users shall request through _____."
- "All distribution of this report is controlled. Qualified DDC users shall request through _____."

If the report has been furnished to the Office of Technical Services, Department of Commerce, for sale to the public, indicate this fact and enter the price, if known.

11. SUPPLEMENTARY NOTES: Use for additional explanatory notes.

12. SPONSORING MILITARY ACTIVITY: Enter the name of the departmental project office or laboratory sponsoring (paying for) the research and development. Include address.

13. ABSTRACT: Enter an abstract giving a brief and factual summary of the document indicative of the report, even though it may also appear elsewhere in the body of the technical report. If additional space is required, a continuation sheet shall be attached.

It is highly desirable that the abstract of classified reports be unclassified. Each paragraph of the abstract shall end with an indication of the military security classification of the information in the paragraph, represented as (TS), (S), (C), or (U).

There is no limitation on the length of the abstract. However, the suggested length is from 150 to 225 words.

14. KEY WORDS: Key words are technically meaningful terms or short phrases that characterize a report and may be used as index entries for cataloging the report. Key words must be selected so that no security classification is required. Identifiers, such as equipment model designation, trade name, military project code name, geographic location, may be used as key words but will be followed by an indication of technical context. The assignment of links, roles, and weights is optional.